X-ray reflectivity and Grazing Incidence Small Angle X-Ray Scattering

G. Renaud,
CEA-Grenoble, France
Département de Recherche Fondamentale sur la Matière Condensée
Service de Physique des Matériaux et des Microstructures
And ESRF, BM32 beamline
grenaud@cea.fr

European School on Magnetism
New Experimental Aproaches in Magnetism

Constantza, Romania, Sept 7-16, 2005

Introduction

Nanoparticles, nanowires, thin films and multilayers… have

New physical properties (e.g. magnetic, but also electronic, catalytic or photonic)

Atomic structure, size, shape & organization

Growth conditions &

Morphology, temperature … of the substrate surface

X-ray

complementary to Near Field Microscopy

- non destructive - statistical information over mm scale
- depth sensitivity, from 20 Å up to several mm
- length scale probed : from a few Å to mm
- quantitative analysis
- following in-time: deposit - annealing - gas adsorption
- *in situ*, in UHV, during growth (and sometimes in real time)
- no charge effects : insulating samples (single crystal oxide substrates)

X-Ray Scattering

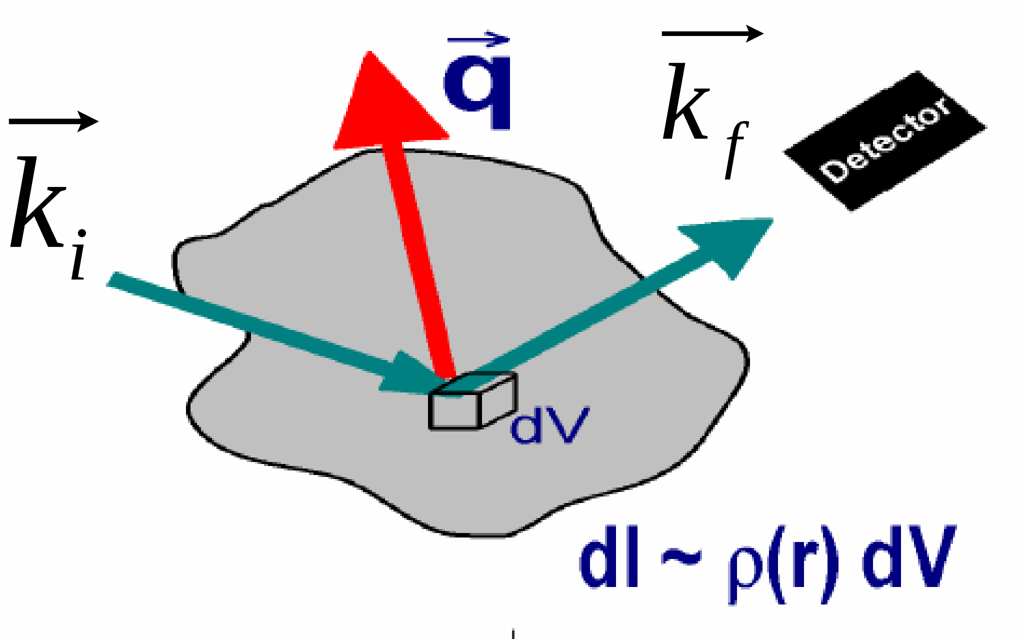

$\vec{q} = \vec{k_f} - \vec{k_i} = \vec{G_{hkl}}$ vector of the reciprocal space

Explores Reciprocal Space

Reciprocal Space of nanostructures deposited on a substrate

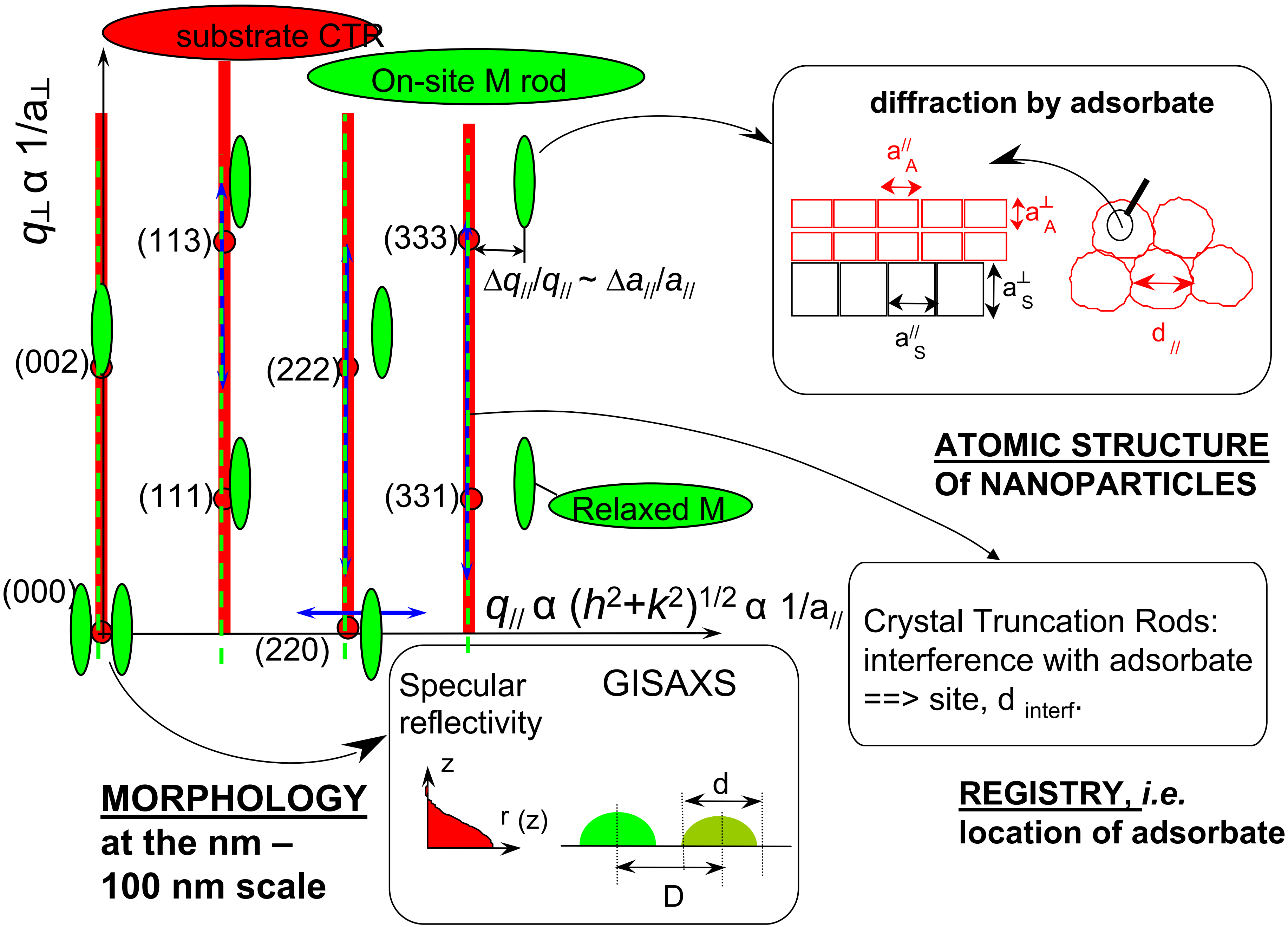

Grazing Incidence X-ray Scattering GIXS (or GID)

Structure @ atomic scale

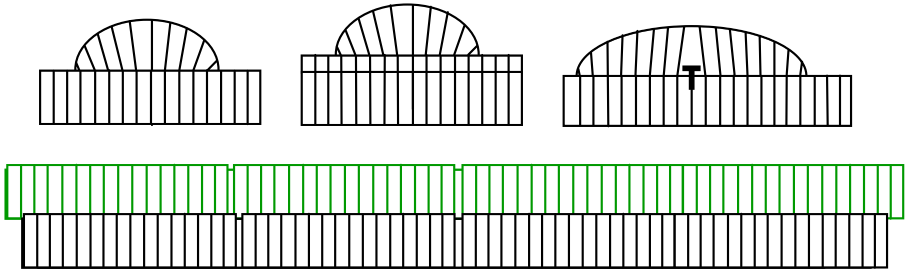

- Structure, composition
- Epitaxial relashionships
- Relaxation
  - Coherent
  - Incoherent (dislocations)
- Registry / substrate lattice
- Intermixing with substrate
- Substrate distortions
- ...

Grazing Incidence Small Angle X-ray Scattering (GISAXS) and X-R Reflectivity (XRR)

Morphology @ nanometer scale

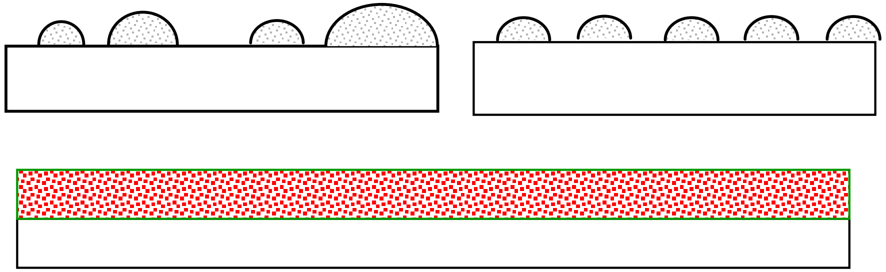

- Shape (facets, equilibrium shape)
- Dimensions
- Size distributions
- Organization
- Growth mode
- Density profile
- Thin film thickness
- Interface roughness
- Buried layers
- ...

Nanostructures (nanoparticles, nanowires, thin films, multilayers ...) & x-rays

X-RAY METHODS AT GRAZING INCIDENCE

STRUCTURE OF THIN LAYERS ON SUBSTRATE

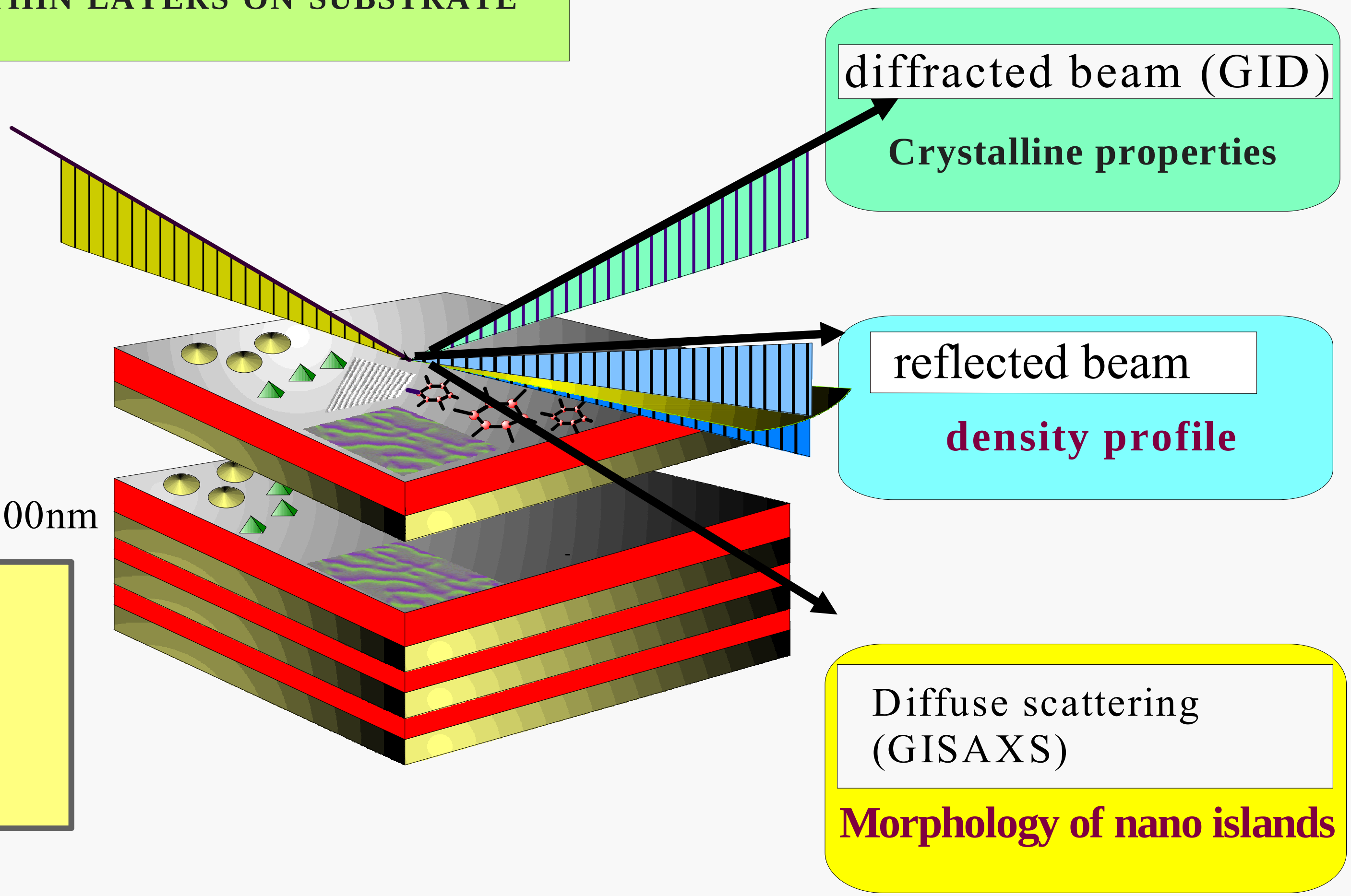

depth resolution 10nm-200nm

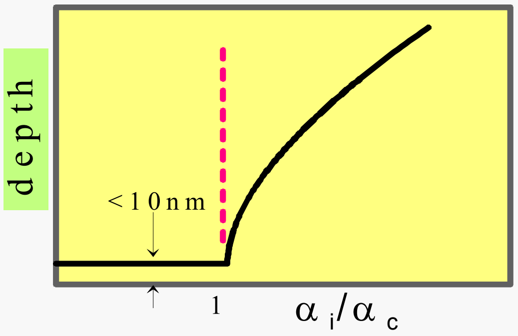

X-Ray Reflectivity: Principle

Visible Light Reflectivity: $n_2 > 1$

n_1

n_2

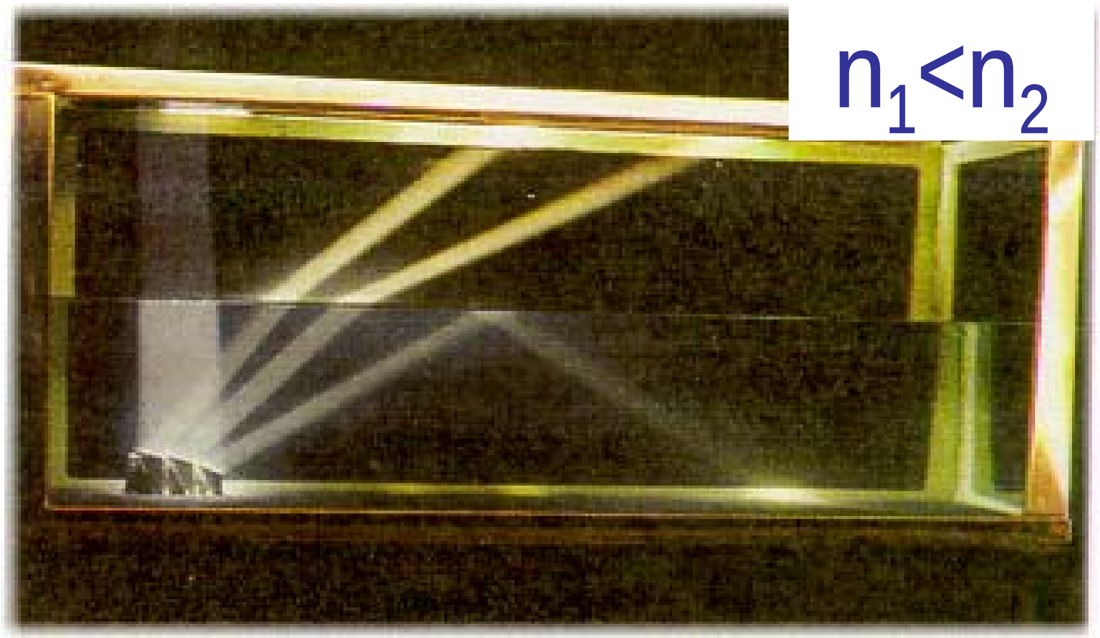

X-Ray Reflectivity: $n_2 < 1$

n_1

n_2

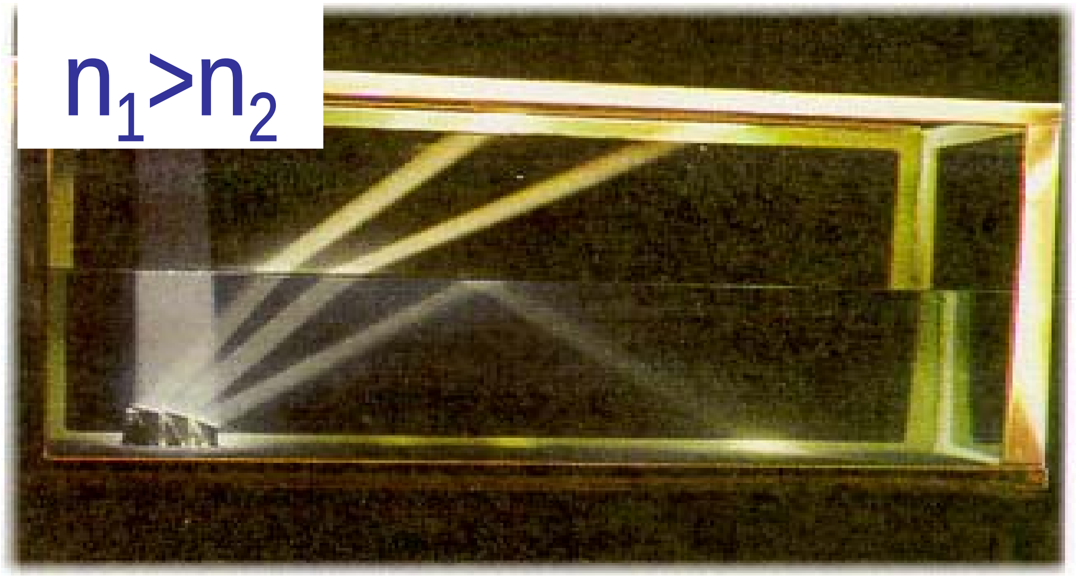

adapted M. Tolan Univ. Dortmund

Reflection and refraction – Perfect surface

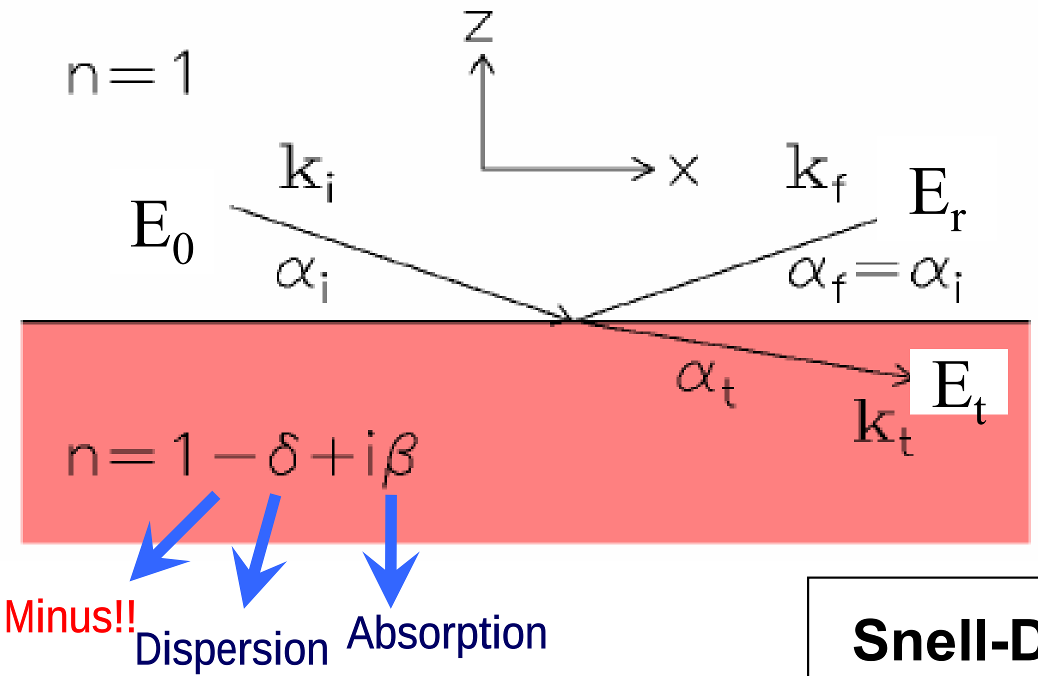

$$\delta = \frac{\lambda^2}{2\pi} r_0 \rho \approx 10^{-4}..10^{-6}$$

$$\beta = \frac{\lambda}{4\pi} \mu \approx 10^{-6}..10^{-9}$$

Snell-Descartes law: $\cos \alpha_i = n \cos \alpha_t$

∃ transmitted wave only if $\cos(\alpha_t) \leq 1$, i.e. $\alpha_\mathrm{i} \geq \alpha_c$

If $\alpha_\mathrm{i} \leq \alpha_c$,
- Incident wave totally externally reflected.
- Transmitted wave exponentially damped with z.

α_c critical angle for total external reflection of X-rays

$$\alpha_c = \sqrt{2\delta} = \sqrt{\frac{r_0}{\pi}} \times \lambda \times \sqrt{\rho} \approx 0.1 \text{ to } 0.5°$$

Reflection and refraction: perfect surface

- Fresnel equations:

Relationships between the amplitudes of incident, transmitted and reflected beam.

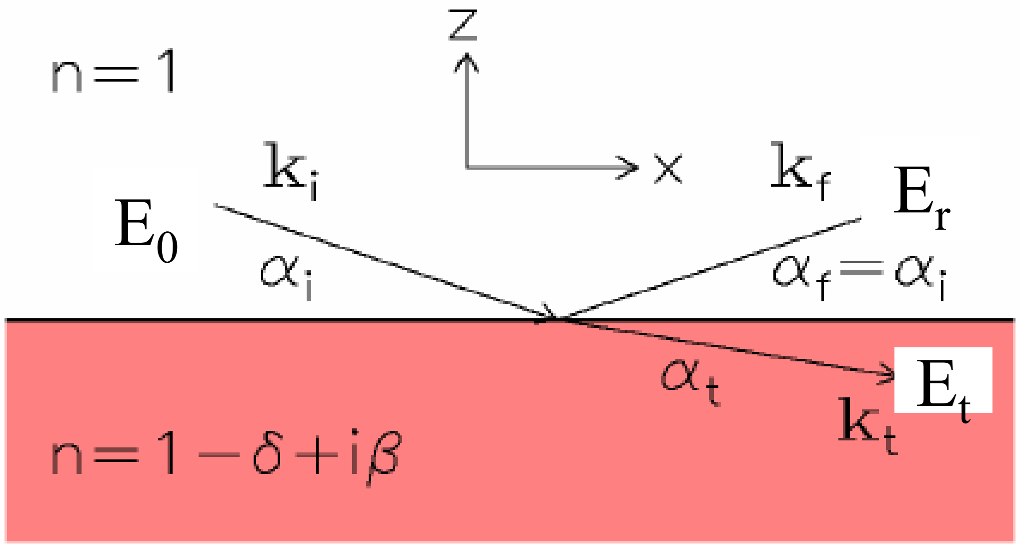

Amplitude

Intensity

Reflection

$$r=\frac{E_r}{E_0}=\frac{\sin(\alpha_i-\alpha_t)}{\sin(\alpha_i+\alpha_t)}\approx\frac{\alpha_i-\alpha_t}{\alpha_i+\alpha_t}$$

$$R=\left|\frac{E_r}{E_0}\right|^2$$

Transmission

$$t=\frac{E_t}{E_0}=\frac{2\sin(\alpha_i)\cos(\alpha_t)}{\sin(\alpha_i+\alpha_t)}\approx\frac{2\alpha_i}{\alpha_i+\alpha_t}$$

$$T=\left|\frac{E_t}{E_0}\right|^2$$

Limiting and asymptotic values for Fresnel equations

Transmission

$$t = \frac{2\alpha_i}{\alpha_i + \sqrt{\alpha_i^2 - 2\delta}} \approx \frac{2\alpha_i}{\alpha_i + \alpha_i(1 + \frac{1}{2}\frac{2\delta}{\alpha_i^2})}$$

$$t \approx \frac{2\alpha_i}{2\alpha_i + \frac{\delta}{\alpha_i}} \approx \frac{\alpha_i}{\delta} \ldots\ldots for \ldots\ldots \alpha_i < \sqrt{2\delta}$$

$$t \approx \frac{2\alpha_i}{2\alpha_i} = 1 \ldots\ldots\ldots\ldots\ldots\ldots\ldots for \ldots\ldots \alpha_i >> \sqrt{2\delta}$$

Reflection

$$r = \frac{\alpha_i - \sqrt{\alpha_i^2 - 2\delta}}{\alpha_i + \sqrt{\alpha_i^2 - 2\delta}} \approx \frac{\alpha_i - \alpha_i(1 + \frac{1}{2}\frac{2\delta}{\alpha_i^2})}{\alpha_i + \alpha_i(1 + \frac{1}{2}\frac{2\delta}{\alpha_i^2})}$$

$$r = 1 \ldots\ldots\ldots\ldots\ldots\ldots for \ldots\ldots\ldots \alpha_i << \sqrt{2\delta}$$

$$r = -\frac{\delta}{2\alpha_i^2} \ldots\ldots for \ldots\ldots\ldots \alpha_i >> \sqrt{2\delta}$$

Amplitude

Intensity

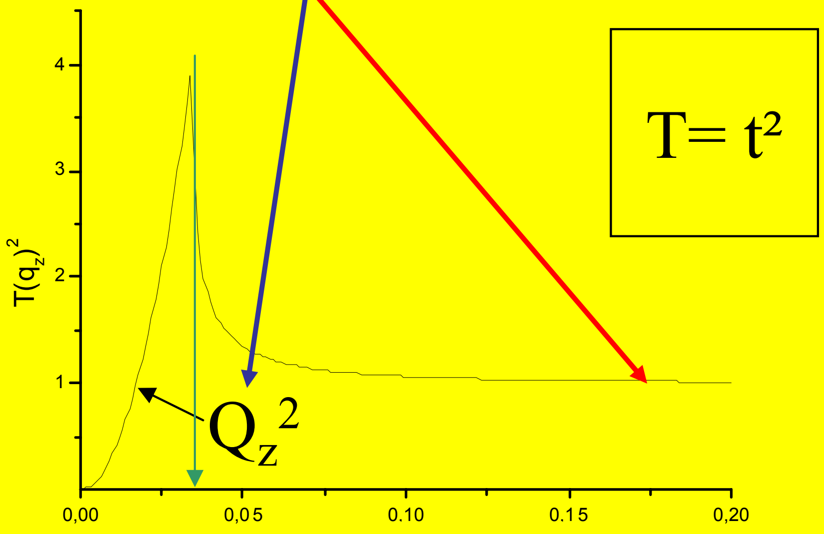

$Q_z = 4\pi/\lambda \sin \Theta_1$

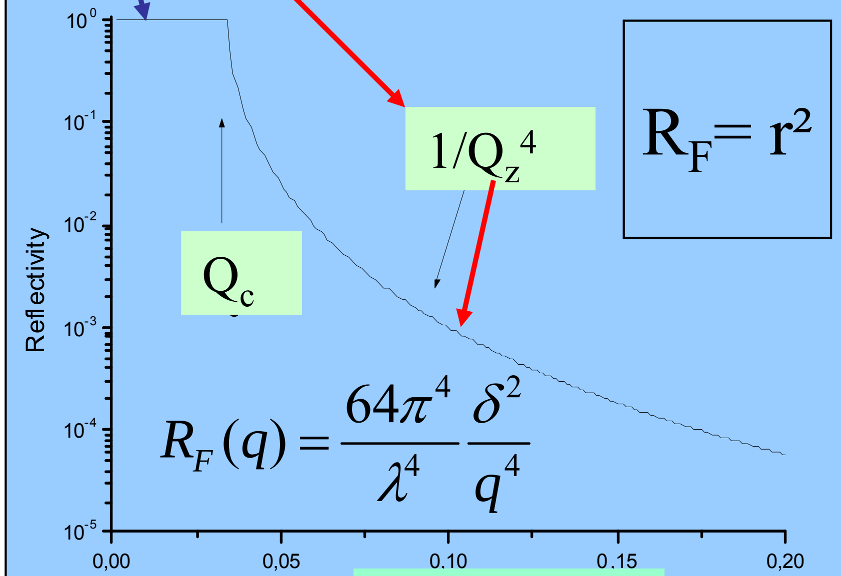

$$R_F(q) = \frac{64\pi^4}{\lambda^4}\frac{\delta^2}{q^4}$$

$Q_z = 4\pi/\lambda \sin \Theta_1$

Exact evaluation of Fresnel reflectivity

$$\boxed{R_F(\alpha_i) = |r|^2 = \frac{(\alpha_i - p_+)^2 + p_-^2}{(\alpha_i + p_+)^2 + p_-^2}}$$

$$\alpha_t = p_+ + \mathrm{i}p_-$$

$$p_{+/-}^2 = \frac{1}{2}\left\{\sqrt{(\alpha_i^2 - \alpha_c^2)^2 + 4\beta^2} \pm (\alpha_i^2 - \alpha_c^2)\right\}$$

➔ Absorption β also play a significant role

Fresnel Reflectivity: $R_F(\alpha_i)$ with absorption

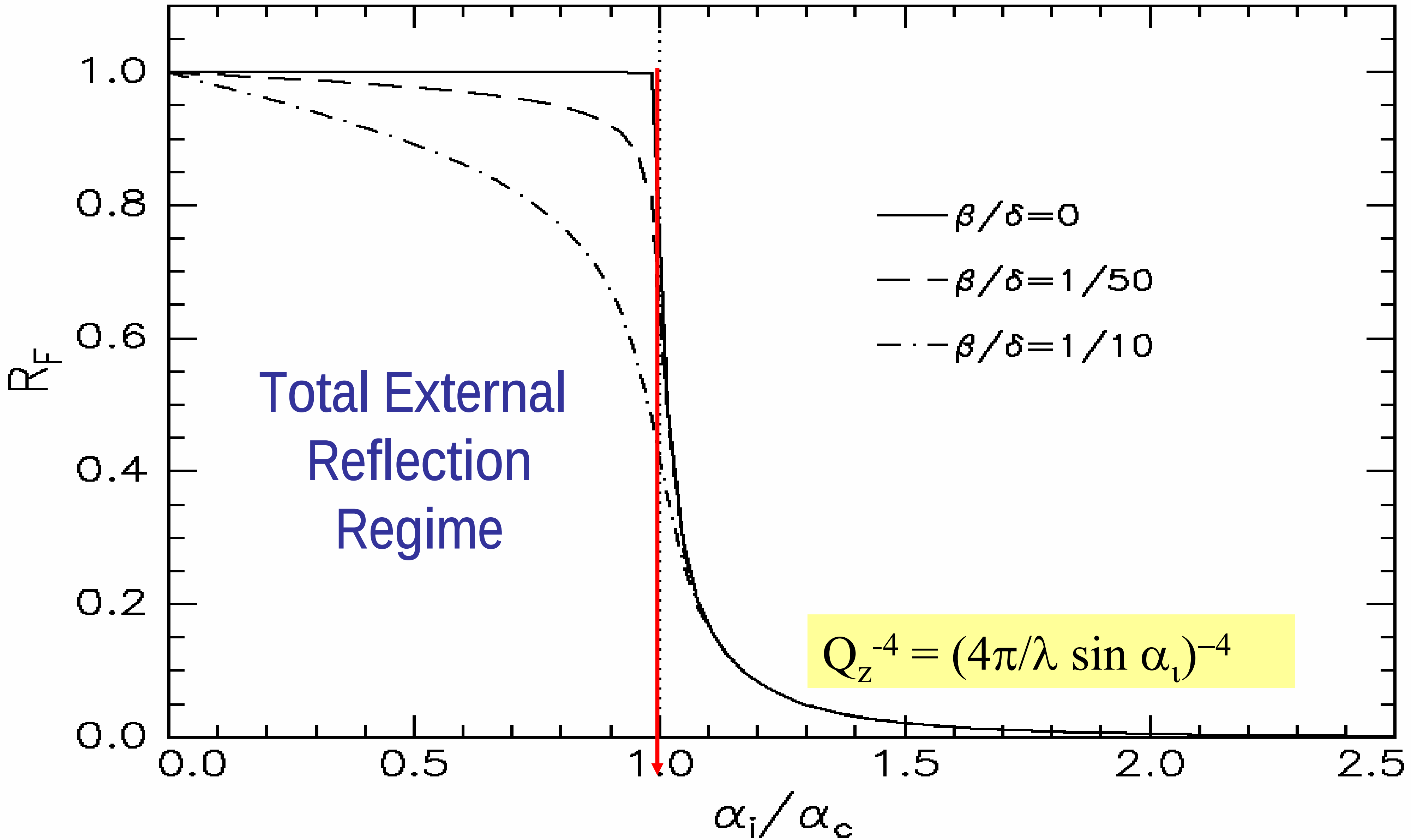

Transmission Function with absorption

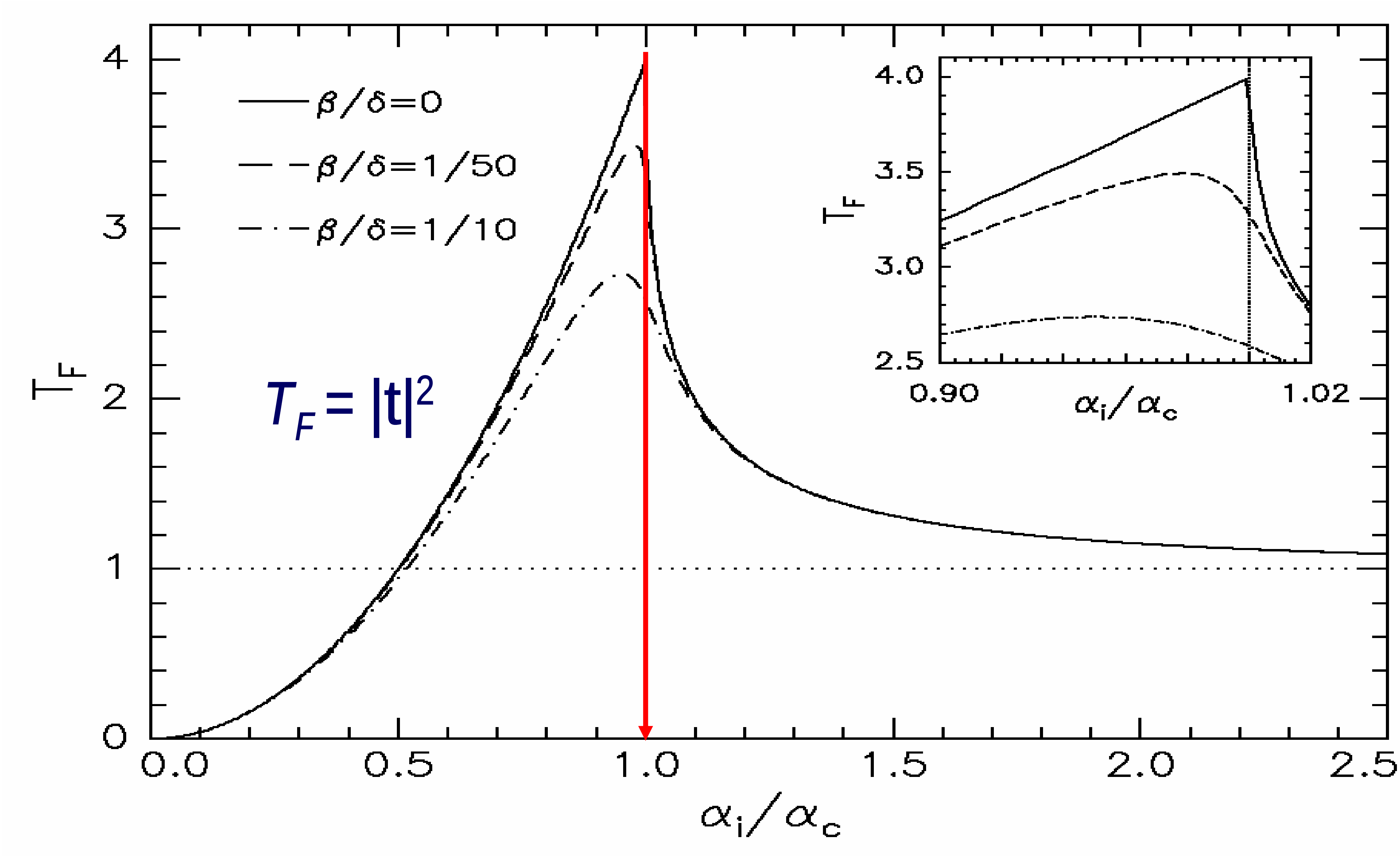

Penetration Depth with absorption

$$L_{i,f} = \left|\mathrm{Im}(k_{t,z})\right|^{-1} = \lambda / 2\pi l_{i,f}$$

$$l_{i,f} = \frac{1}{\sqrt{2}}\left\{\left(2\delta - \sin^2\alpha_{i,f}\right) + \left[\left(\sin^2\alpha_{i,f} - 2\delta\right)^2 + 4\beta\right]^{1/2}\right\}^{1/2}$$

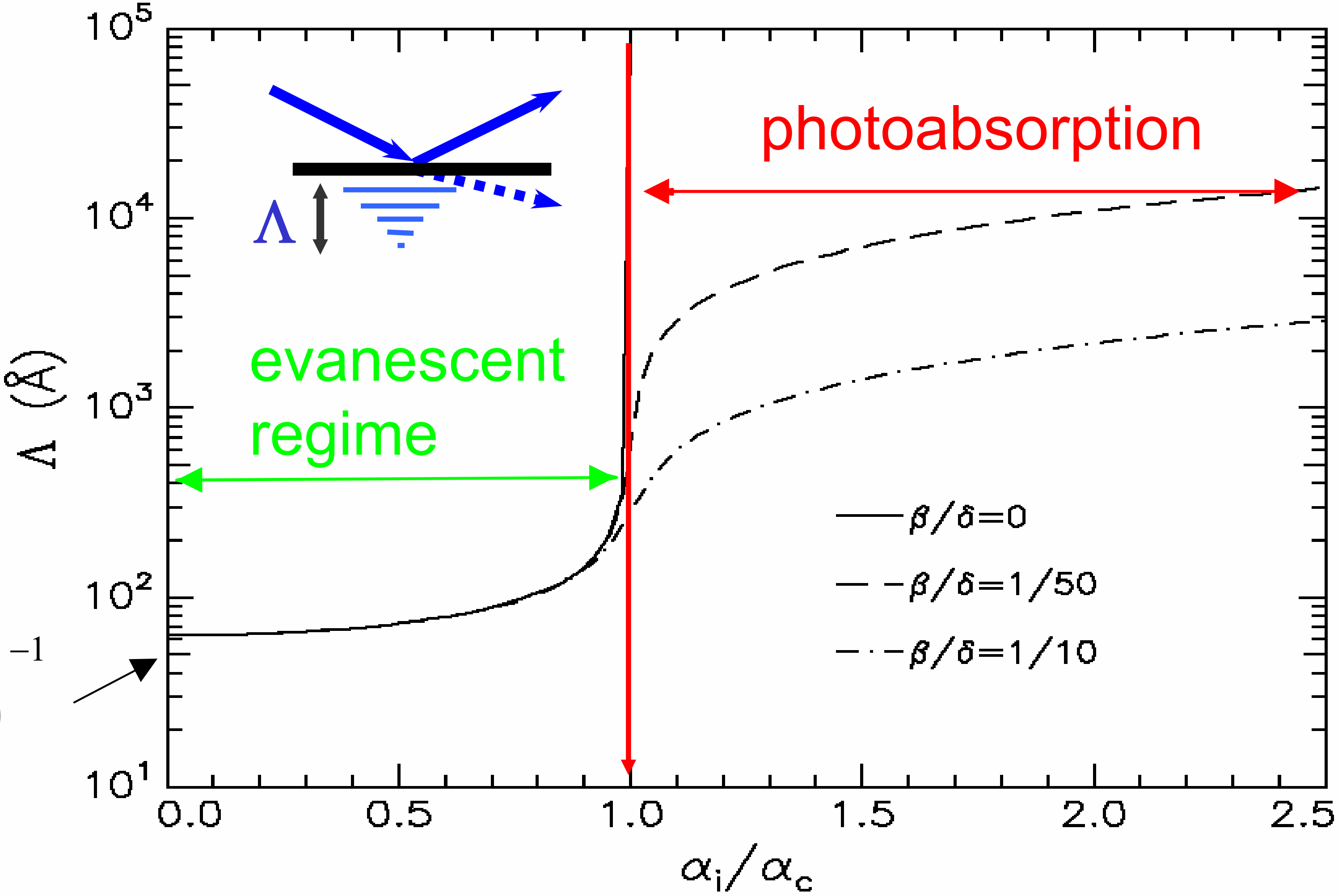

$$(\pi r_0 \rho)^{-1}$$

The geometry of X-ray reflectivity

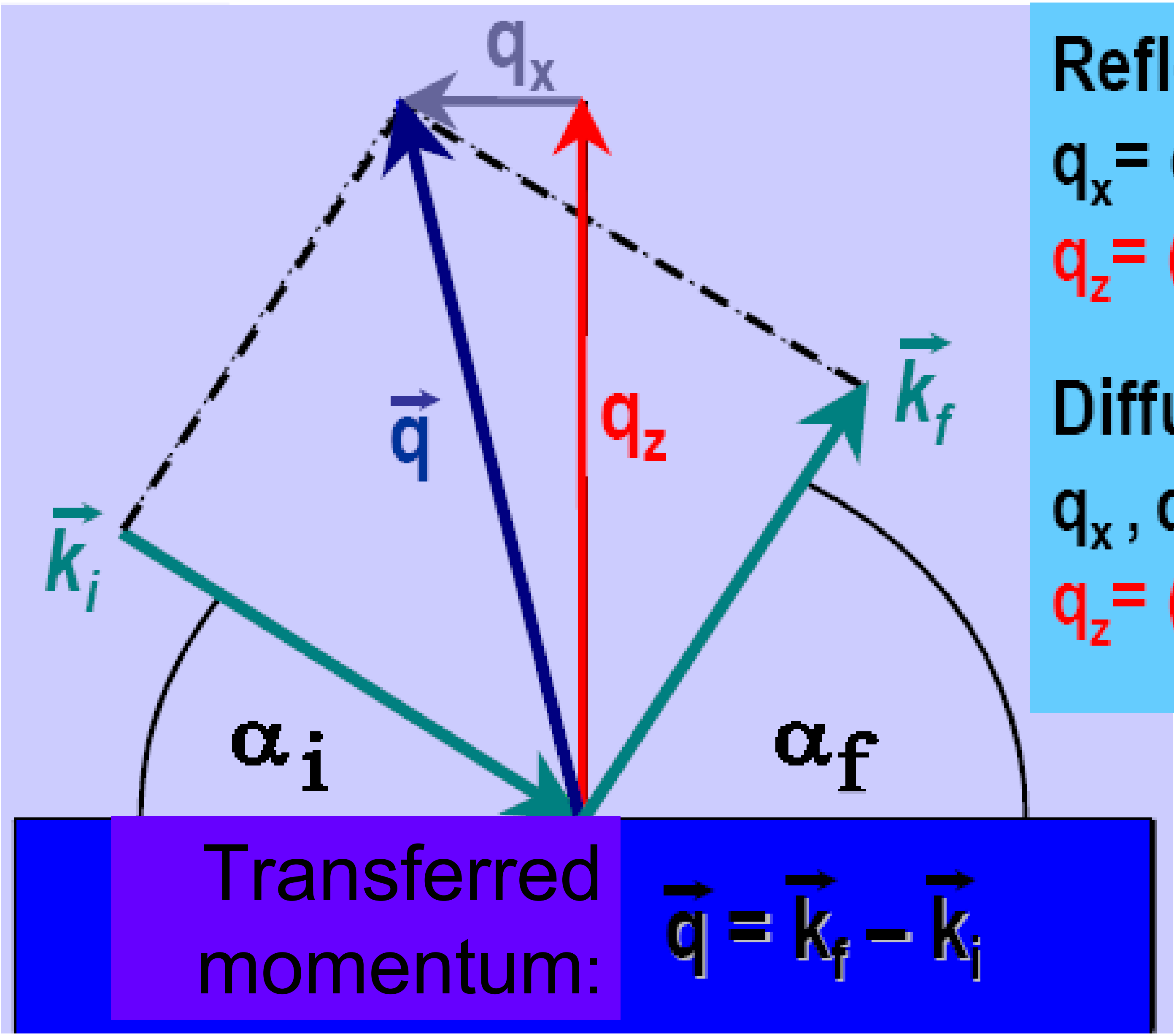

Reflectivity:

$q_x = q_y = 0$

$q_z = (4\pi/\lambda)\sin\alpha_i$

Diffuse Scattering:

$q_x, q_y \neq 0$

$q_z = (4\pi/\lambda)\sin(\alpha_i+\alpha_f)/2$

$\alpha_i, \alpha_f < 5°$

X-ray reflectivity: main equation

Helmholtz equation $$\Delta E(\vec{r}) + k^2\, n_X^2(\vec{r})\, E(\vec{r}) = 0$$

Formal solution:

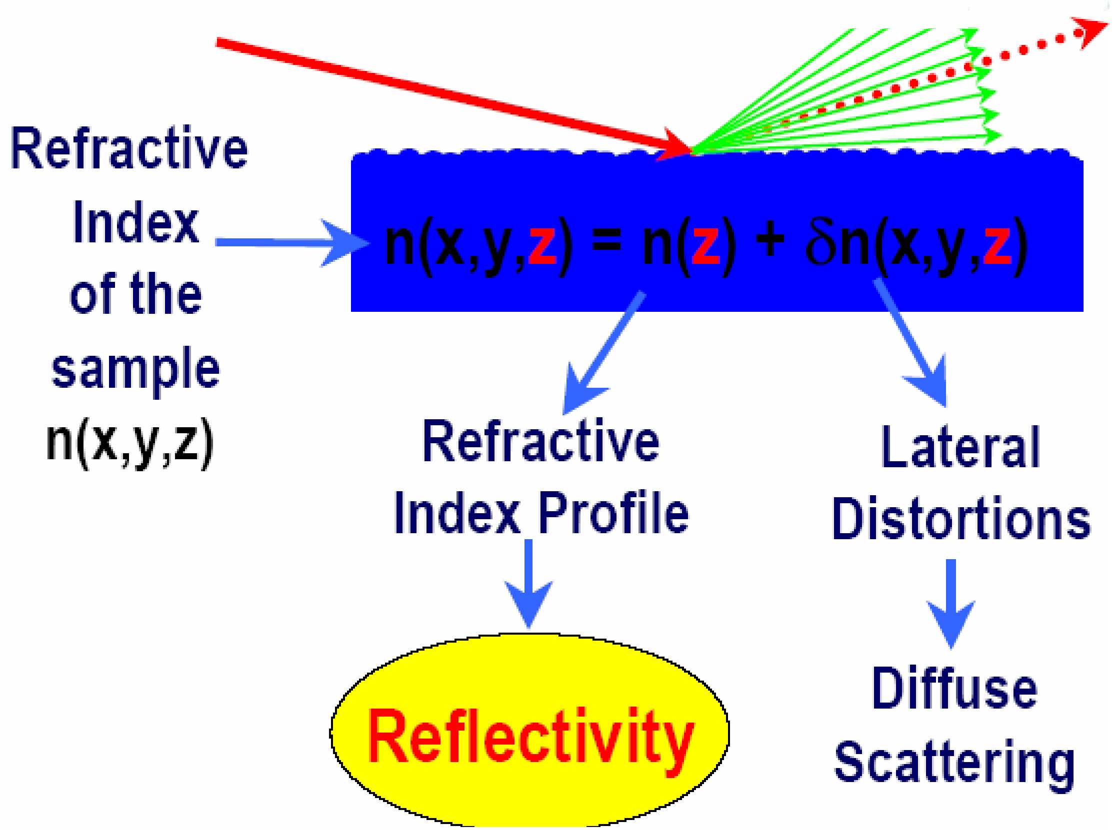

$$n(z) = 1 - \frac{\lambda^2}{2\pi} r_e\, \varrho(z) + \mathrm{i}\, \frac{\lambda}{4\pi}\, \mu(z)$$

➔ Electron density profile $\varrho(z) = \langle \varrho(x,y,z) \rangle_{x,y}$

adapted from M. Tolan Univ. Dortmund

Reflectivity from multilayers

Multiple scattering (dynamical calculation)

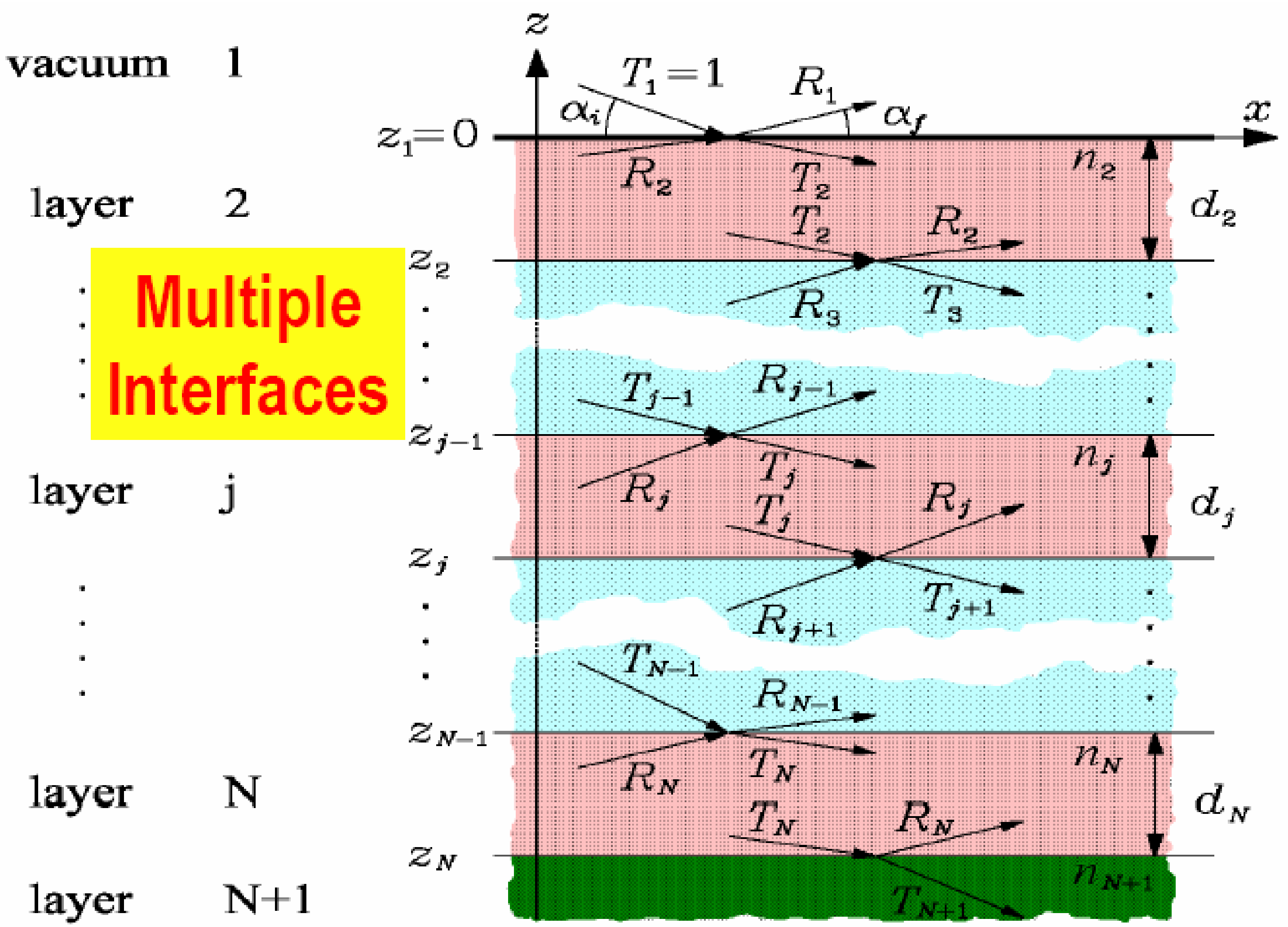

Matrix formalism:

Parrat iterations
Parrat, 1954

adapted M. Tolan Univ. Dortmund

Reflectivity from layer on substrate. Ex: PS on Si

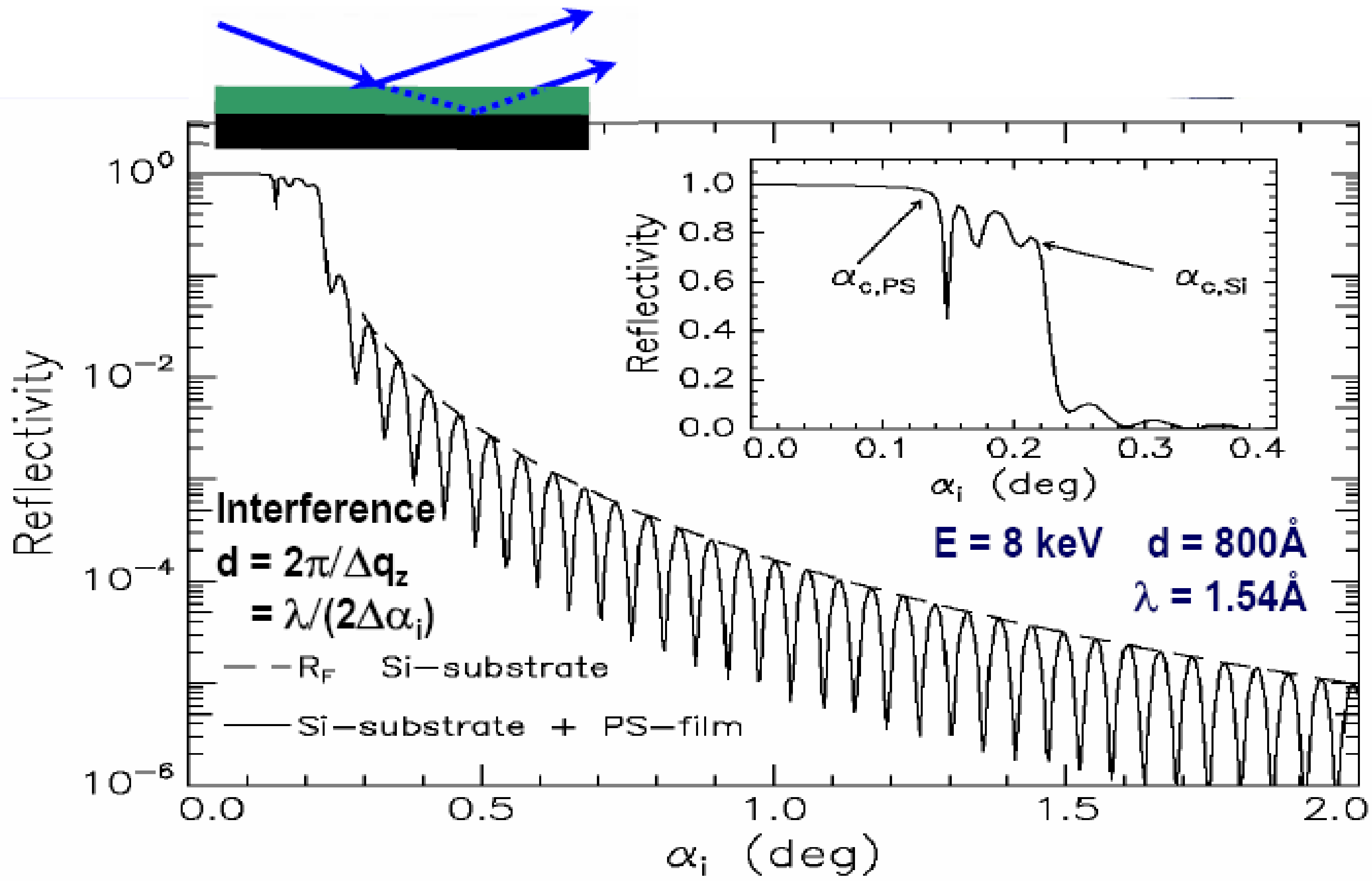

➔Reflectivity used as an everyday laboratory tool to measure the thickness of layers deposited on a substrate

adapted from M. Tolan Univ. Dortmund

Rough interfaces: statistics

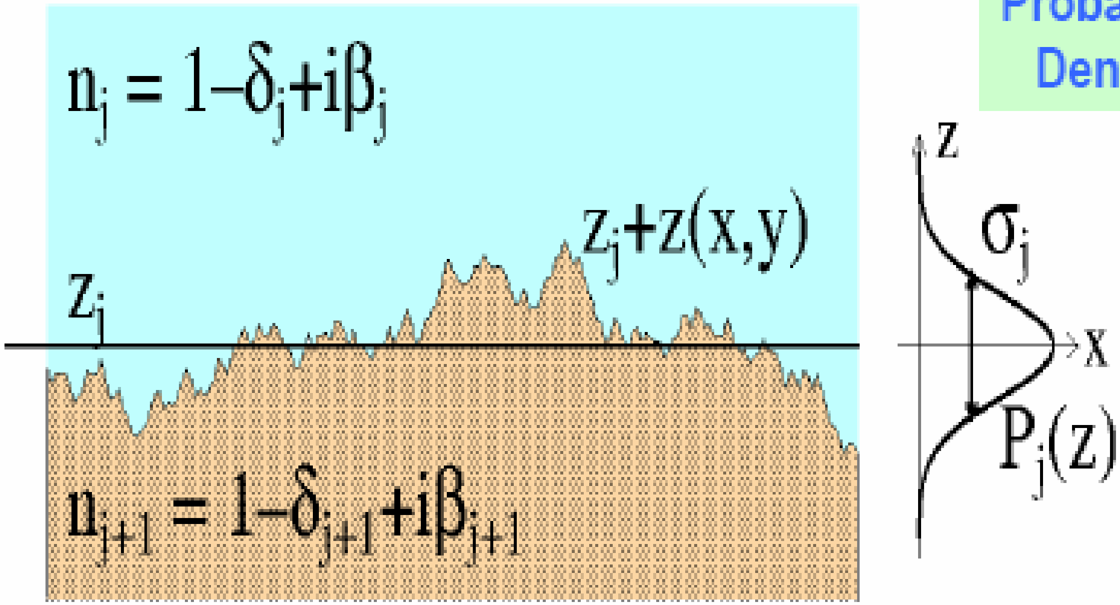

Probability Density

$$P_j(z) = \frac{1}{\sqrt{2\pi}\sigma_j}\exp\left(-\frac{z^2}{2\sigma_j^2}\right)$$

Integration

$$n_j(z) = \frac{n_j+n_{j+1}}{2} - \frac{n_j-n_{j+1}}{2}\,\mathrm{erf}\left(\frac{z-z_j}{\sqrt{2}\sigma_j}\right)$$

Refractive Index Profile n(z)

Electron Density Profile $\rho(z)$

adapted M. Tolan Univ. Dortmund

Reflectivity by a rough surface : which roughness ?

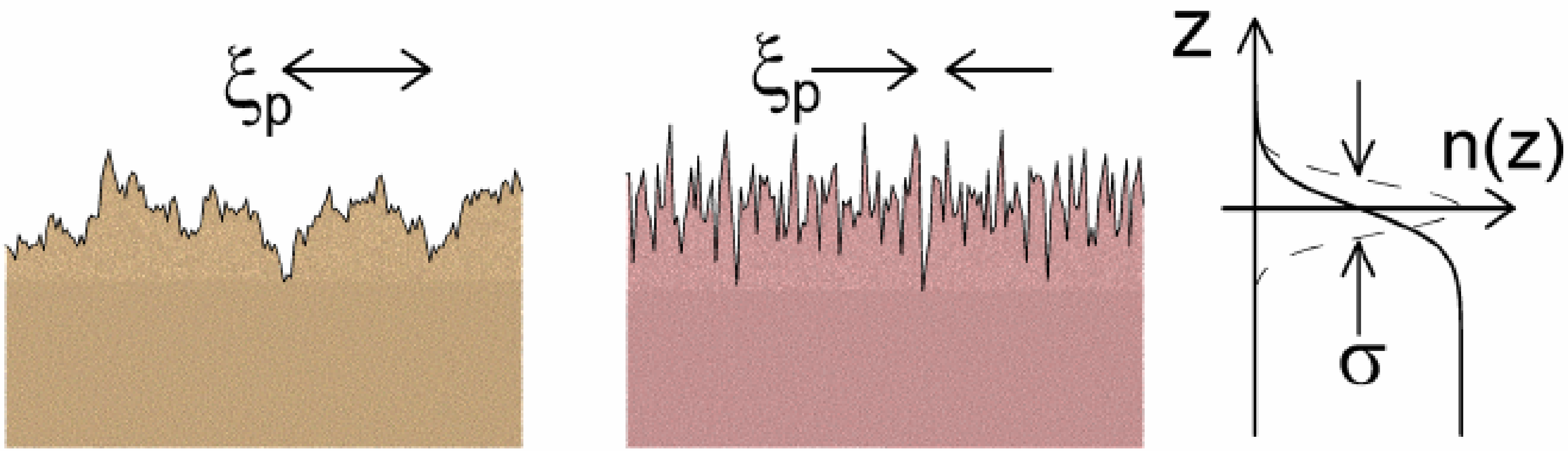

Same Roughness σ & Refractive Index Profile *n(z)* !

Lateral Structure Different

Different *Averaging* Procedures: $\sigma/\xi_p < 1$ or $\sigma/\xi_p > 1$

Roughness in multilayers?

Beckmann-Spizzichino Result (1963):

$\sigma/\xi_p < 1$

Reflection Coefficient

$$\tilde{r}_{j,j+1} = r_{j,j+1}\, e^{-2 k_{z,j}^2 \sigma_j^2}$$

Transmission Coefficient

$$\tilde{t}_{j,j+1} = t_{j,j+1}\, e^{-(k_{z,j}-k_{z,j+1})^2 \sigma_j^2/2}$$

Nevot-Croce Result (1980):

$\sigma/\xi_p > 1$

Reflection Coefficient

$$\tilde{r}_{j,j+1} = r_{j,j+1}\, e^{-2 k_{z,j} k_{z,j+1} \sigma_j^2}$$

Transmission Coefficient

$$\tilde{t}_{j,j+1} = t_{j,j+1}\, e^{+(k_{z,j}-k_{z,j+1})^2 \sigma_j^2/2}$$

$\sigma_j \Rightarrow$ **Exponential Damping of Reflectivity !**

Effect of interfacial roughness on reflectivity: single interface

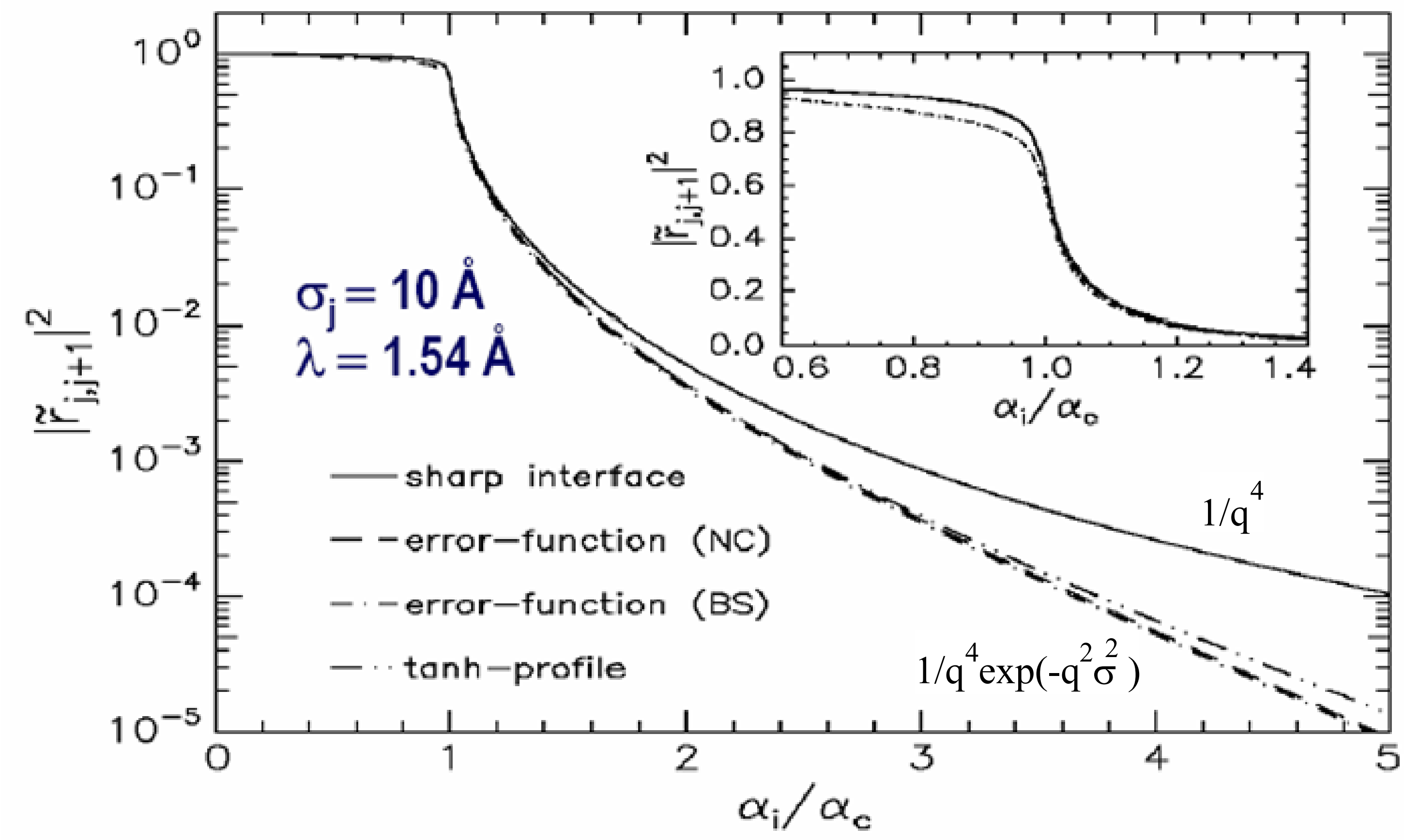

$$R(q_z) = R_F(q_z)\exp(-q_z^2\sigma^2)$$

➔ Reflectivity very efficient to measure (small) (statistically averaged) roughness of surfaces or interfaces.

Roughness at several interfaces

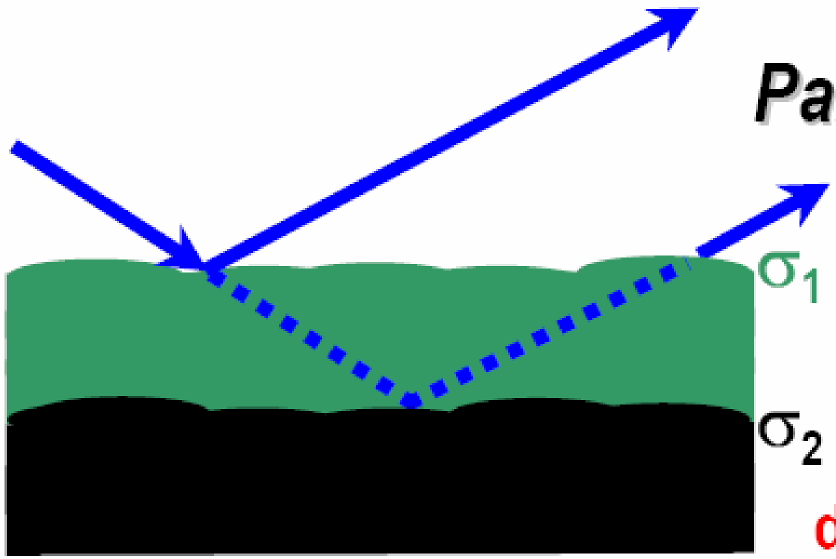

Parratt-Iteration
& Roughness:

Interference:

$$d = 2\pi/\Delta q_z = \lambda/(2\Delta\alpha_i)$$

+

Damping:

Roughness σ_1 , σ_2

Thin film with surface and interface roughness.
Example: PS layer on Si, with roughness

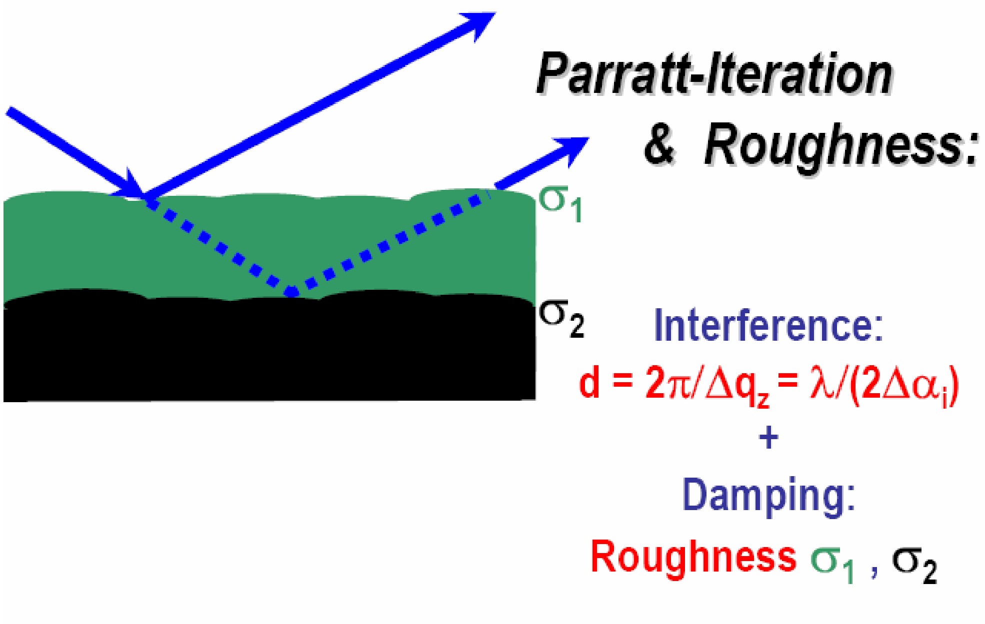

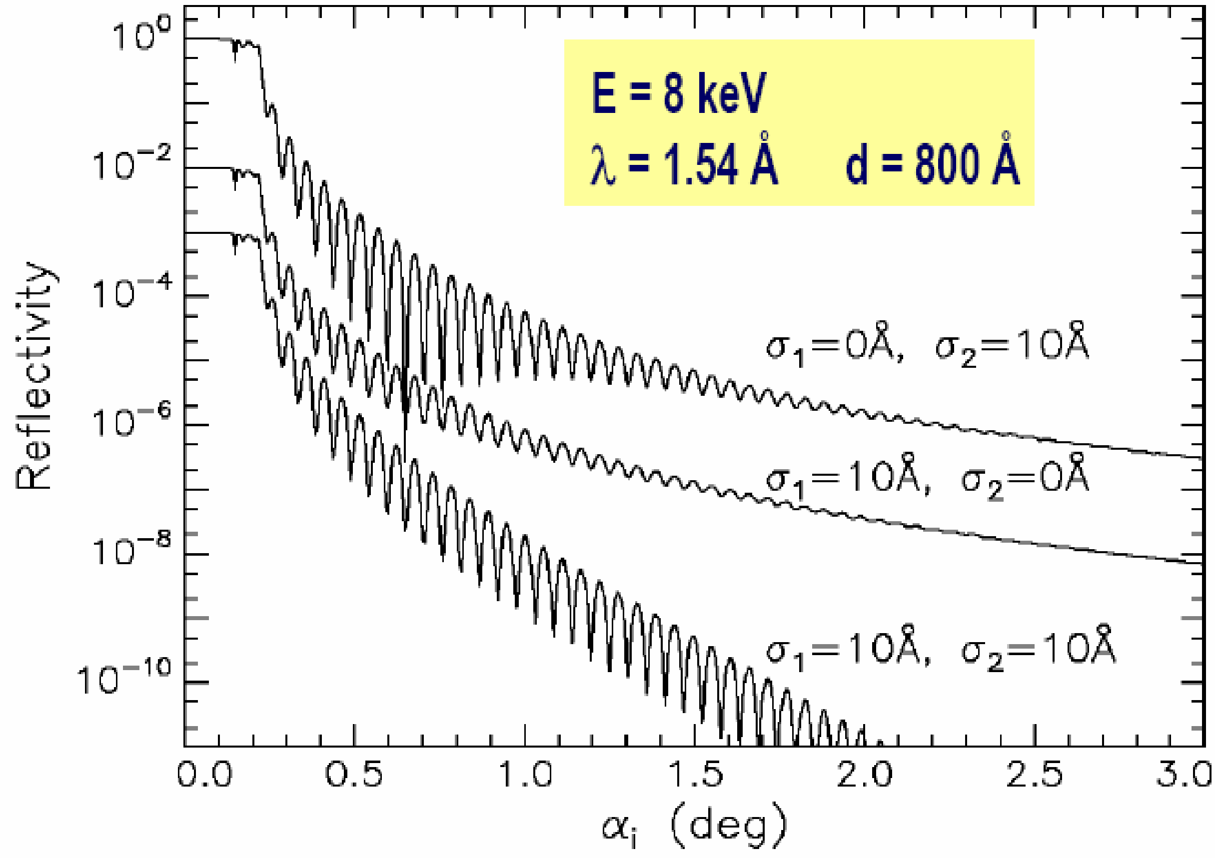

➔Effects of surface and interface roughness very different

➔σ_1, σ_2 and d can be determined independantly

Reflectivity calculation for arbitrary density profiles

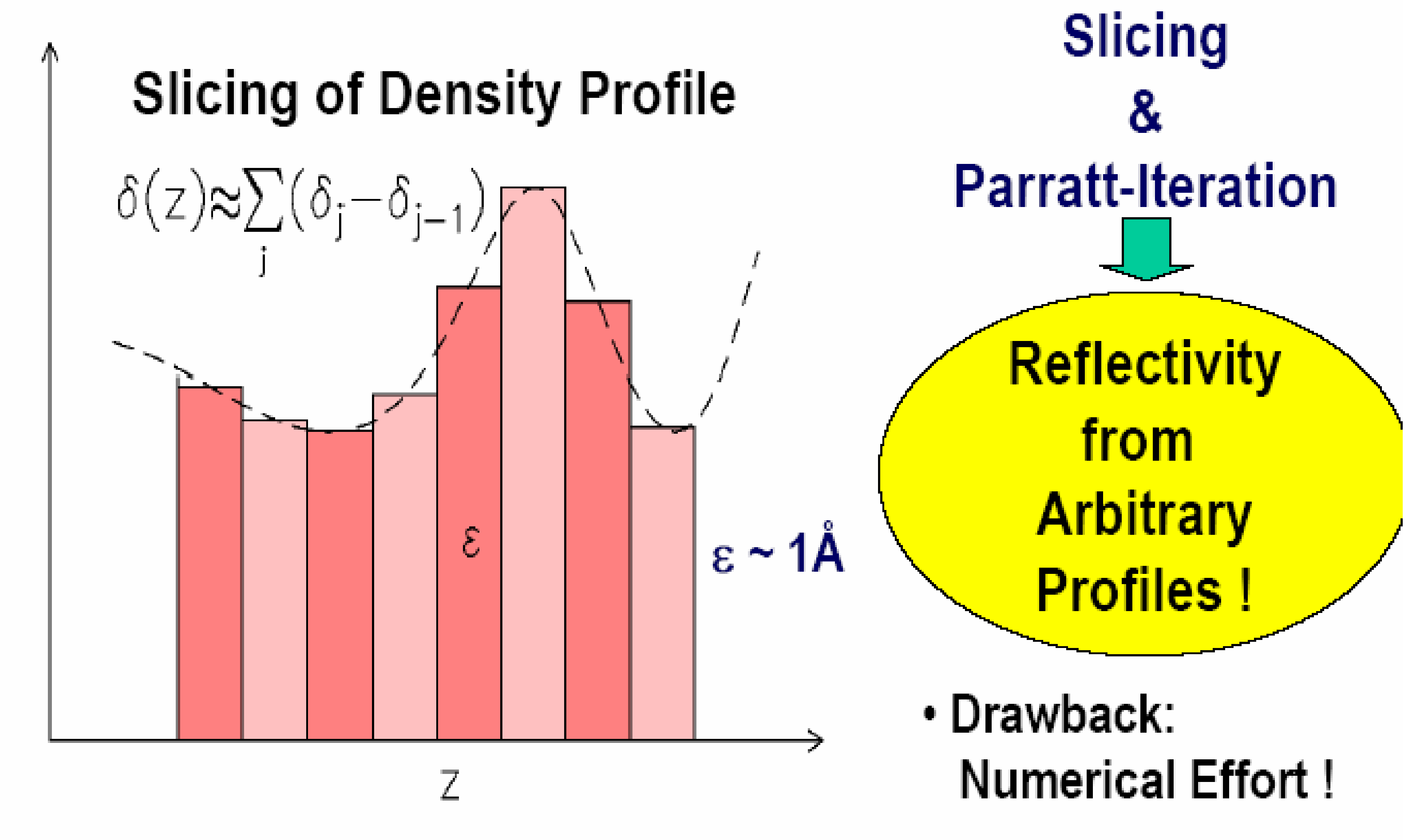

Example of fit of reflectivity curve:

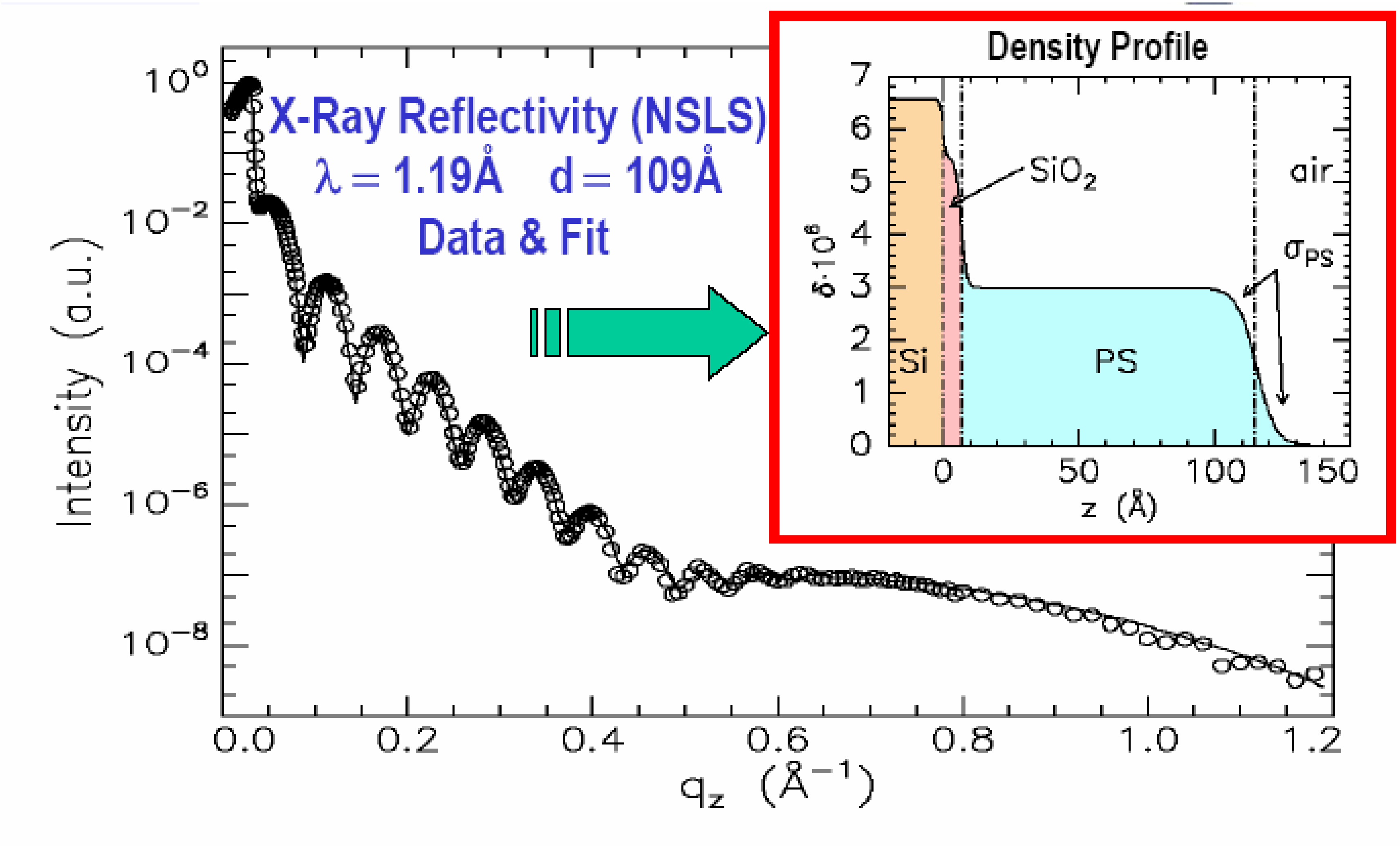

adapted M. Tolan Univ. Dortmund

Simplier aproach: Kinematical approximation

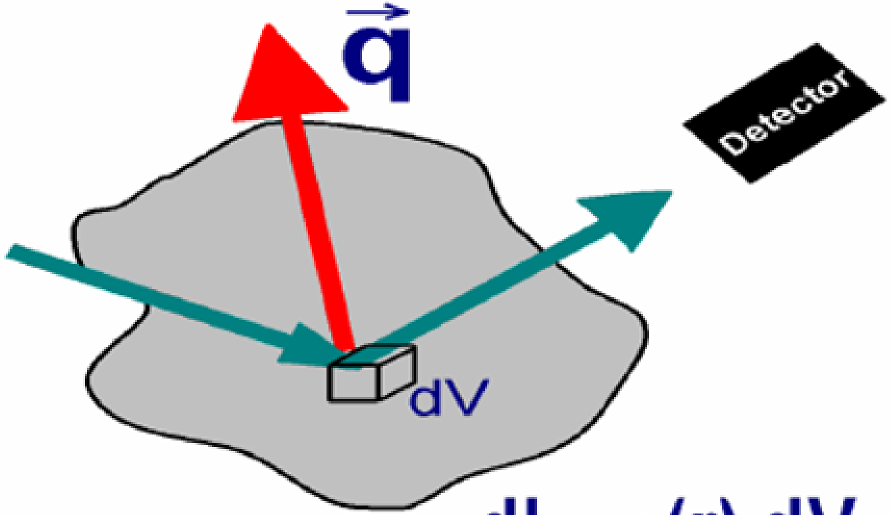

Multiple Scattering Negligible!

$$dI \sim \rho(r)\, dV$$

$$I(\vec{q}) \propto \left| \int \varrho(r)\ \exp(\mathrm{i}\,\vec{q}\cdot\vec{r})\,\mathrm{d}\vec{r} \right|^2$$

The « master » formula

$$I(\vec{q}) \propto \left| \int \varrho(r) \exp(\mathrm{i}\,\vec{q}\cdot\vec{r})\,\mathrm{d}\vec{r} \right|^2$$

Reformulation for Interfaces

$$R(q_z) = R_\mathrm{F}(q_z) \left| \frac{1}{\varrho_\infty} \int \frac{\mathrm{d}\varrho(z)}{\mathrm{d}z} \exp(\mathrm{i}\,q_z z)\,\mathrm{d}z \right|^2$$

Fresnel-Reflectivity of the Substrate

Electron Density Profile

Example: roughness

$$\rho'(z) = \frac{1}{\sqrt{2\pi}\sigma} \exp\left(-\frac{z^2}{2\sigma^2}\right) \Rightarrow R(q) = R_F(q) \exp\left(-q^2\sigma^2\right)$$

Kinematical versus dynamical calculation

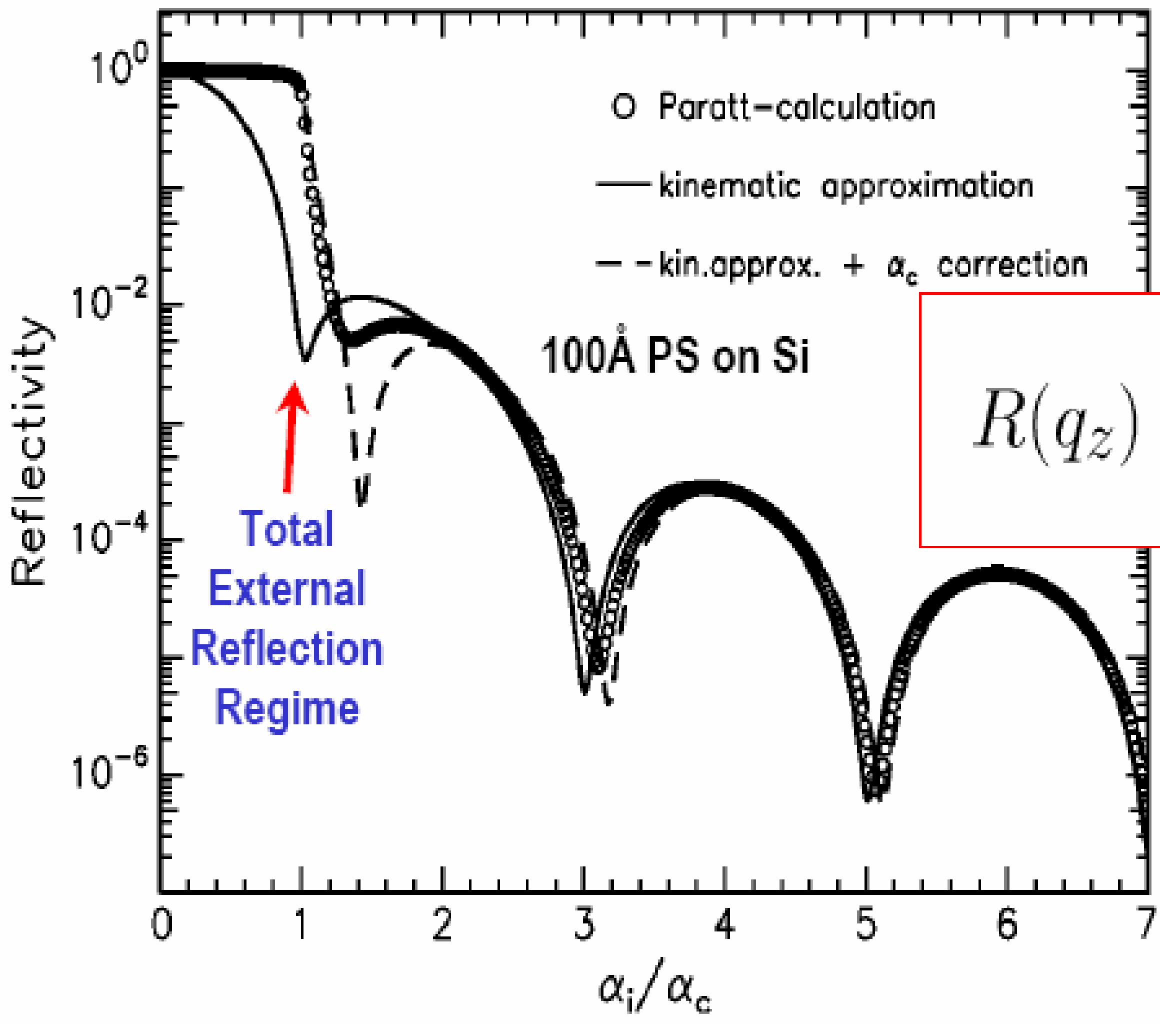

$$R(q_z) = R_{\mathrm{F}}(q_z)\,|F(q_z)|^2$$

„Phase Problem“
Data Fitting!

$$R(q_Z) \xrightarrow{?} \rho(z)$$

$$R(q_Z) \xleftarrow{\boxed{|T.F.|^2 \text{ Matrices}}} \rho(z)$$

Pb: Loss of the phase:

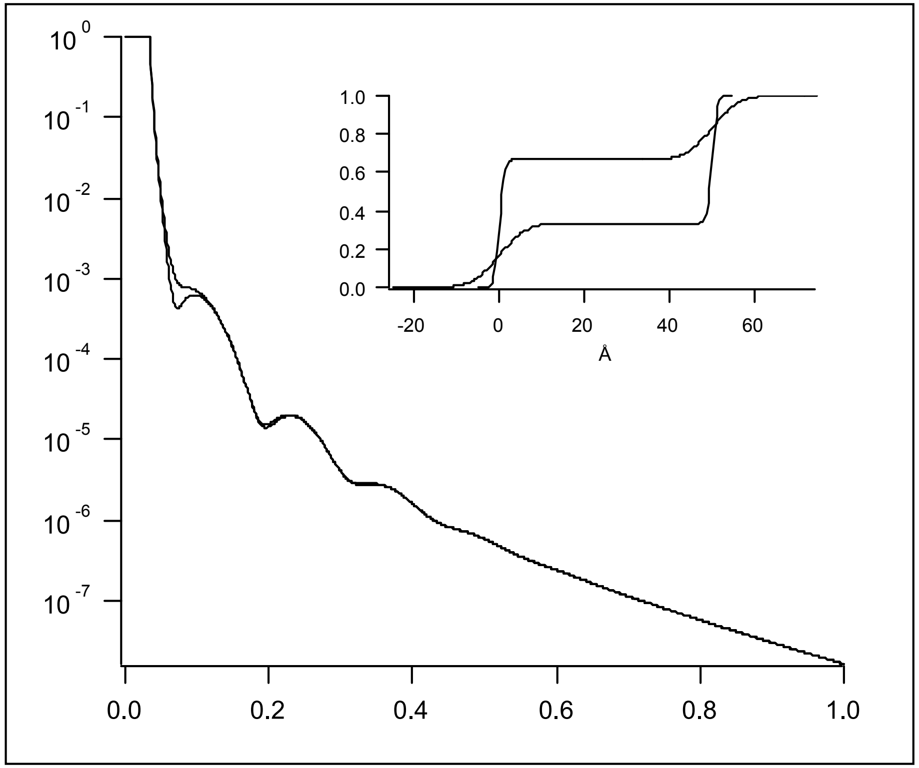

Different ways to solve the phase problem:

-Inclusion of pre-knowledge

-Anomalous reflectivity

Ex: Multilayers:

- Complex index profile

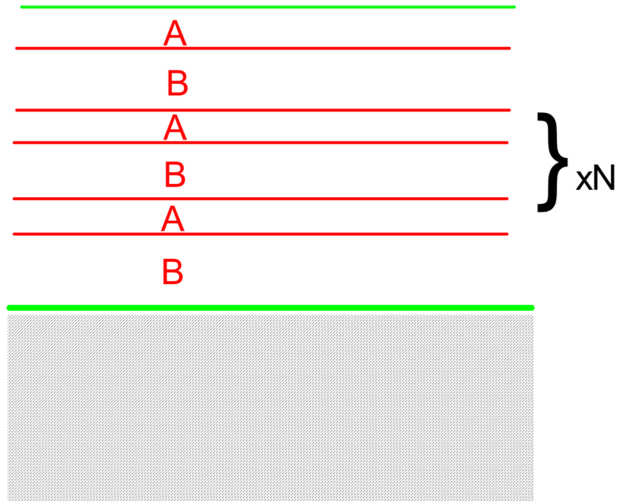

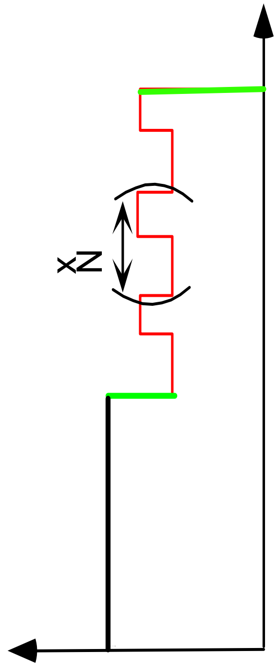

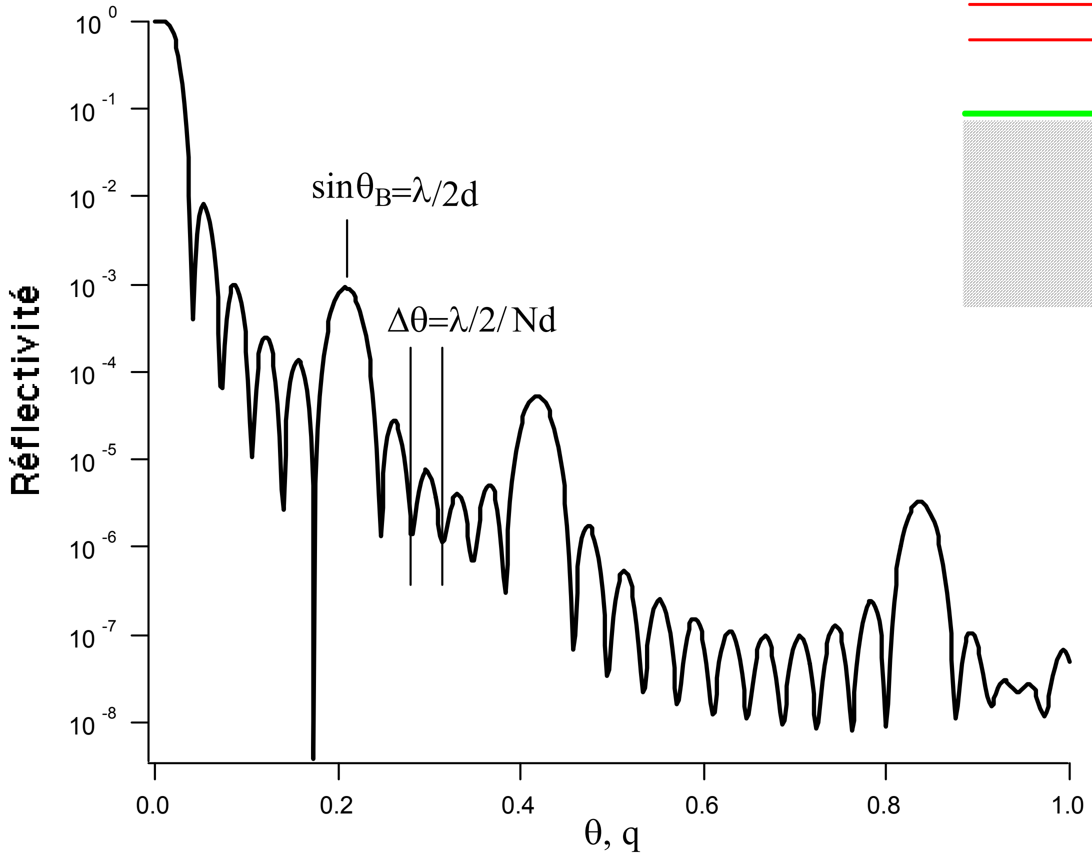

➔X-ray reflectivity used to characterize the thickness, period and roughnesses of multilayers.

Rough surfaces → diffuse scattering

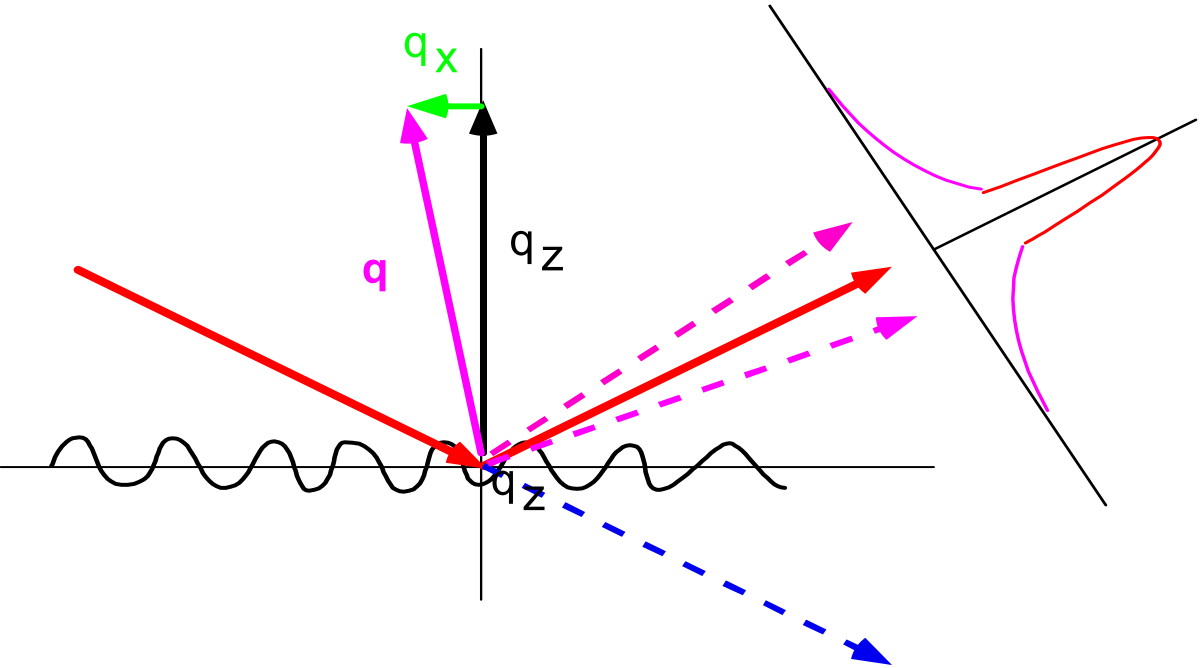

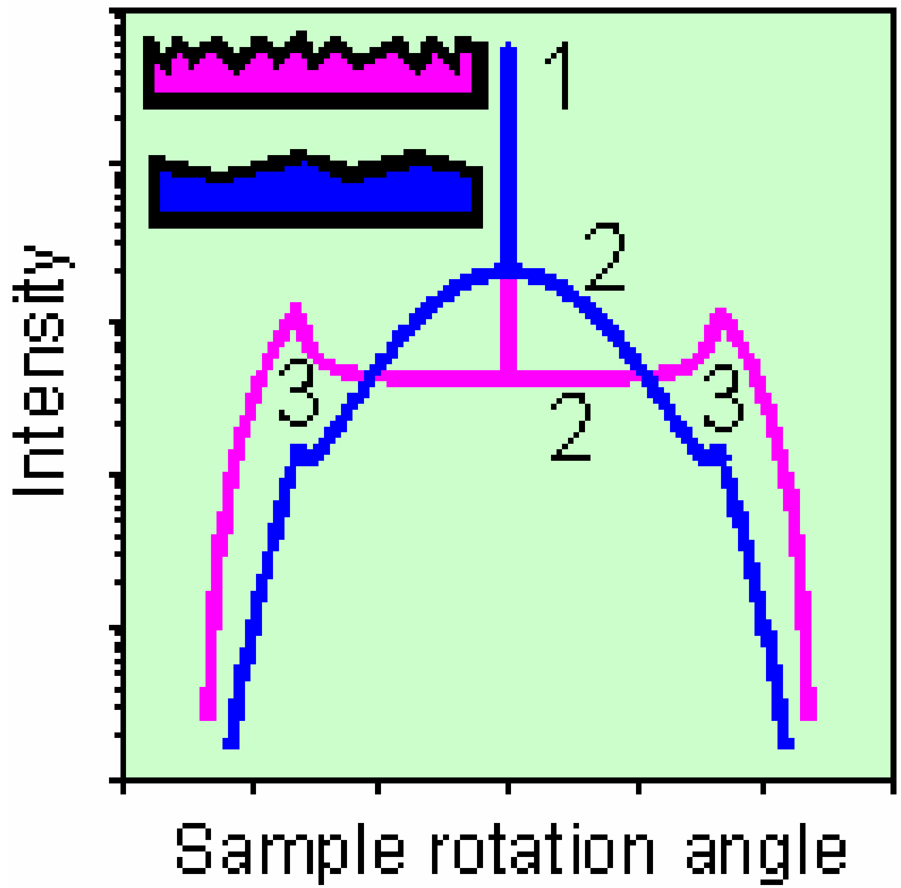

→ Lateral features of the roughness – Height-height correlations

Ex.: Roughness correlations in multilayers?

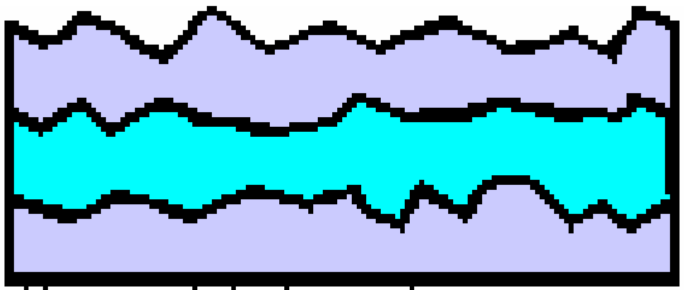

Uncorrelated roughness

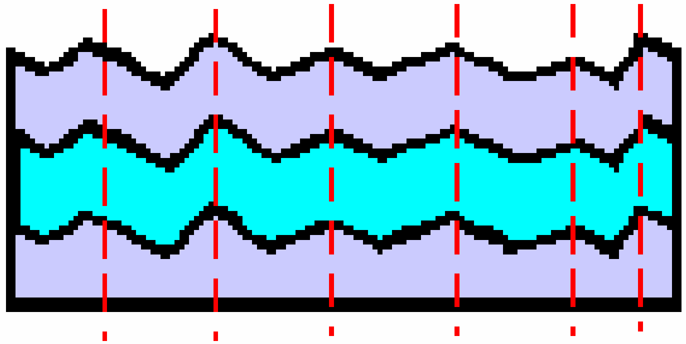

Correlated (repeated) roughness

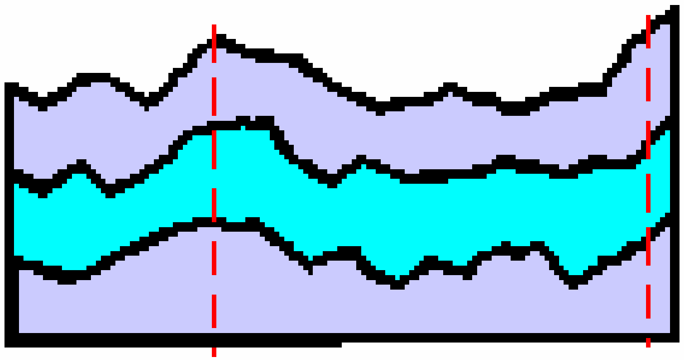

Wavelength-dependent inheritance of roughnes.

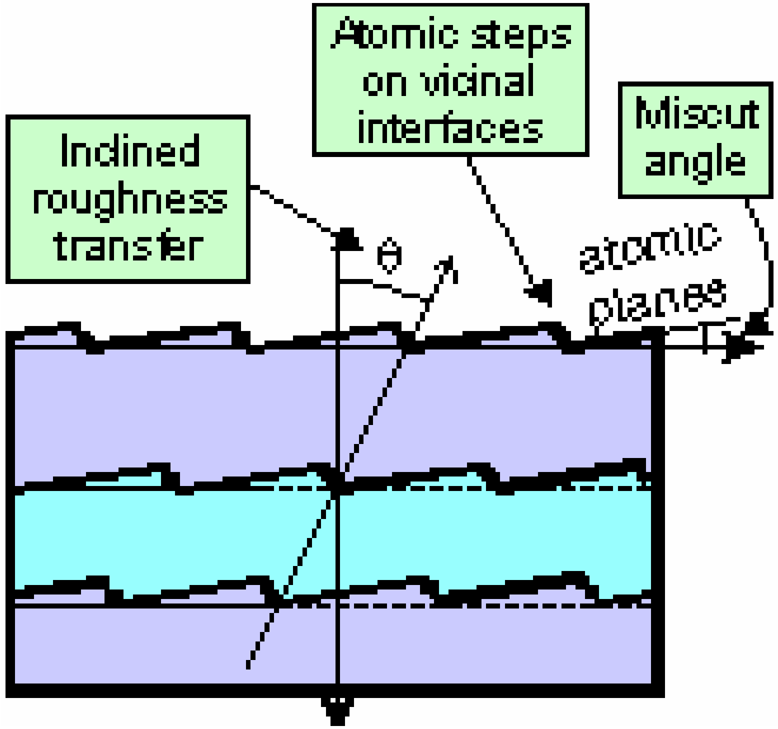

Conclusions on reflectivity

Specular reflectivity measures

- average density (mass and electron density)
- layer thicknesses
- interface roughness

Off-specular reflectivity probes

- Height-height correlations
- lateral order at nanometer-micrometer scale

- Refraction under grazing incidence

➔ tuneable scattering depth

Why GISAXS ?

GISAXS

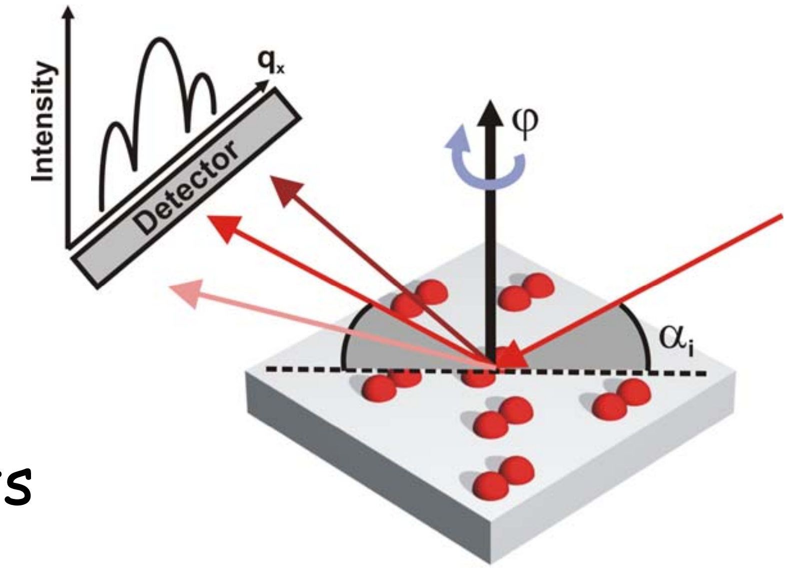

- Statistical information
- Lateral and vertical correlation
- shape as seen by x-rays:
  input for diffraction experiments
- Information about buried objects

AFM / STM

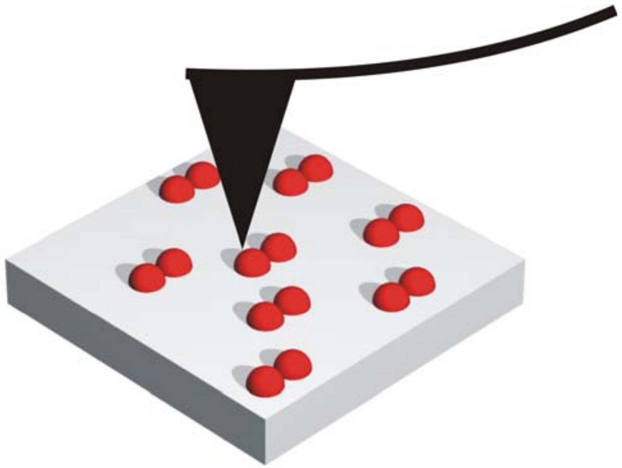

- Local information
- Detailed shape

Grazing Incidence Small Angle X-ray Scattering (GISAXS)

Principle

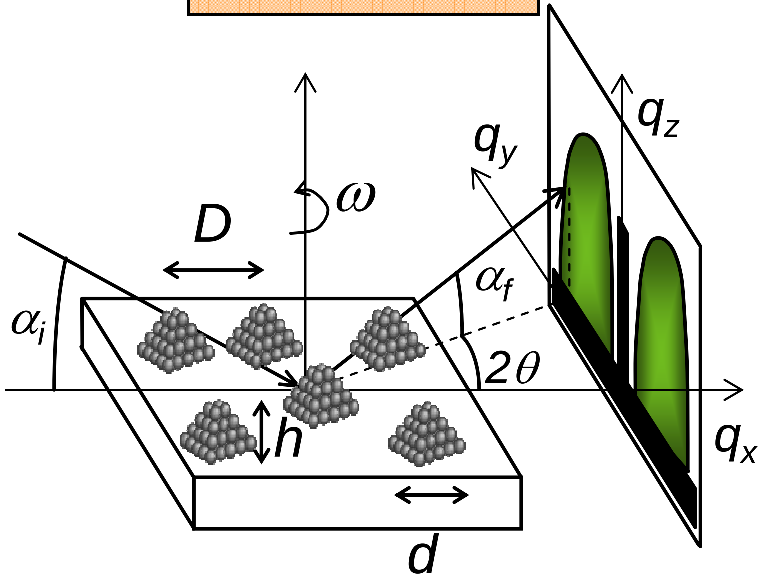

2D image around direct beam:
Fourier transform of objects

Morphology

- Shape
- Sizes
- Size distributions
- Particle-particle pair correlation function

Standard 3D growth (Volmer-Weber)

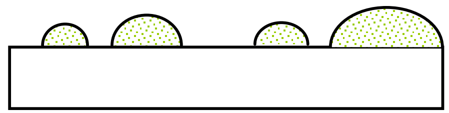

Example : **20 Å Ag/MgO(001) 500K**

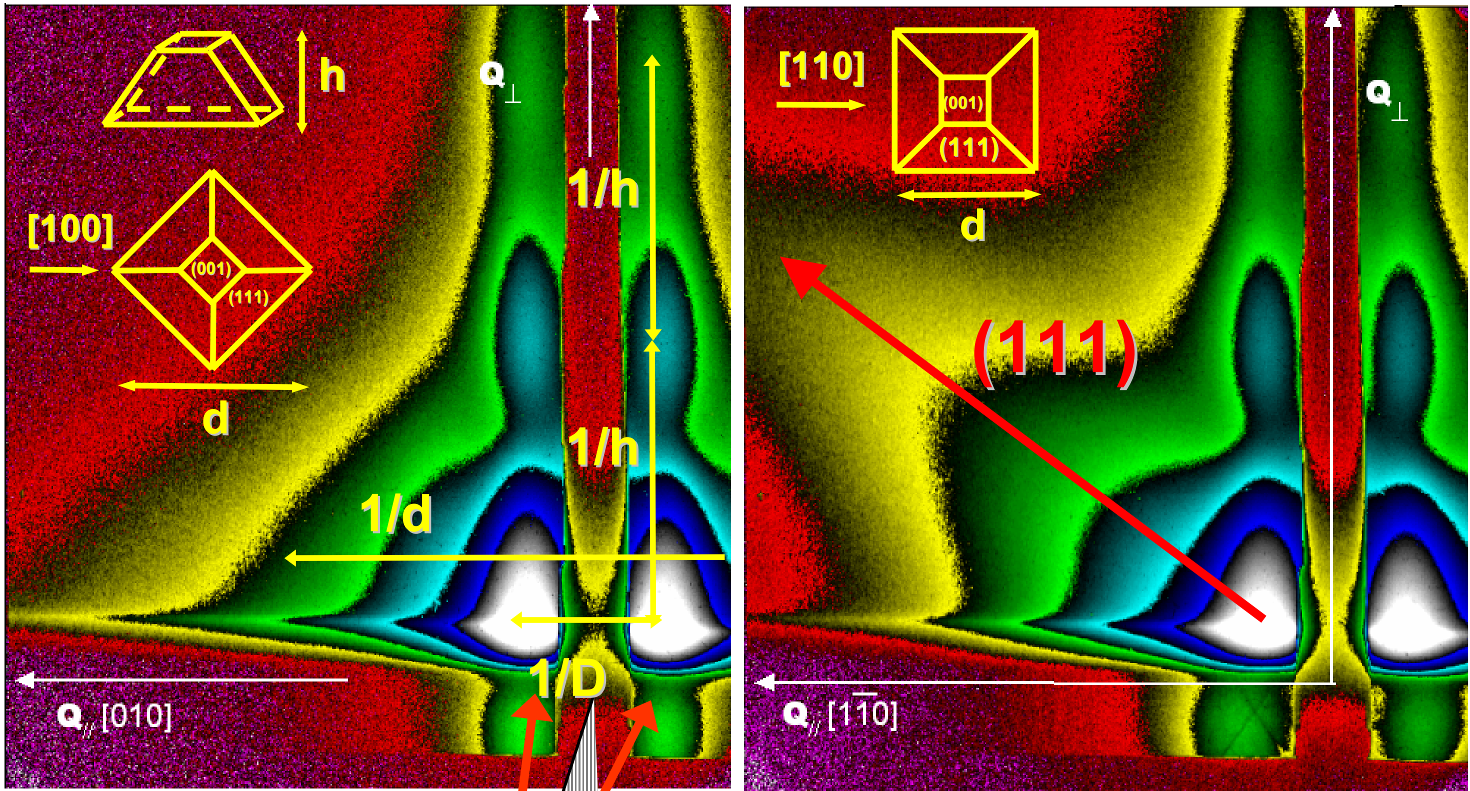

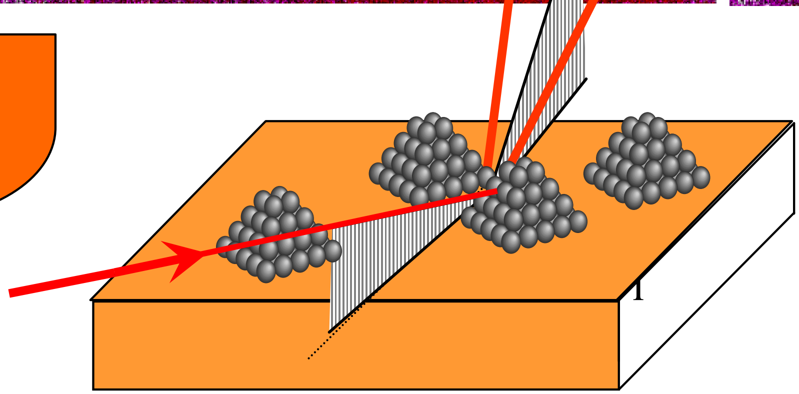

Anisotropic islands: truncated square pyramids with (111) facets

Off-specular reflectivity:

Probed length scales?

La géométrie de diffusion : GISAXS et réflectivité

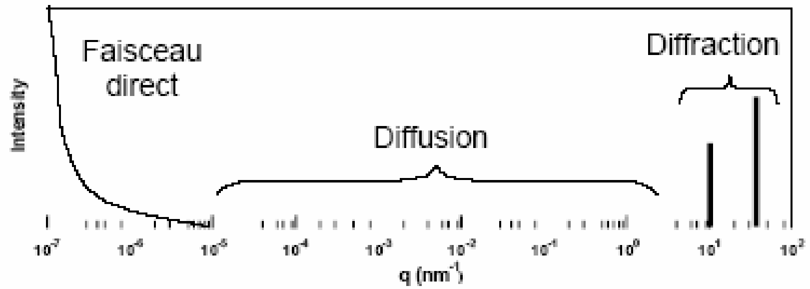

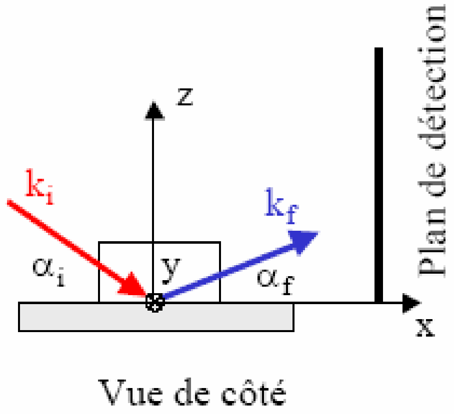

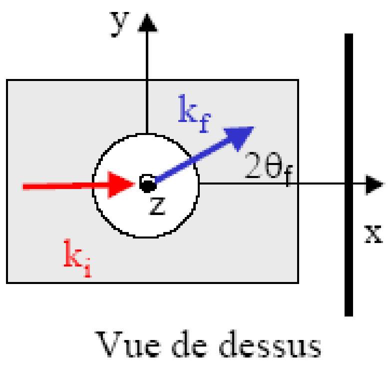

Le GISAXS ou comment mesurer des distances de l'ordre du nanomètre avec des rayons X ?

Le transfert de moment : grandeur pertinente ?

$$\vec{q} = \vec{k}_f - \vec{k}_i$$

$$q_x = \frac{2\pi}{\lambda}\left[\cos\alpha_f \cos 2\theta_f - \cos\alpha_i\right]$$

$$q_y = \frac{2\pi}{\lambda}\left[\cos\alpha_f \sin 2\theta_f\right]$$

$$q_z = \frac{2\pi}{\lambda}\left[\sin\alpha_f + \sin\alpha_i\right]$$

Réflectivité X

$\alpha_i = \alpha_f,\ 2\theta_f = 0$

GISAXS

λ=1Å - E=12keV

$\alpha_i = \alpha_f/2 = 0.2°$

$2\theta_f = 1°$

q_x= -0.011 nm^{-1} $\Rightarrow$ d_x=580nm

q_y= 1.1 nm^{-1} $\Rightarrow$ $d_{y=}$=5.7nm

q_z= 0.66 nm^{-1} $\Rightarrow$ d_z=9.5nm

Small angles of incidence and exit: plane of incidence

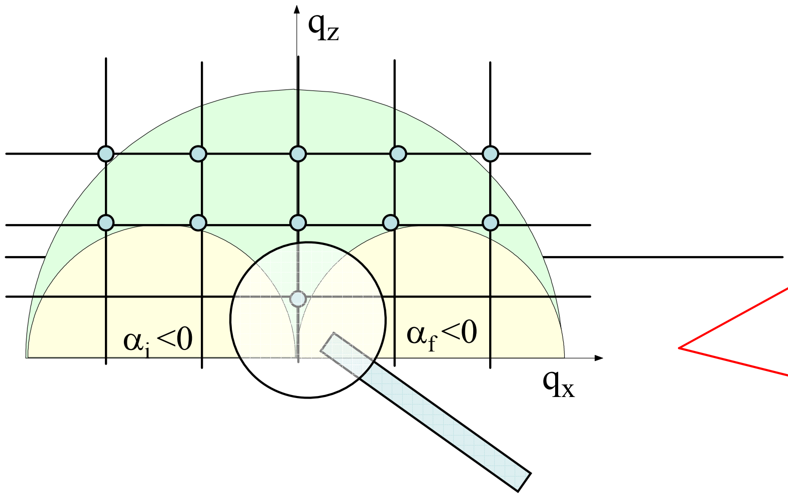

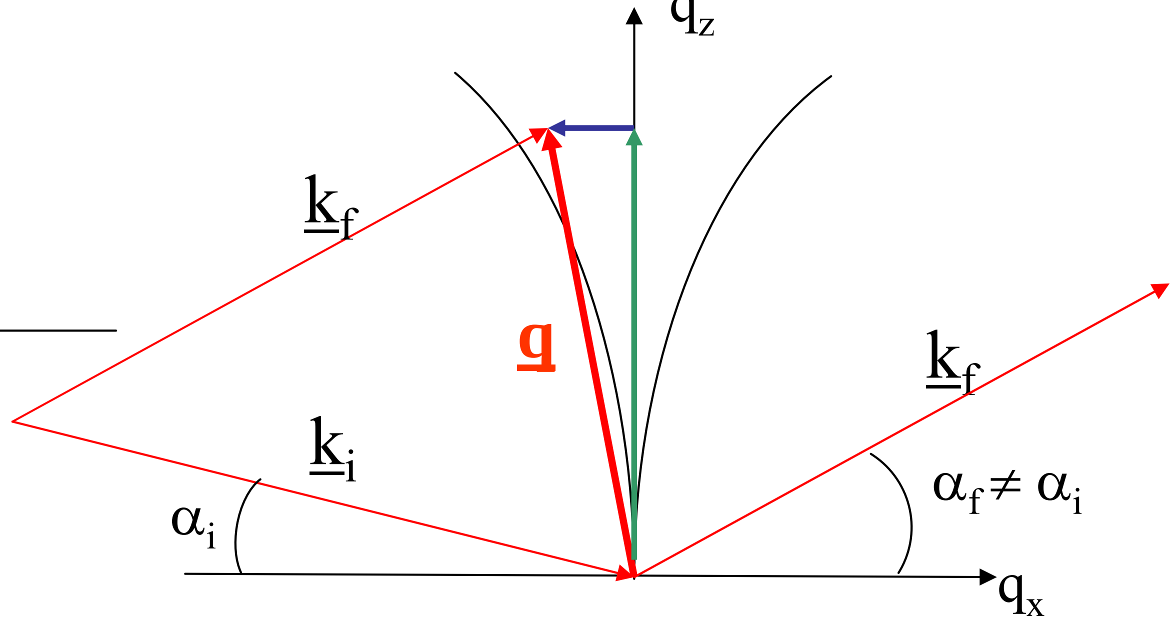

$\underline{\mathbf{q}} = \underline{\mathbf{k}_f} - \underline{\mathbf{k}_i}$

Specular direction: $\alpha_f = \alpha_i$: $q_z = 4\pi/\lambda(\sin \alpha_i) = 2\pi/d$

$q_x = (2\pi/\lambda)(\cos \alpha_f - \cos \alpha_i)$ $q_z = (2\pi/\lambda)(\sin \alpha_f + \sin \alpha_i)$

Lengthscales d: lateral and vertical

$\lambda = 1.54$Å $\alpha_i = 0.5^o$ $\mathbf{d_x = 2\pi/ q_{x,\,max} \leq \lambda / (\cos \alpha_f - 1) \approx 10\,000}$ **Å**

$\mathbf{d_z = 2\pi/ q_{z,} \approx 20}$ **Å for** $\boldsymbol{\alpha_f = \alpha_i}$

GISXAS or how to measure **nm** lateral lengthscales

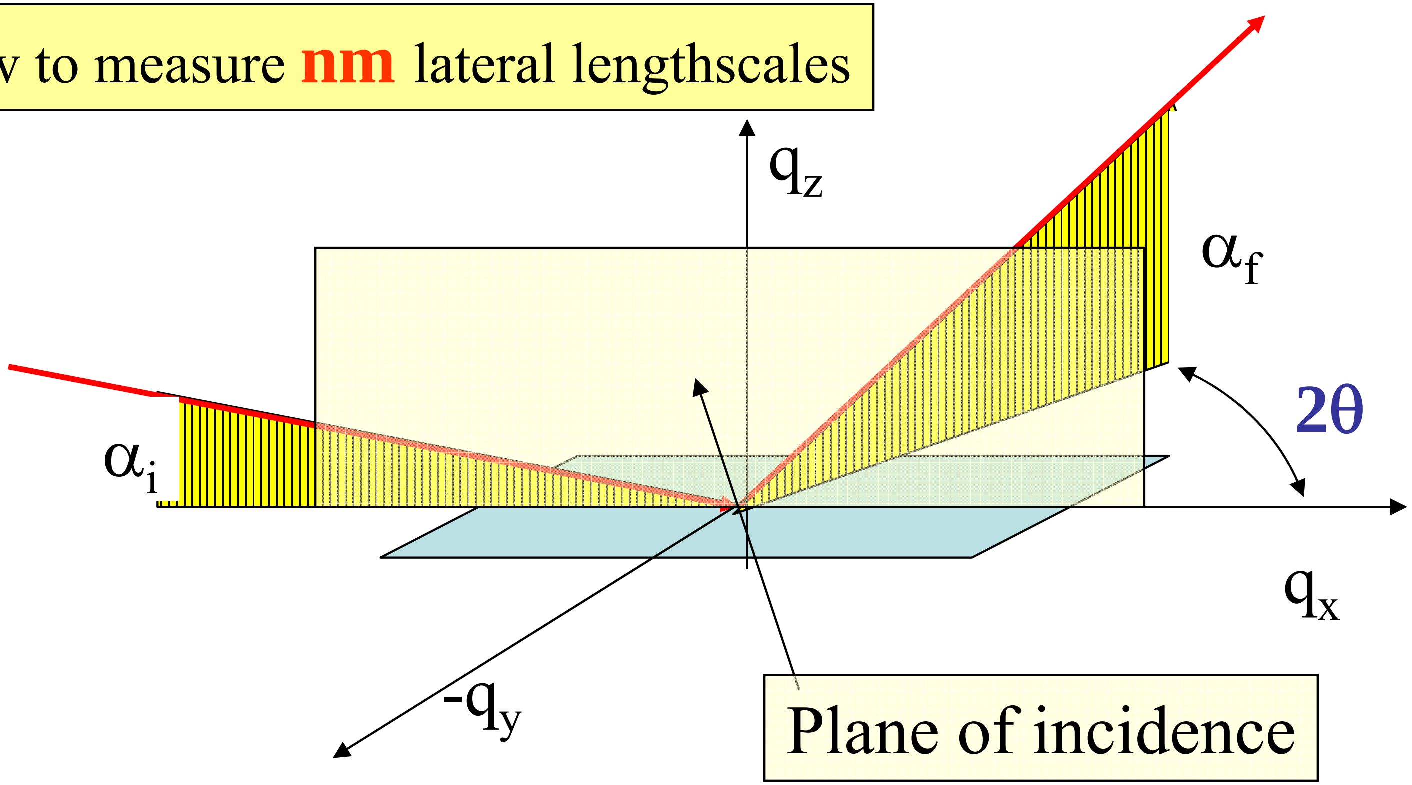

$\underline{Q} = \underline{k_f} - \underline{k_i}$

$$q_x = (2\pi/\lambda)(\cos\alpha_f \cos 2\theta - \cos\alpha_i)$$

$$q_y = (2\pi/\lambda)(\cos\alpha_f \sin 2\theta)$$

$$q_z = (2\pi/\lambda)(\sin\alpha_f + \sin\alpha_i)$$

Lengthscales d: lateral

$\lambda = 1.54$Å $2\theta = 2^o$ $\alpha_f = 0.5^o$ **$d_y = 2\pi / q_y \leq \lambda / (\cos\alpha_f \sin 2\theta) \approx 44$ Å !!!**

Out-of plane scattering suited for nanostructure investigations

"No" limitation in 2θ : d from 100nm to 0.1nm

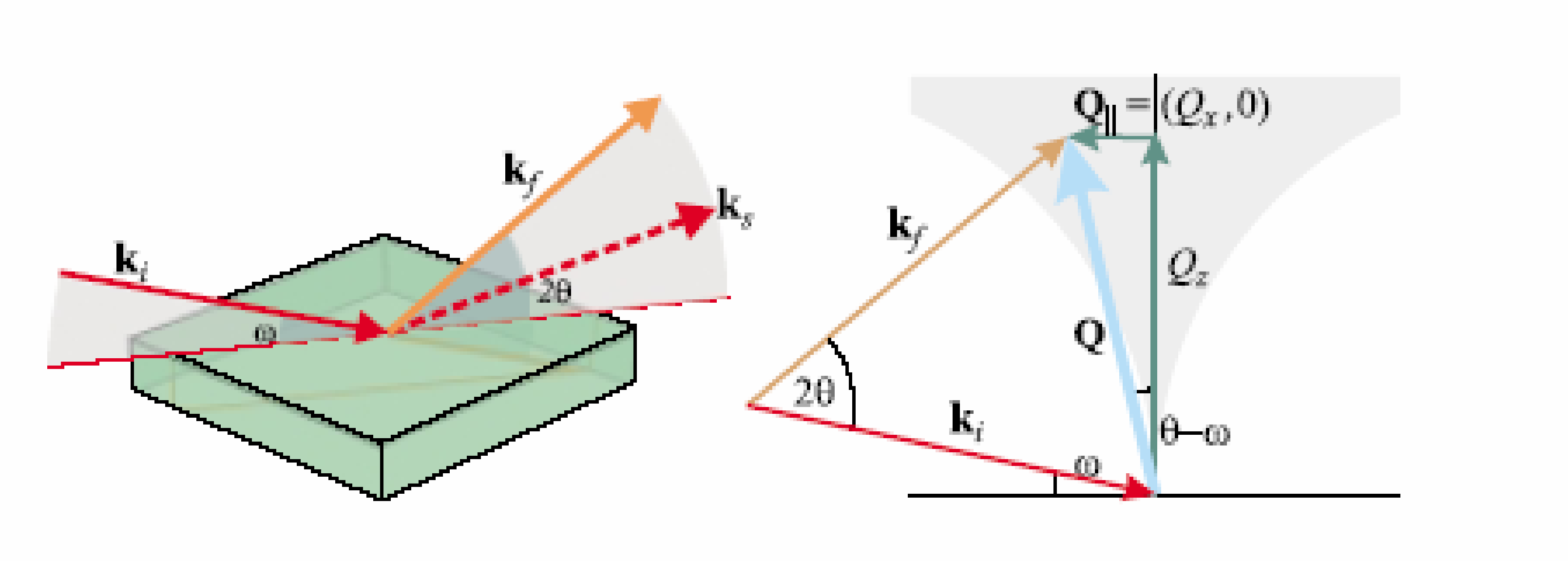

$$Q_x = 2k\,\sin\theta\,\sin(\omega-\theta)$$
$$Q_z = 2k\,\sin\theta\,\cos(\omega-\theta)$$

$$|Q_x| \simeq \frac{1}{2k}\,Q_z^2,$$

As the scattered intensity usually drops quite fast as a function of Q_z, the range of lateral momentum transfer is limited. Typically achievable scattering angles are in the order of $2\theta = 3°$.[3] This puts an upper limit to the the accessible range of lateral structure dimension:

$$d_{\|} > \frac{2\pi}{|Q_{x,\max}|} \simeq \frac{\pi}{k\,\sin^2\theta}.$$

Using $2\theta = 3°$ and $k \simeq 4\,\text{Å}^{-1}$ (for copper radiation), we obtain $|Q_{x,\max}| \simeq 0.005\,\text{Å}^{-1}$, i.e., XRR is suitable only for the investigation of *lateral* structures with dimensions $d >$ 1000 Å(this value depends, of course, on the wavelength and on how rapidly the intensity drops with Q_z, which depends, e.g., very sensitively on surface and interface roughnesses).

usually named α_i, the exit angle is α_f correspondingly. The reciprocal space coordi
are given by the relations

$$Q_x = k\,(\cos\alpha_i - \cos\alpha_f\,\cos 2\theta)$$
$$Q_y = k\,\cos\alpha_f\,\sin 2\theta$$
$$Q_z = k\,(\sin\alpha_i + \sin\alpha_f)\,.$$

Q_z is equivalent to the corresponding expression in XRR, Eq. (2.2), but now Q_x is vir
zero, and Q_y is finite instead. Hence for the determination of parameters of the ve
sample structure, XRR and GISAXS are equivalent. However, as is obvious from Fi
no restriction of Q_y due to the Laue zones exists, and consequently GISAXS is the m
of choice for the investigation of small lateral structures ($d_{\|} < 1000$ Å). As a "priz
the enlarged range of lateral momentum transfer, the lateral resolution is much sr
than for XRR:

$$|\Delta Q_y| = \left|\frac{\partial Q_y}{\partial\theta}\right|\Delta\theta + \left|\frac{\partial Q_y}{\partial\alpha_f}\right|\Delta\alpha_f =$$
$$= 2k\,\cos\alpha_f\,\cos 2\theta\,\Delta\theta + k\,\sin\alpha_f\,\sin 2\theta\Delta\alpha_f$$
$$\simeq 2k\,(\Delta\theta\ + \alpha_f\,\theta\,\Delta\alpha_f)$$
$$|\Delta Q_y| \simeq 1.5\cdot 10^{-3}\,\text{Å}^{-1}.$$

Quantitative analysis of GISAXS

$$I(q_{//},q_{\perp}) \approx \left\langle |F|^2 \right\rangle \times S(q_{//})$$

*Is*GISAXS program :
http://www.esrf.fr/computing/scientific/joint_projects/IsGISAXS/
R. Lazzari, J. Appl. Cryst. 35, 406 (2002)
F. Leroy, R. Lazzari and G. Renaud, Acta. Cryst. A 60, 565, (2004)

Form factor :
a kind of shape FT
with refraction effects

×

Interference function:
FT of pair
correlation function

$$S(q_{//}) = 1 + \rho_S \int \left(g(r) - 1\right) e^{-iq_{//} r} d^2 r$$

$$F_{DWBA}(q_{//}, k_i, k_f)$$

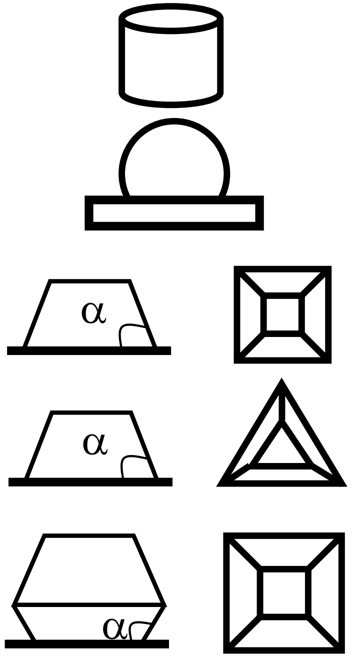

- Cylinder
- Troncated sphere
- Pyramid
- Tetraedron
- Cubooctaedron

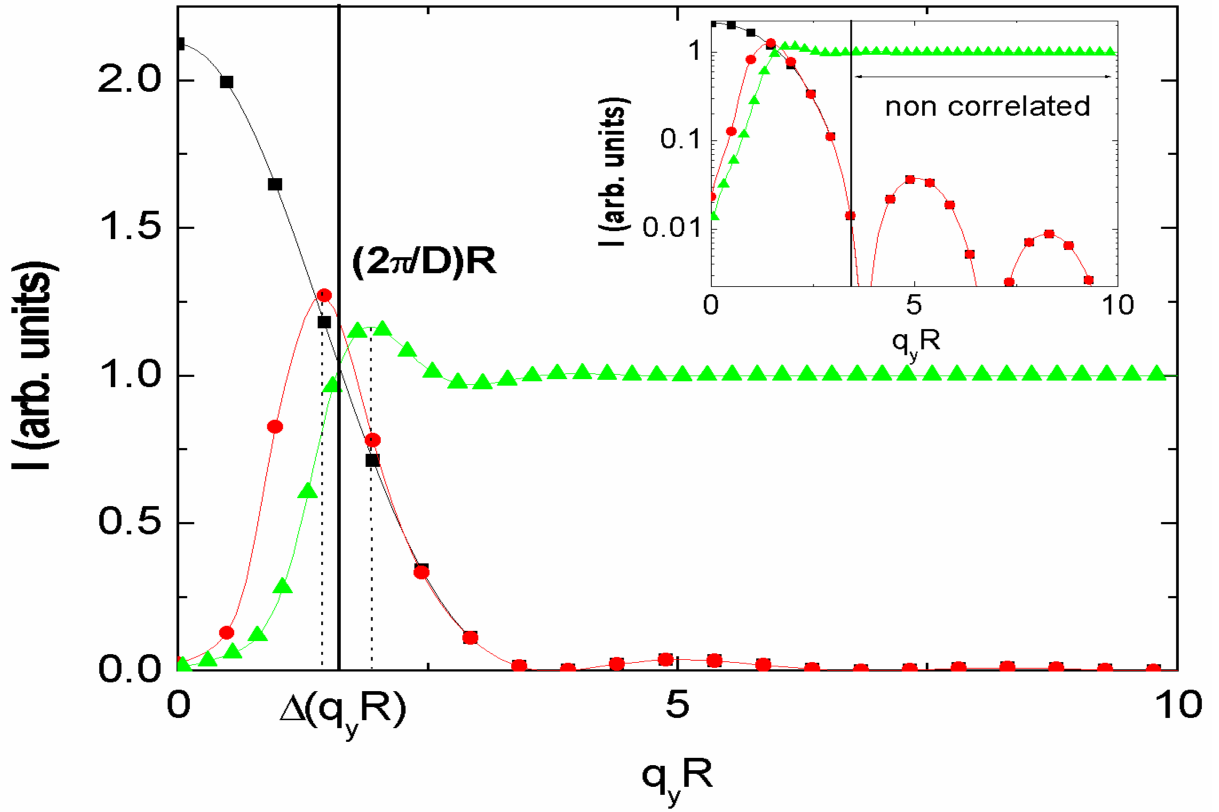

Analyse quantitative du signal GISAXS

*Is*GISAXS program :
http://www.esrf.fr/computing/scientific/joint_projects/IsGISAXS/
R. Lazzari, J. Appl. Cryst. 35, 406 (2002)
F. Leroy, R. Lazzari and G. Renaud,
Acta. Cryst. A 60, 565, (2004)

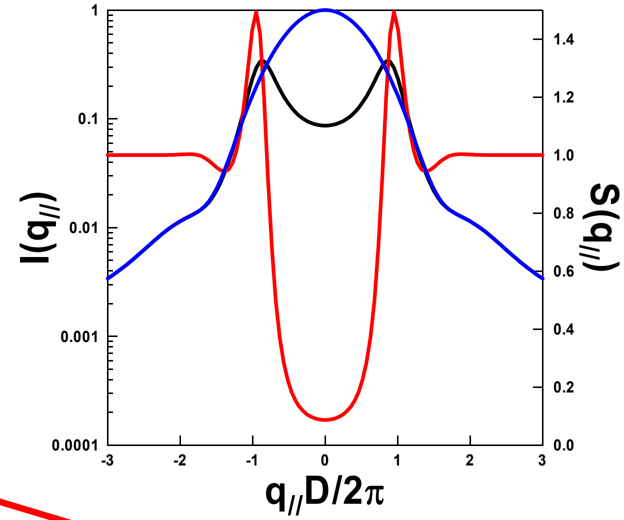

$$I(\vec{q}) = \left\langle \left| F \right|^2 \right\rangle S(q_{//})$$

Facteur de forme

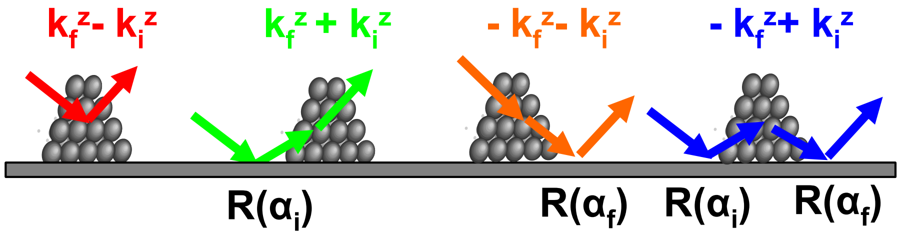

Forme, taille et orientation

• cylindre

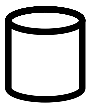

• sphère tronquée

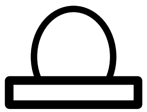

• pyramide

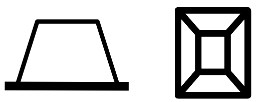

+ distributions

Fonction d'interférence

$$S(q_{//}) = \text{TF}\left\{\text{Fonction de corrélation de paires}\right\}$$

Arrangement spatial

• réseau

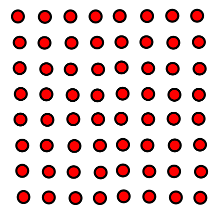

• modèle de désordre (paracristal...)

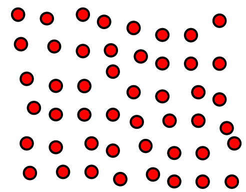

distance moyenne + distribution de distances

Growth of Au on TiO_2(110)

12 Å flashed annealed @ 800K

STM pictures
Goodman et al.

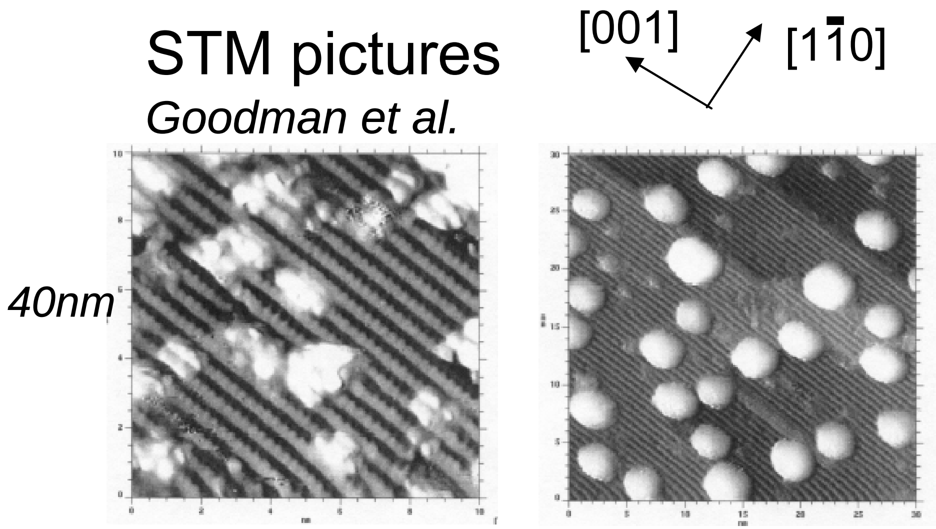

FITS:
Truncated spheres

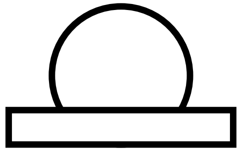

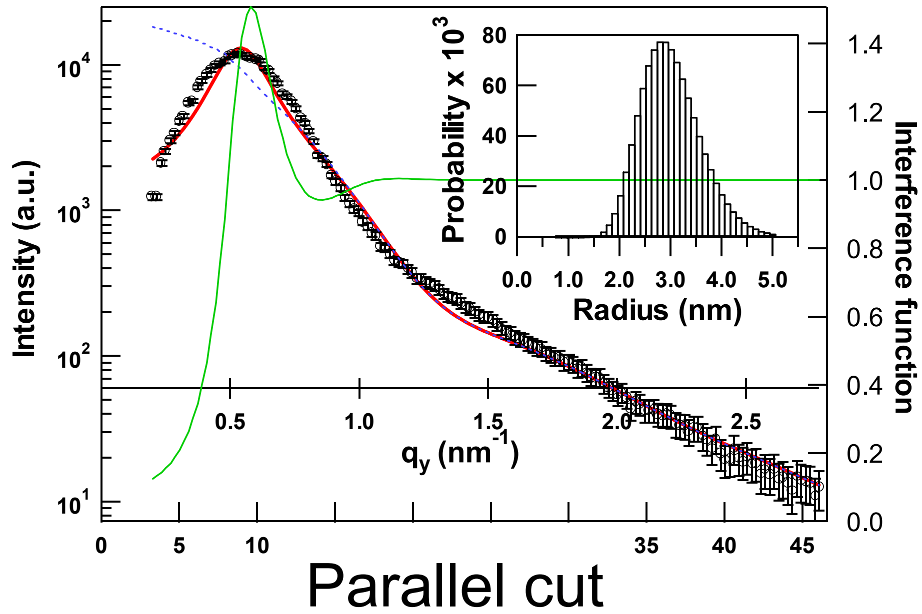

R = 2.9 nm s_R(log normal) = 1.2
H= 4.9 nm s_H(gaussian) = 0.1
r=9.1 10^{11} part/$cm^{2;}$ q_c=132°

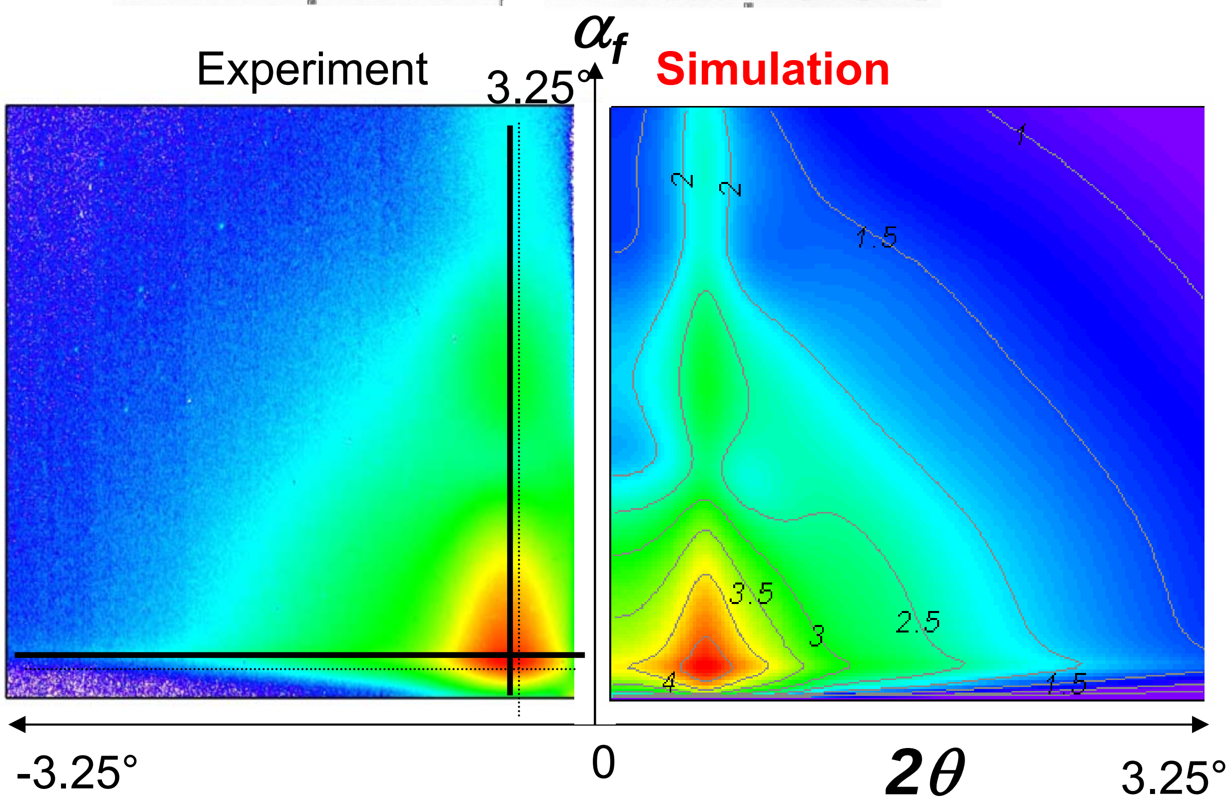

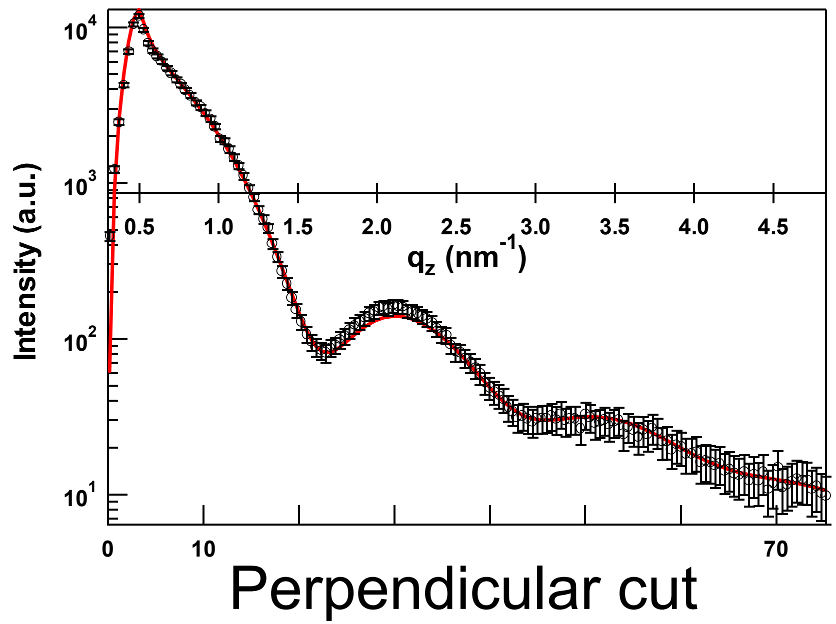

Equilibrium shape of particles. Ex: 1.5nm Pd/MgO @ 650 K

Fit with truncated octaedron

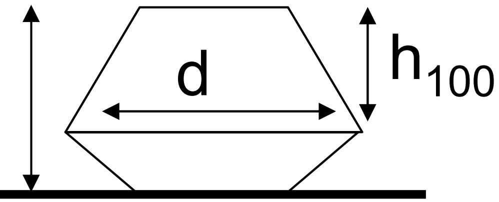

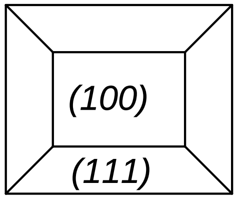

D=22±0.2nm
d=11.4 ±0.4nm - σ_{FWHM}=6nm
h=6.2 ±0.4nm - σ_{FWHM}=0.8nm
$h_{(001)}$/d=0.46
h/d=0.62 ±0.2

H/d = cte = 0.62
➔
Equilibrium island shape

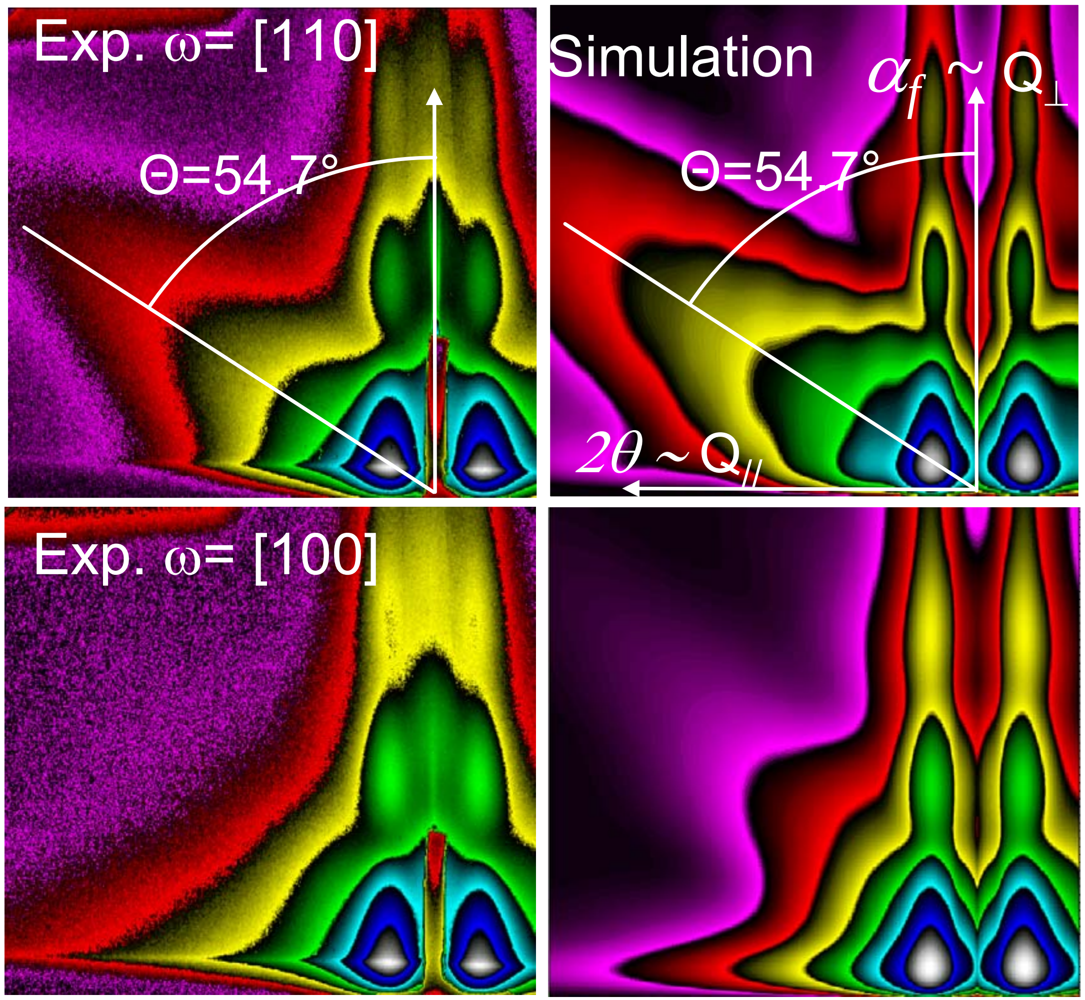

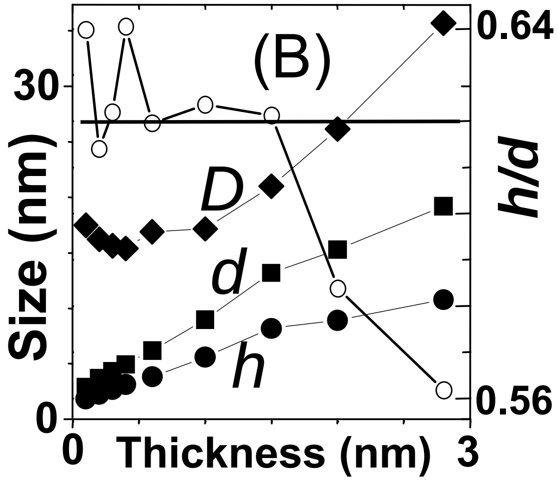

Wulff's construction

Adhesion energy from GISAXS: β=1.12 J/m²

To be compared with TEM : β = 0.95 J/m²

GISAXS →
Equilibrium shape, *in situ*,
non destructively during growth

G. Renaud, et al., Science 300, 1416 (2003).
C. Revenant, F. Lazzari, F. Leroy, G. Renaud, C.R. Henry, PRB 69 (2004)

Self-organized growth : systems

3 main types of surface structuration

Surface reconstruction	Vicinal surface	Dislocation Network
Co dots on Au(111)	Co wires on Pt(997)	Fe islands on a bilayer of Cu/Pt(111)
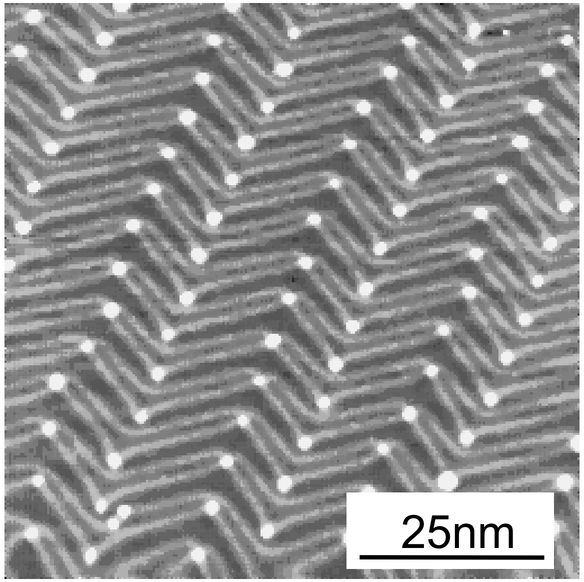	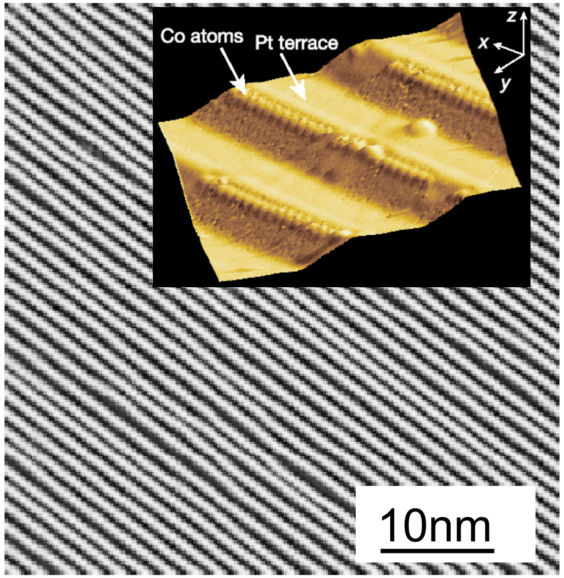	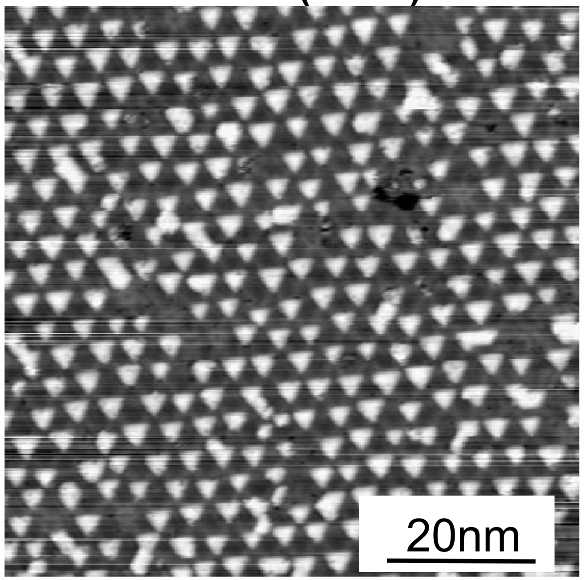
B. Voigtländer et al.	P. Gambardella et al.	H. Brune et al.
Phys. Rev. B **44** (1991) 10354	Nature **416** (2002) 301	Nature **394** (1998) 451

- **Self-organized growth of cobalt islands on a**

–Au(677) kinked surface

The kinked Au(677) surface

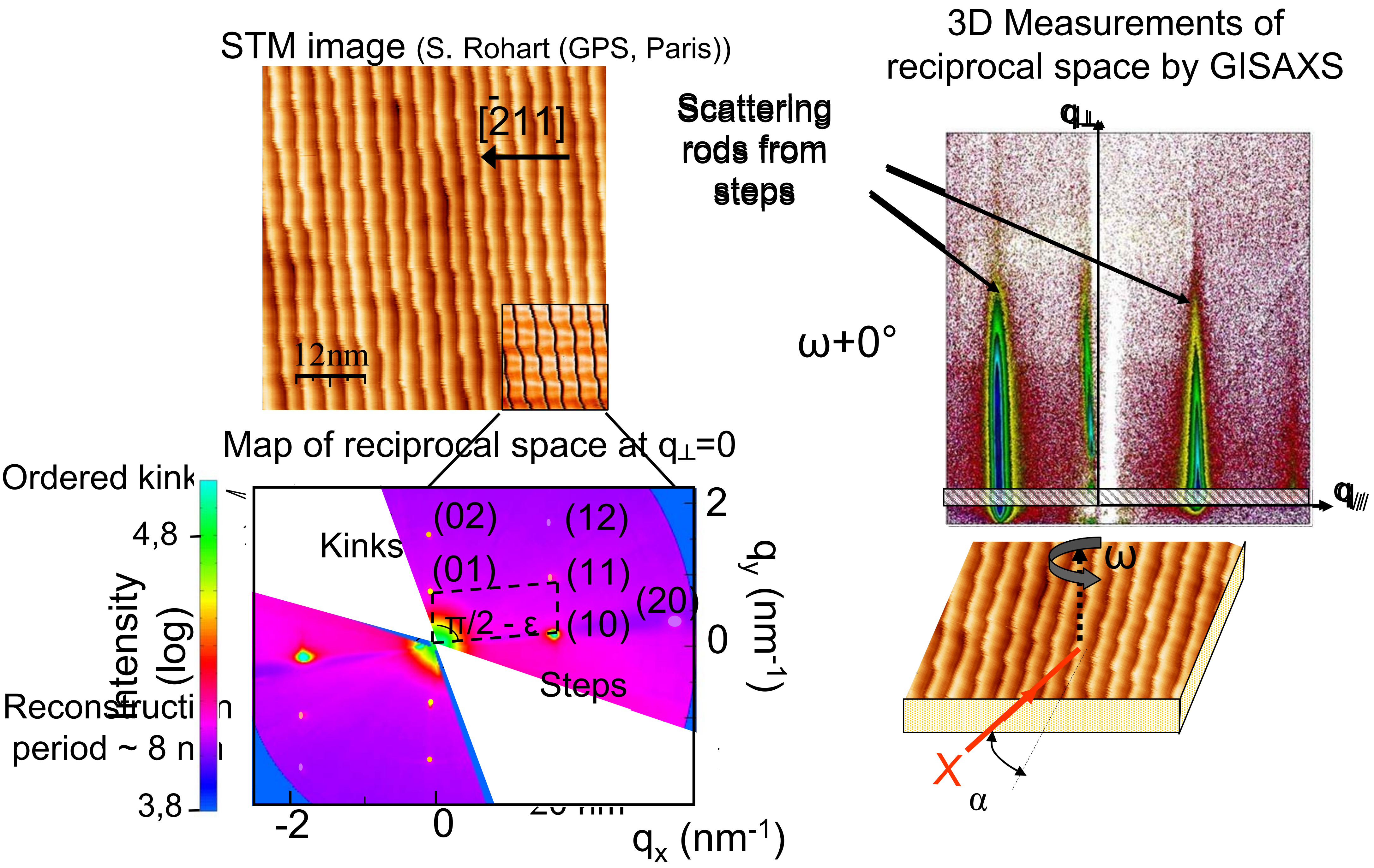

Modelisation of a kinked Au(677) surface

Principle : Paracrystal

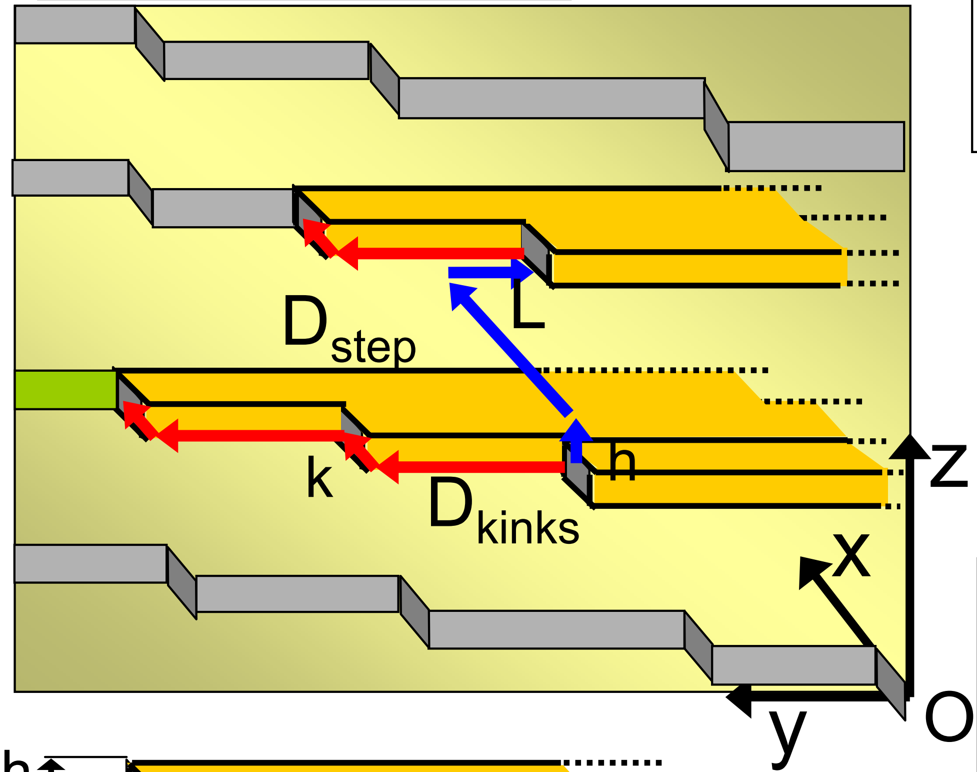

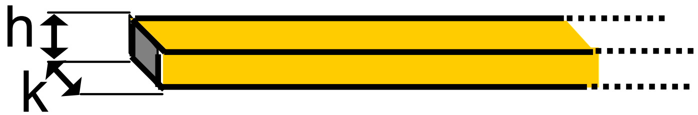

Elementary object

$$I(\vec{q}) = \left[\underbrace{\frac{4 \sin\left(\frac{q_z h}{2}\right) \sin\left(\frac{q_x k}{2}\right)}{q_x q_y q_z}}_{\text{Shape and size of kinks}} \right]^2$$

Steps

$D_{step} = 3.42 \pm 0.23$ nm

Kinks position

$D_{kink} = 8.04 \pm 0.62$ nm

$L = 0 \pm 0.3$ nm

Determined by the reconstruction

Kinks size

$k = 0.7 \pm 0.35$ nm

Monoatomic kinks

Packed

by 3±1.5

GISAXS data and fits

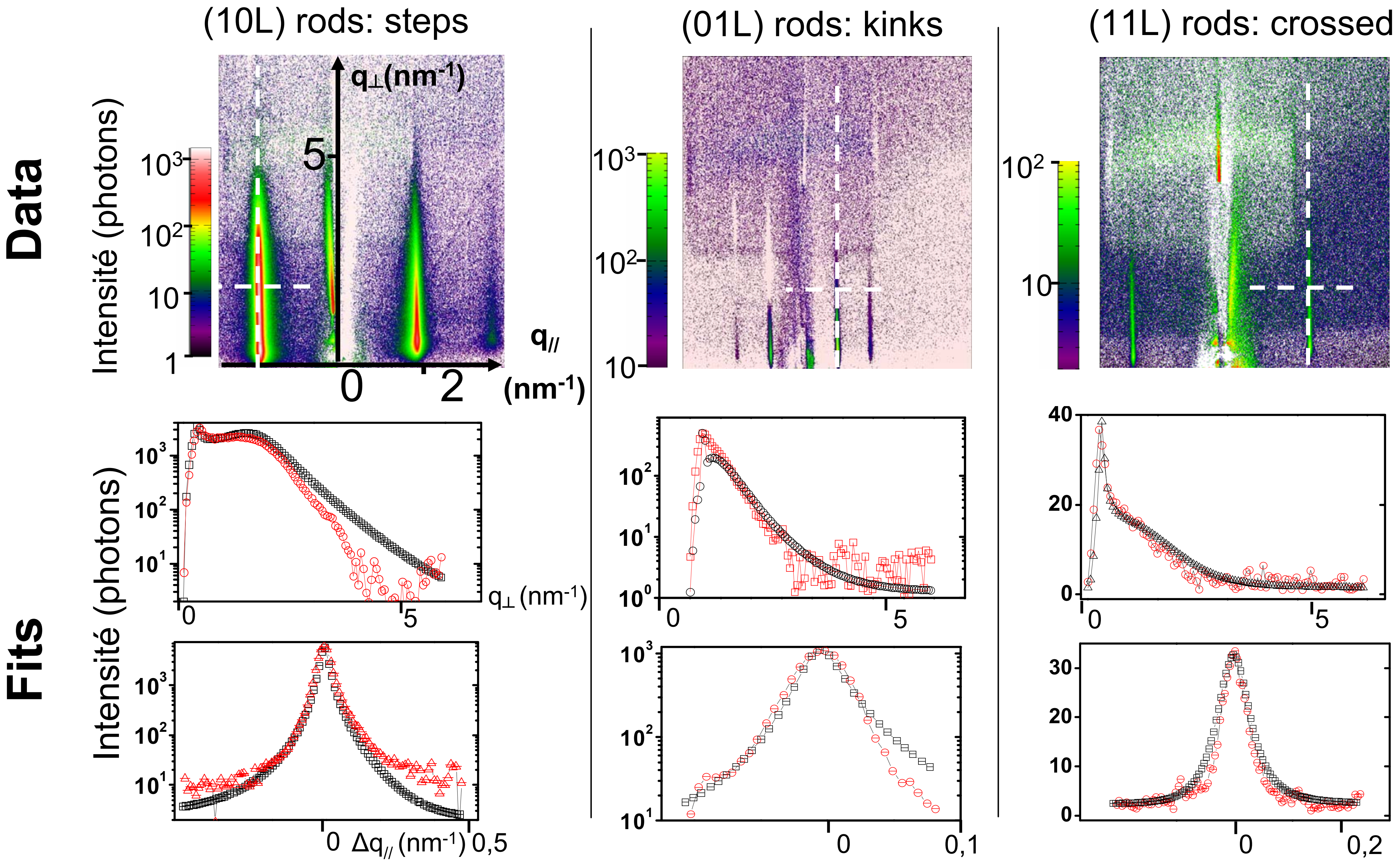

Co growth at room temperature

STM image

S. Rohart (Au(788) surface)

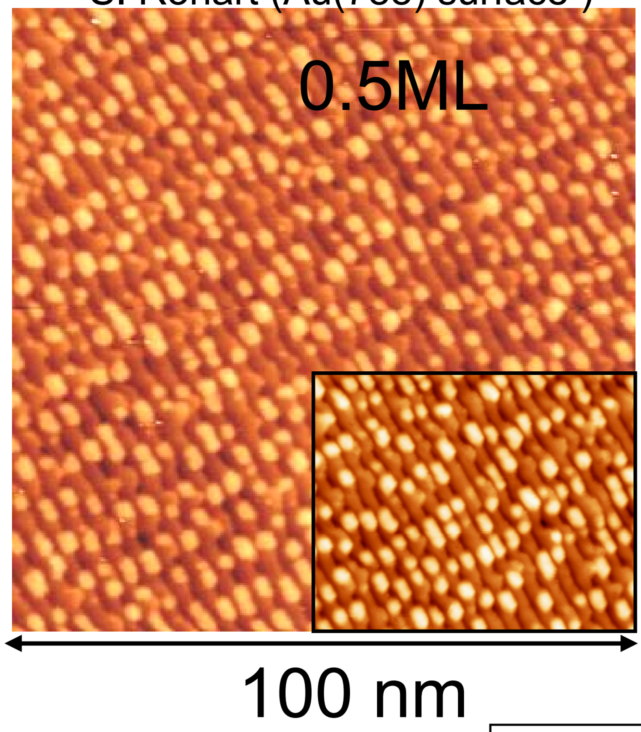

Model

Shape and size

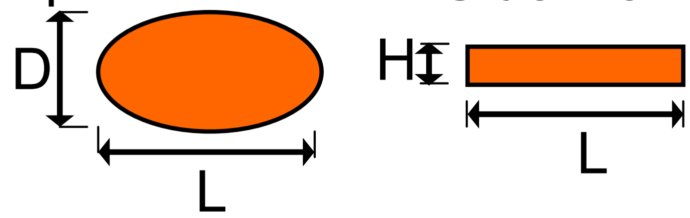

Position

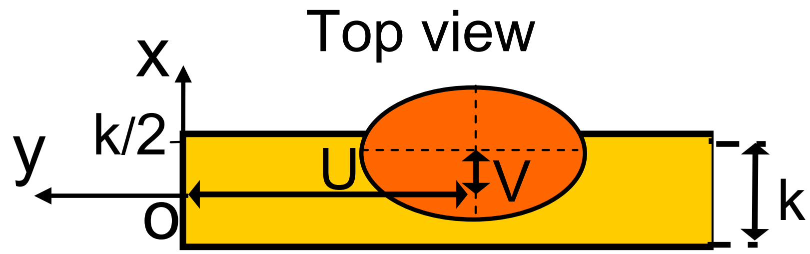

Island position
- in between kinks
- at the step edge

Shape and size
- anisotropic growth
- bilayer islands

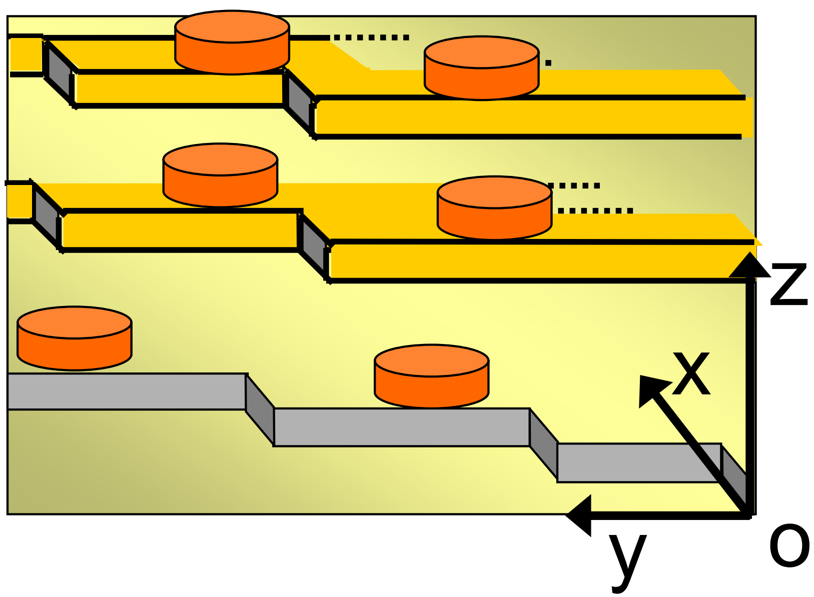

Self-organized growth : Systems

3 main surface structuration

Surface reconstruction	Vicinal surface	Dislocation Network

Co dots on Au(111)

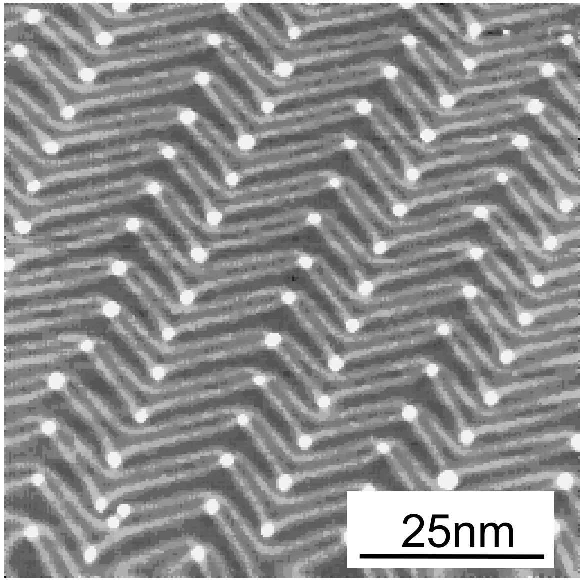

B. Voigtländer et al.

Phys. Rev. B **44** (1991) 10354

Co wires on Pt(997)

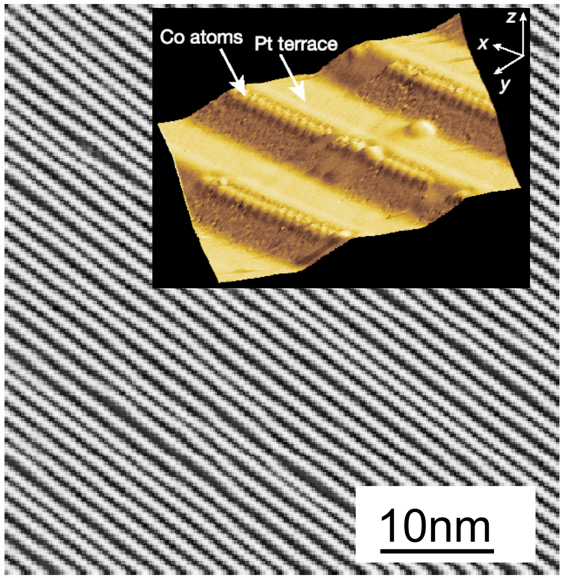

P. Gambardella et al.

Nature **416** (2002) 301

Fe islands on a bilayer of Cu/Pt(111)

Co dots on a dislocation network buried at the Ag/MgO(001) interface

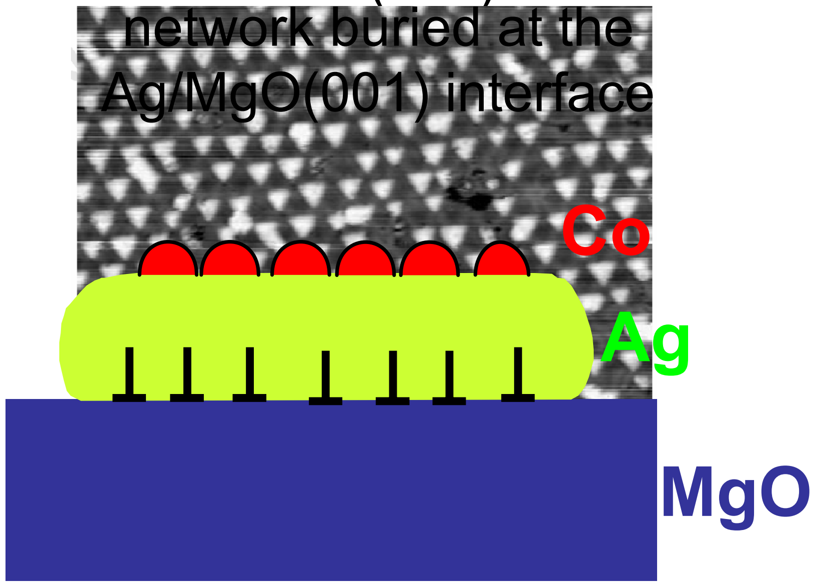

H. Brune et al.

Nature **394** (1998) 451

- **Self-organized growth of cobalt islands on a**
  - **dislocations network at the Ag/MgO(001) interface**

Ordering of nanostructures induced by a dislocation network : principle

- Misfit dislocation network

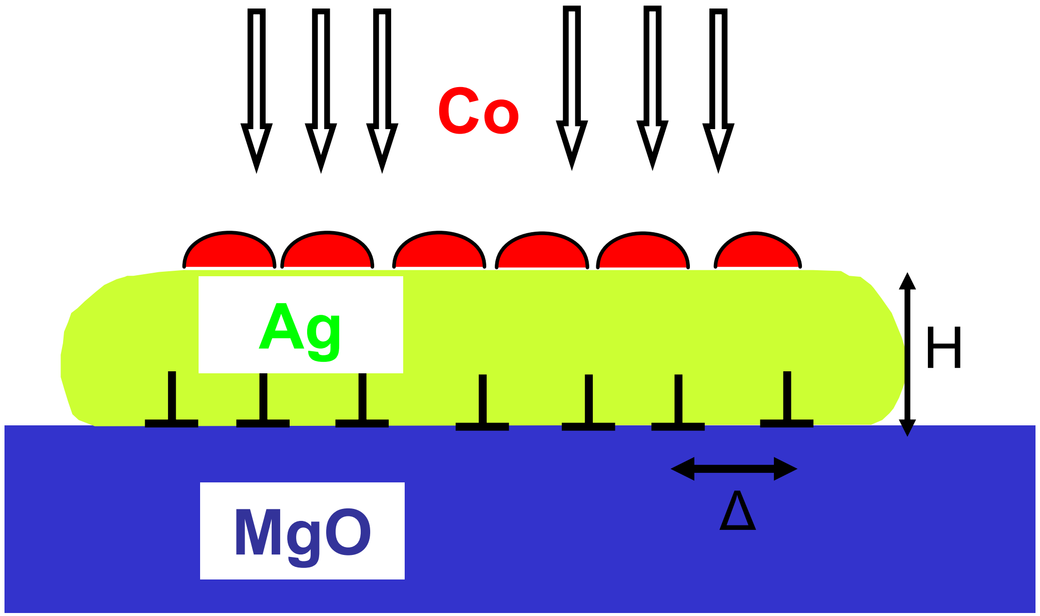

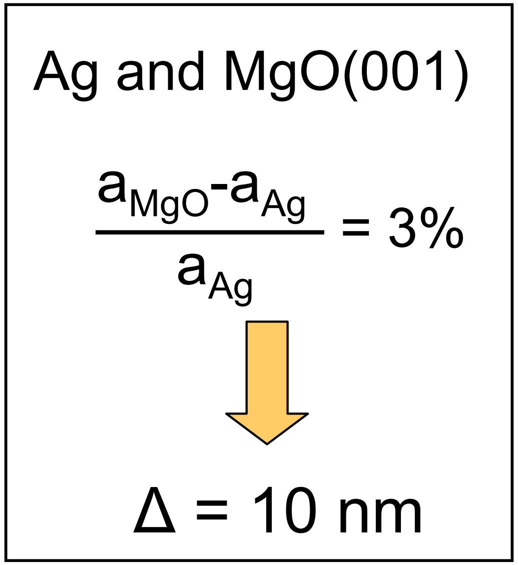

- Significant surface strain if : H<Δ

Ag/MgO(001) ultra-thin film: *in situ* GIXS, XRR and GISAXS

1. Growth of 100 nm Ag(001)/MgO

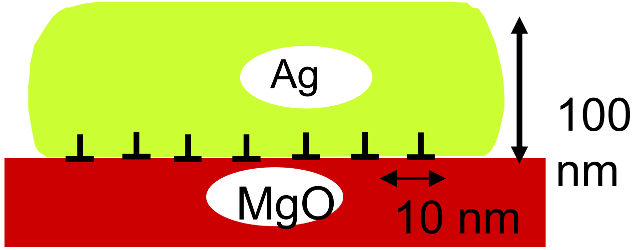

2. Annealing 900 K

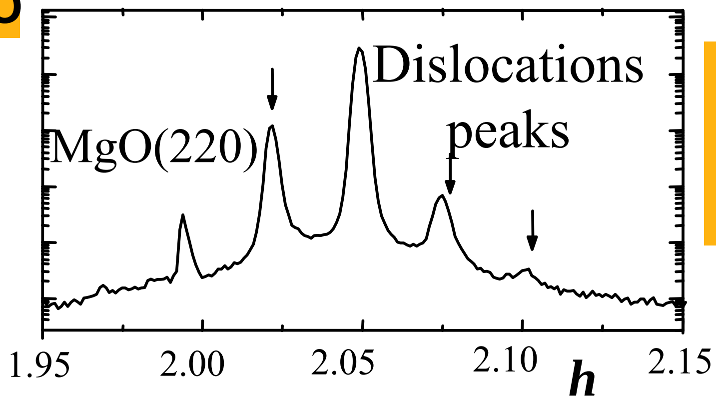

- ➔ **Ordered dislocation network**
- ➔ **Very low roughness**
- ➔ **Large terraces (100nm)**

3. Ion Beam thinning down to 5 nm while keeping large terraces and low roughness.

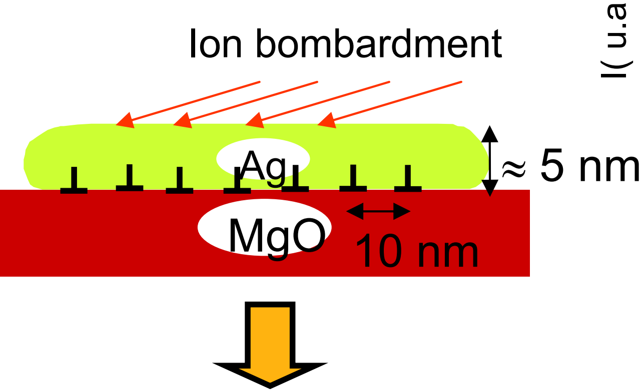

Monitored *in situ* by Anti-Bragg GIXS

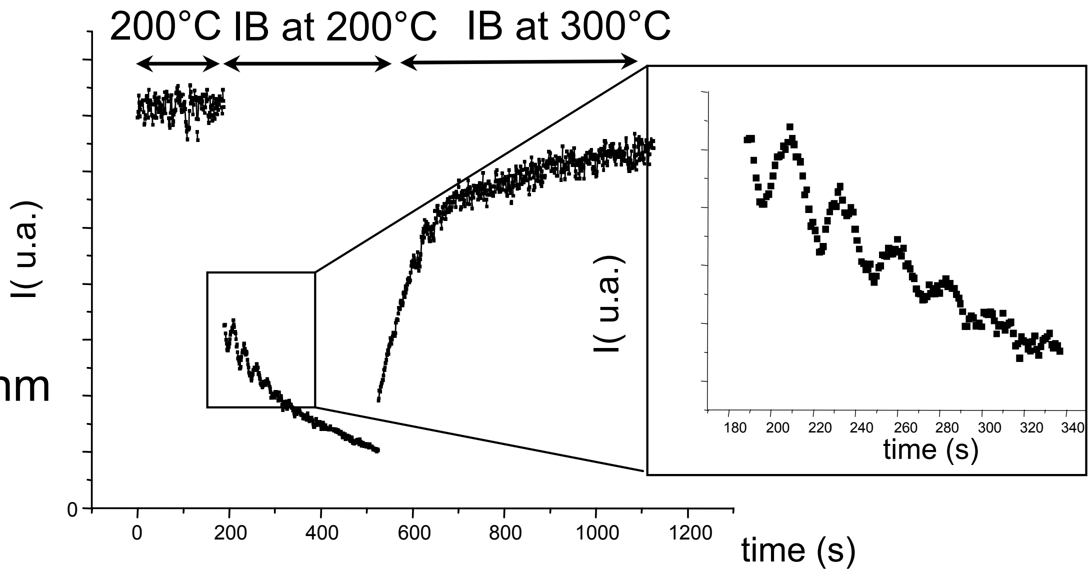

and reflectivity

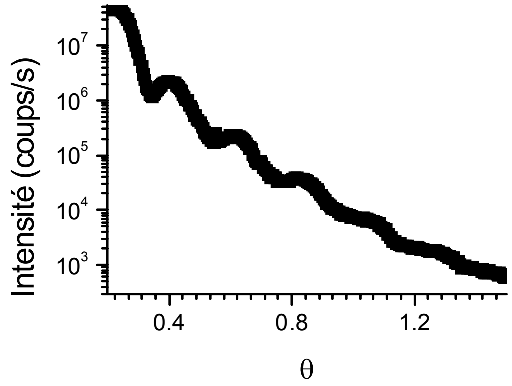

Ultra-thin (5nm) Ag film of homogeneous thickness, with an ordered array of dislocation

4. Co Deposition

- **Room temperature : trap energy >> thermal energy**
- **Deposition rate (0.05 Å/min): diffusion length of Co adatoms >>10 nm**

Self-organized growth of magnetic cobalt dots on an interfacial dislocation network : Co/Ag/MgO(100)

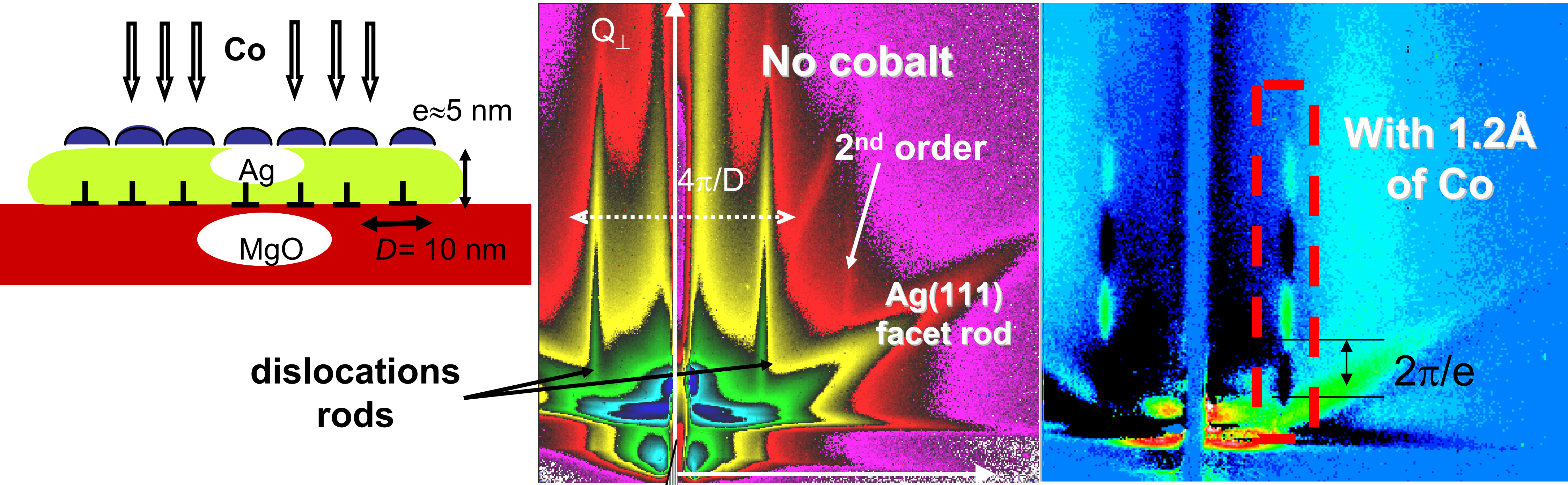

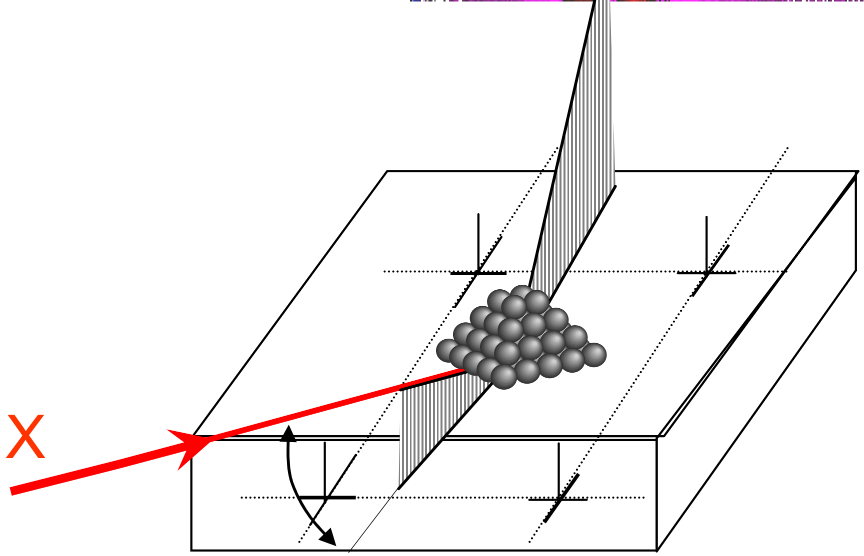

Interferences

↓

Co islands are ordered

Position of Co islands / dislocation cores

$$I(\vec{q}) - I_{disloc}(\vec{q}) = \cancel{I_{Co}(\vec{q})} + \underbrace{2\sqrt{I_{disloc}(\vec{q}) \times I_{Co}(\vec{q})} \times \cos \quad +}_{\text{interferences}}$$

After - before **negligible**

interferences

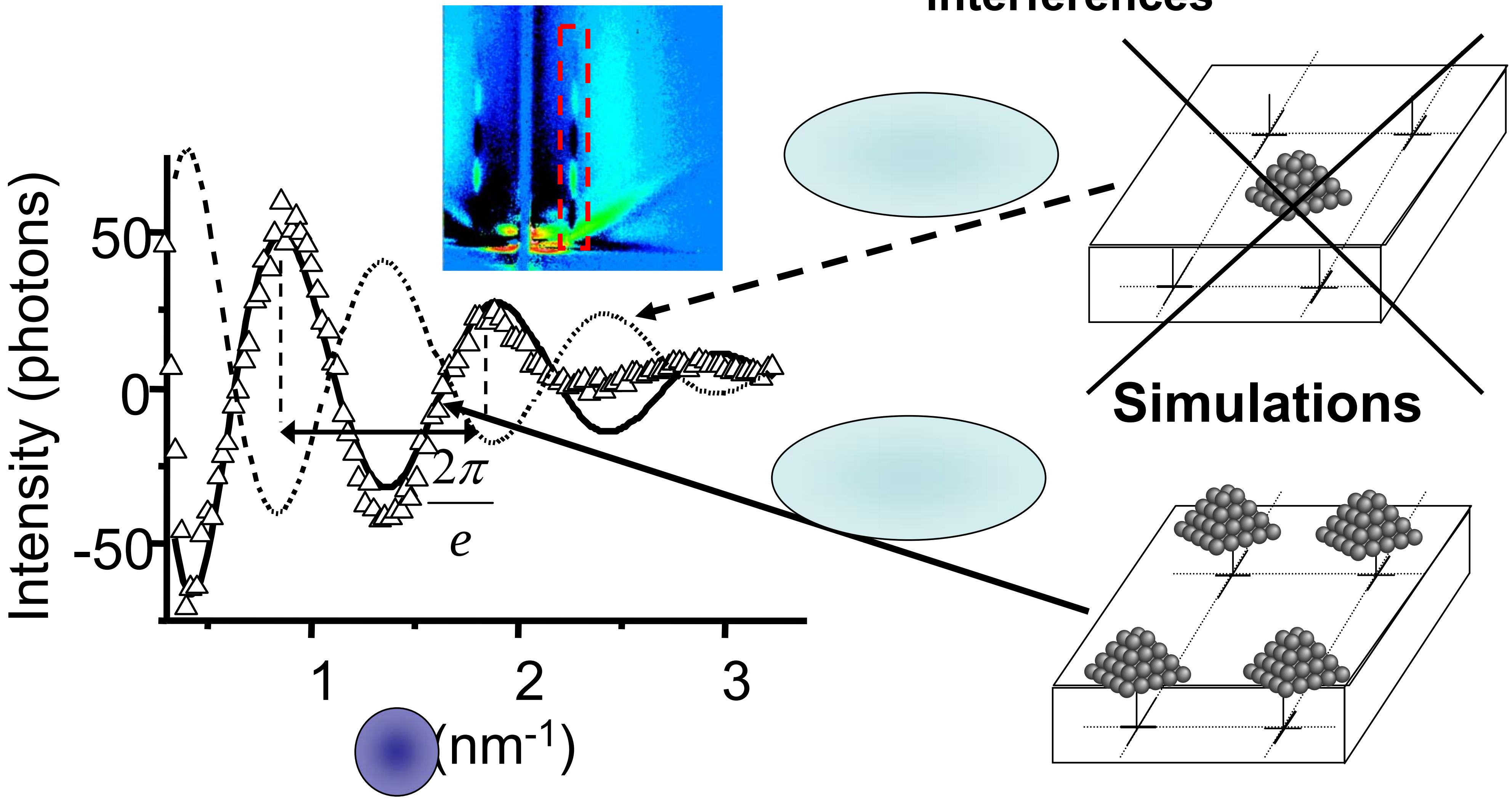

Size and shape evolution of Co dots upon deposition time

$$I_{\mathrm{int}\,erference}(\vec{q},time) = 2\sqrt{I_{disloc}(\vec{q}) \times \quad} \times \cos\left(\vec{q}_{//}\vec{d}_{//} + q_{\perp}H\right)$$

Interference(q⊥,time)

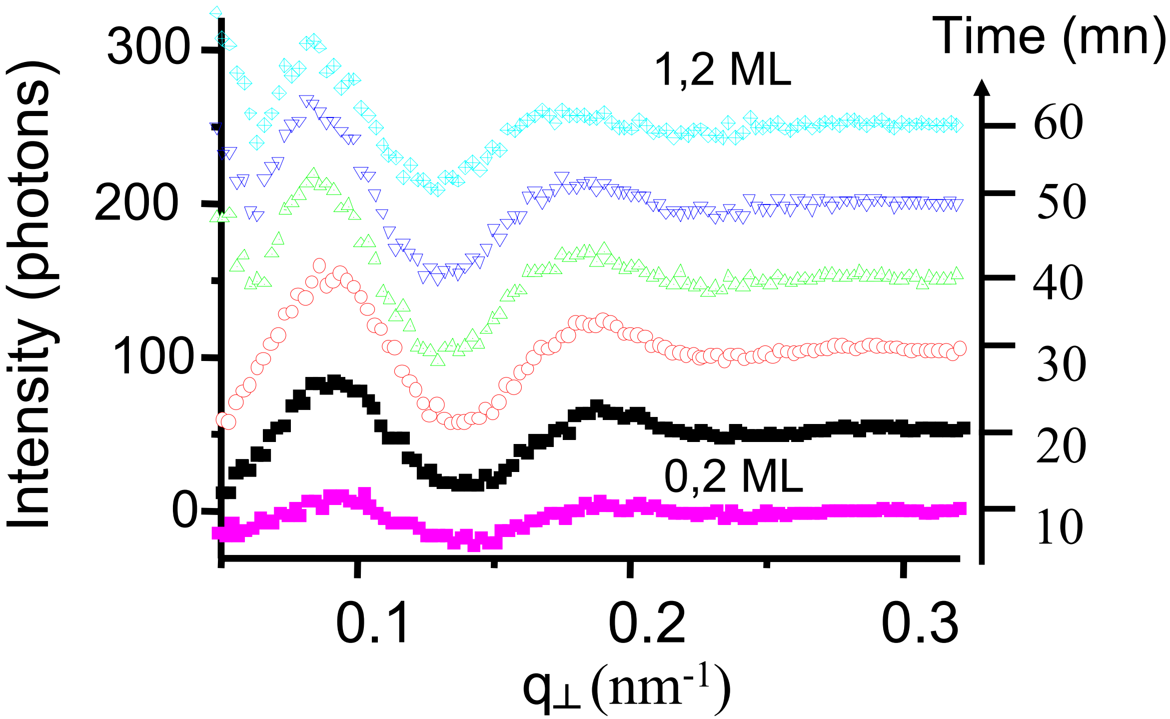

Fit : 2ML height islands

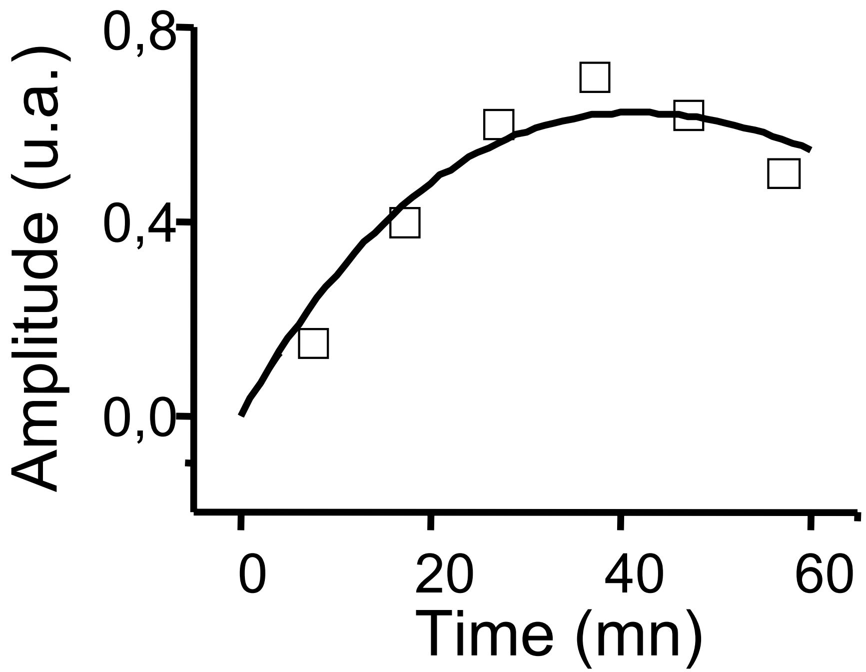

Conclusions

- GISAXS for the first time *in situ* during growth
- Combined with GIXS ➔ Atomic structure + Morphology
- Quantitative information on nano-particles shape/size/ordering
- Very sensitive to the ordering of nanostructures

- *In situ* surface X-ray diffraction and GISAXS combined

for determining conditions for ordering of Co islands on a Ag/MgO dislocation network

Determination of the nucleation site, size and shape of islands during organized growth of :

- Co on Au(111)
- Co on kinked Au(677) : in between kinks and at the step edges
- Co on Ag/MgO(001) : upon the dislocation core

Potential and future directions

•GISAXS extremely sensitive to the very premisses of organization

➔ used to monitor organized growth in real-time and quickly reach the right thermodynamical and kinetic conditions for the organization.

•*In situ* studies during

→ surface reactivity (e.g. catalytic reactions, annealings ...)
→ growth (during MBE, (MO)CVD, LPE);
→ use of gaseous, liquid or solid surfactants, at High p, T …

•Eventually probing the shape & 2D organization of biological molecules deposited on surfaces?

➔Conformation and function of selected bio-molecules?

La section efficace de diffusion en GISAXS et l'approximation de l'onde distordue DWBA

- « petits angles »
  - pas d'effets de polarisation
  - **diffusion par des écarts $\delta\rho$ à la densité électronique moyenne** = rugosité ou des variations de contraste électronique
- formulation cinématique de la diffusion (expression volumique)

$$\frac{d\sigma}{d\Omega} \propto \left| \int \delta\rho(\vec{r}) \exp(i\vec{q}.\vec{r}) \right|^2$$

- α_i et α_f proches de l'angle critique de réflexion totale externe = **effet de réfraction du faisceau ou pic de Yonéda**

- **DWBA = combinaison du traitement dynamique et cinématique de la diffusion**
  - réflexion-réfraction aux interfaces
  - traitement cinématique de la diffusion par $\delta\rho$, sans inclure les effets de diffusions multiples
  - approche similaire en réflexion neutronique
- section efficace calculée **au premier ordre en théorie des perturbations** par rapport au système idéal

Historique

1982 : DWBA et la diffraction en incidence rasante, G. Vineyard Phys. Rev. B26, 4146 (1982)
1988 : Théorie DWBA pour les surface rugueuses, S.K. Sinha et al., PRB 38, 2297 (1988)
1993 : DBWA et multicouches rugueuses corrélées, V. Holy et T. Baumbach, Phys. Rev. B 47, 15896 (1993), 49, 10668 (1994)
1994 : DWBA d'ordre 2 en réflectivité, D.K.G. De Boer, Phys. Rev. B 49, 5817 (1994), 51, 5297 (1995)
1995 : DWBA : rugosité et variation de contraste électronique, M. Rauscher, Phys. Rev. B 52, 16855 (1995)
1999 : GISAXS pour des îlots sur une surface, *J. Appl. Phys., 86, 673 (1999)*

Formulation de la DWBA

Point de départ : équation de Helmholtz pour l'onde électromagnétique

$$\left(\nabla^2 + k^2\right)|\psi\rangle = V(r)|\psi\rangle$$

Potentiel diffusant

$$V(\vec{r}) = k^2\left[1 - n(\vec{r})^2\right] = \overline{V(\vec{r})} + \delta V(\vec{r})$$

Élément de matrice de transition $\langle f|T|i\rangle = \langle \tilde{\psi}_f|\overline{V}|\phi_i\rangle + \langle \psi_f|\delta V|\chi\rangle \approx \underbrace{\langle \tilde{\psi}_f|\overline{V}|\phi_i\rangle}_{\overline{V}_{if}} + \underbrace{\langle \psi_f|\delta V|\psi_i\rangle}_{\delta V_{if}}$

Les ondes

$\phi_i(\vec{r}) = \exp(i\vec{k}_i.\vec{r}) \longrightarrow$ Onde incidente

$$\left.\begin{aligned}\psi_i(\vec{r}) &= T_i \exp(i\vec{k}_i.\vec{r}) + R_i \exp(i\vec{k}'_i.\vec{r}) \\ \tilde{\psi}_f(\vec{r}) &= T_f^* \exp(i\vec{k}_f.\vec{r}) + R_f^* \exp(i\vec{k}'^*_f.\vec{r})\end{aligned}\right\}$$

Vecteurs propres du système idéal avec renversement temporel

Règle d'or de Fermi

$$\frac{d\sigma}{d\Omega} \propto \left\langle \left|\langle i|T|f\rangle\right|^2 \right\rangle = \left\langle \left|\overline{V}_{if} + \delta V_{if}\right|^2 \right\rangle$$

$$\left.\frac{d\sigma}{d\Omega}\right)_{spec} \propto \left|\overline{V}_{if} + \langle \delta V_{if}\rangle\right|^2, \left.\frac{d\sigma}{d\Omega}\right)_{diff} \propto \left\langle \left|\delta V_{if}\right|^2 \right\rangle - \left|\langle \delta V_{if}\rangle\right|^2$$

Quelques exemples de sections efficaces en GISAXS

Développement suivant la géométrie du potentiel de diffusion

Rugosité de surface

$$\frac{d\sigma}{d\Omega} \propto \left|T_i(\alpha_i)\right|^2 S(\vec{q}) \left|T_f(\alpha_f)\right|^2 \Longrightarrow$$ *Pic de Yonéda*

$$S(\vec{q}) = \frac{(\Delta\rho)^2}{\left|q_{zt}\right|^2} \exp\left\{-\left[q_{zt}^2 + q_{zt}^{*2}\right]\sigma^2/2\right\} \times \iint_S \left[\exp\left\{\left|q_{zt}\right|^2 C(\vec{r}_{//})\right\} - 1\right] \exp(i\vec{q}_{//}.\vec{r}_{//}) d^2 r_{//} \qquad C(r_{//}) = \left\langle z(r'_{//}) z(r'_{//} + r_{//}) \right\rangle$$

Remarques : principe de réciprocité

Cas limites : α_i, α_f • •α_c q_{zt}• q_z et |T| • 1 -approximation de Born valide

$q_{zt}\,\sigma$• 1 - TF de la fonction d 'autocorrélation de la rugosité

Multicouches rugueuses corrélées

Traitement analogue mais plus complexe !
Point de départ = optique des multicouches
Complexité = corrélation hauteur-hauteur inter-couches

Inclusions sous la surface

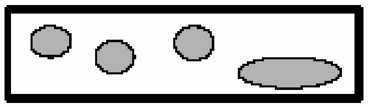

$$\frac{d\sigma}{d\Omega} \propto \left|T_i(\alpha_i)\right|^2 S(q_{//}, q_{zt}) \left|T_f(\alpha_f)\right|^2$$

$$S(\vec{q}) = \left|\int_V \exp(i\vec{q}.\vec{r}) d^3 r\right|^2$$ Transformée de Fourier de la forme de l'objet diffusant

Îlots sur une surface

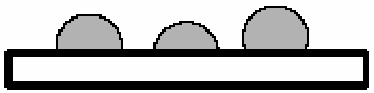

$\longrightarrow$ Cas approfondi par la suite !

Programme d'analyse ***IsGISAXS***

Distorted Wave Born Approximation (DWBA) for supported islands

M. Rauscher, T. Salditt et H. Spohn, Phys. Rev. B 52, 16855 (1995)
M. Rauscher et al. J. Appl. Phys. 86 (12), 6763 (1999)

1st term : $q_z = k_{fz} - k_{iz}$ 2nd term : $q_z = k_{fz} + k_{iz}$ 3rd term : $q_z = -k_{fz} - k_{iz}$ 4th term : $q_z = -k_{fz} + k_{iz}$

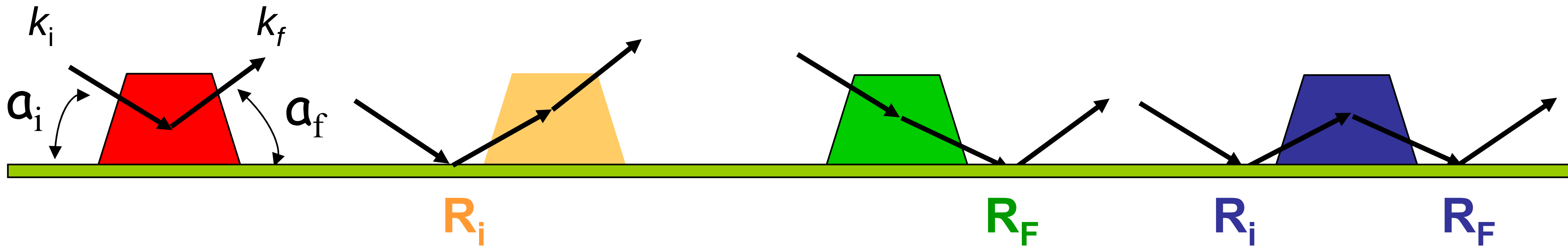

Coherent interferences between 4 waves with different q_z !

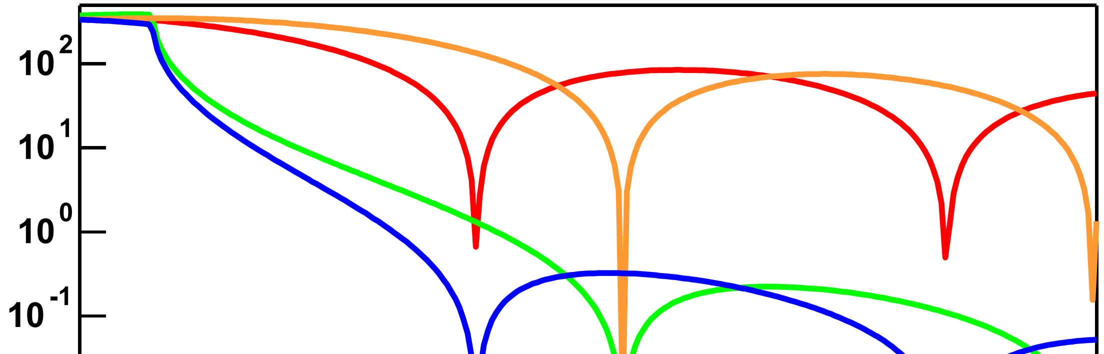

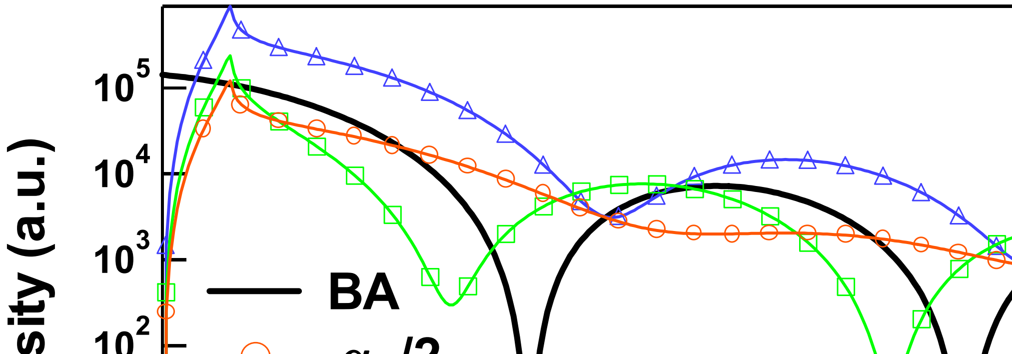

α_i =

$$\frac{d\sigma}{d\Omega} \propto \left| \underbrace{F(\vec{q}_{//}, k_{fz} - k_{iz})}_{\text{Born term}} + R(\alpha_i) F(\vec{q}_{//}, k_{fz} + k_{iz}) + R(\alpha_f) F(\vec{q}_{//}, -k_{fz} - k_{iz}) + R(\alpha_i) R(\alpha_f) F(\vec{q}_{//}, -k_{fz} + k_{iz}) \right|^2$$

with $F(\vec{q}) = \int_V \exp(i\vec{q}.\vec{r}) d^3r$

DWBA form factor of a cylinder

Modulus square of the each term

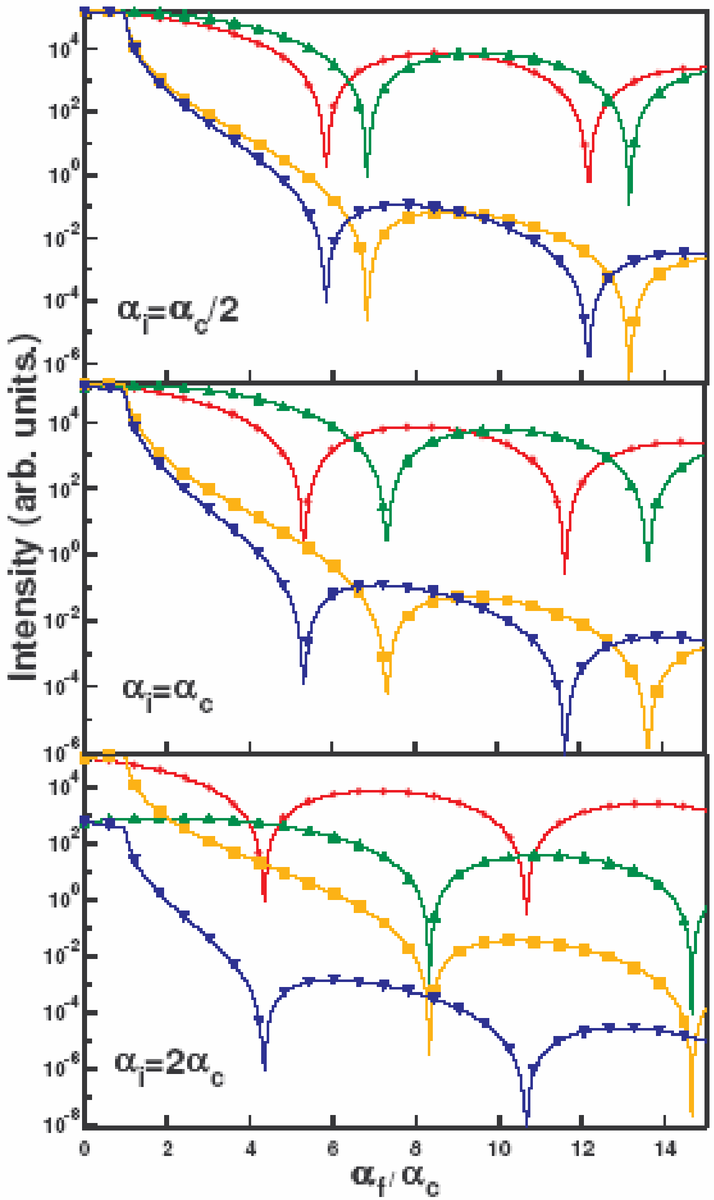

+ Phases

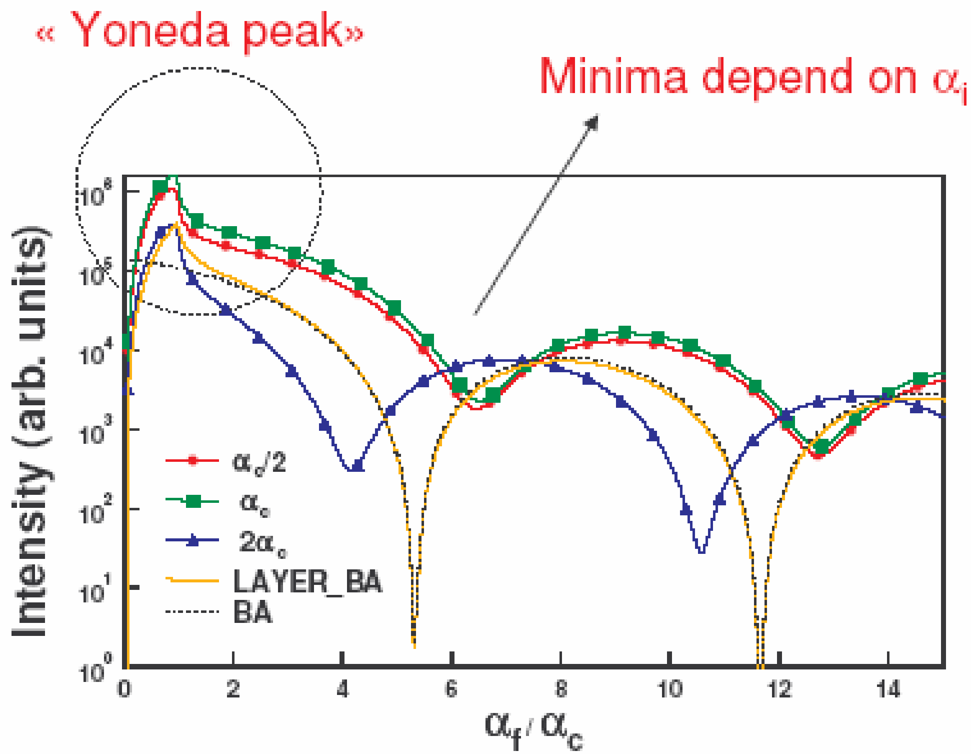

Scattered intensity along α_i

Diffuse Scattering due to size distributions, and sizes-distances and sizes-sizes correlations

Two usual extreme approximations neglecting correlations:

1 – DA (Decoupling Approximation):
Size and positions completely un-correlated

$$\cancel{I(q_{//},q_{\perp}) \propto \underbrace{\left\langle |F|^2 \right\rangle - \left|\left\langle F \right\rangle\right|^2}_{\textit{Diffuse scattering}} + \underbrace{\left|\left\langle F \right\rangle\right|^2 \times S(q_{//})}_{\textit{Coherent scattering}}}$$

2 - LMA : Local monodisperse approximation

$$\cancel{I(q_{//},q_{\perp}) \propto \left\langle |F|^2 \right\rangle \times S(q_{//})}$$

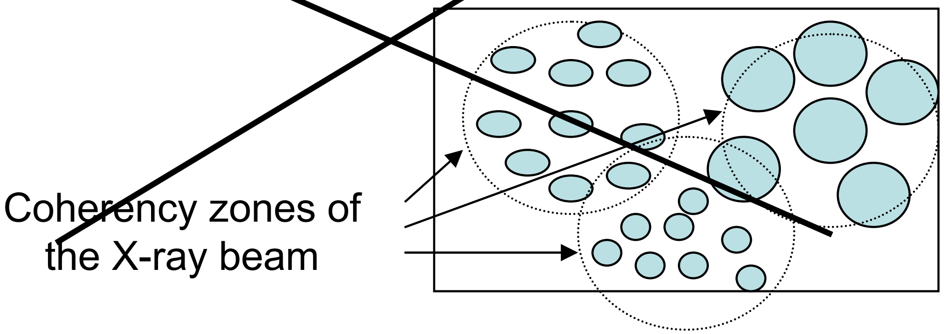

•Correlations deduced from analysis of TEM images Pd/MgO(001)

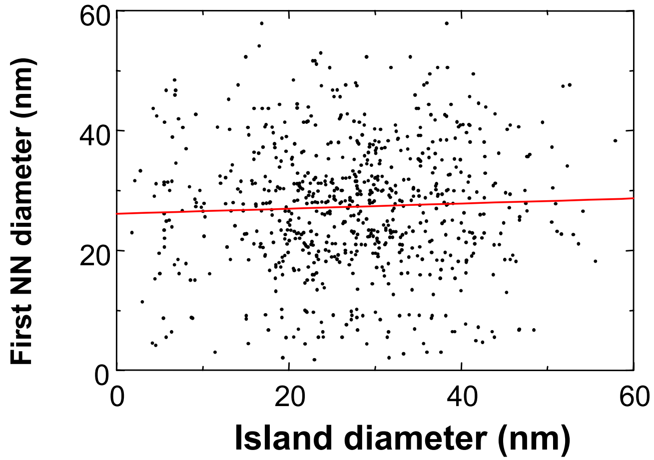

No sizes-sizes correlation LMA wrong

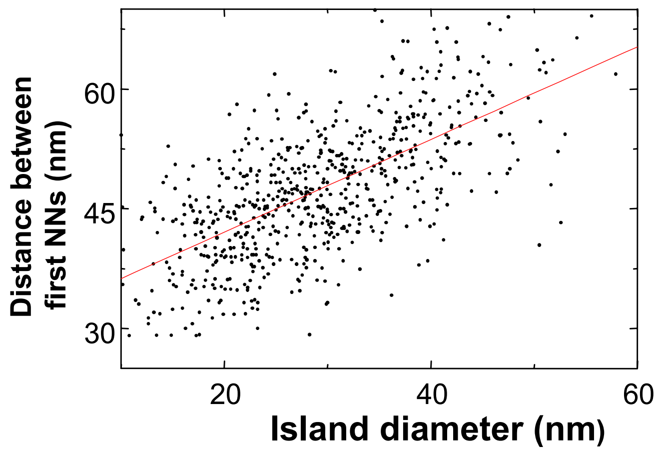

Sizes-separations correlations

In plane scattering : coherent versus incoherent ?

$$\frac{d\sigma}{d\omega} \propto \frac{1}{N}\left\langle \left| \sum_i F_i(\vec{q}_{//},k_{fz},k_{iz})\exp(i\vec{q}_{//}.\vec{r}_{i//}) \right|^2 \right\rangle$$

Configuration average over the coherently illuminated areas

Knowledge of all the partial pair correlation functions ?

2 simple limit cases

Decoupling approximation DA

$$\frac{d\sigma}{d\Omega} \propto \underbrace{\left\langle|F|^2\right\rangle - \left|\langle F\rangle\right|^2}_{\textit{Incoherent scattering}} + \underbrace{\left|\langle F\rangle\right|^2 \times S(q_{//})}_{\textit{Coherent scattering}}$$

Total disorder – no correlations

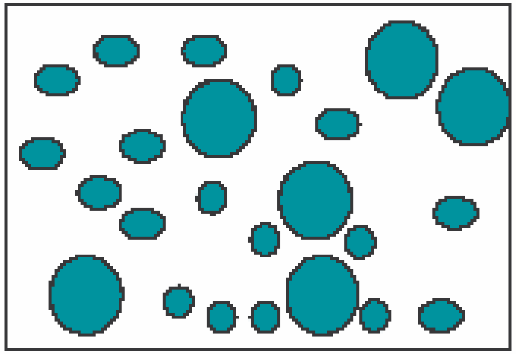

Local Monodisperse Approximation LMA

$$\frac{d\sigma}{d\Omega} \propto \left\langle|F|^2\right\rangle \times S(q_{//})$$

Incoherent sum of scattering from Monodisperse domains

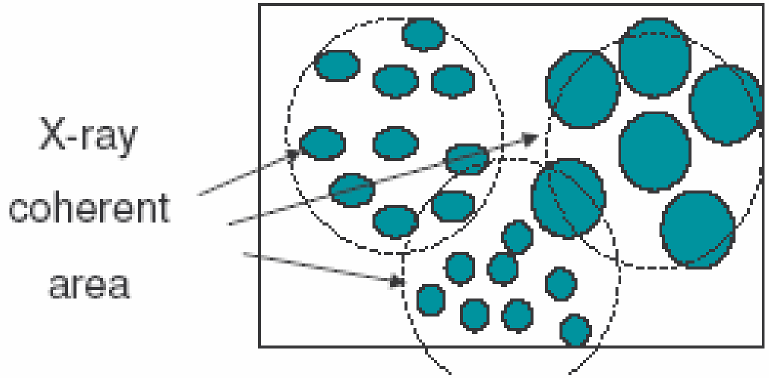

Result from scattering theory

form factor of a single object

correlation function of the positions

$$\left(\frac{d\sigma}{d\omega}\right)_{\text{diff}} = \text{const.} \sum_p \left| A_p F(\mathbf{Q}_p) \right|^2 P(\mathbf{Q}_p)$$

over the processes

amplitude of the *p*-th process

$P(Q_p)$ = FT of pair correlation in real space

Short range order

Long range order

Courtesy of V. Holy

Lateral size distribution and zeros of the form factor

Cylindrical particles and gaussian distributions

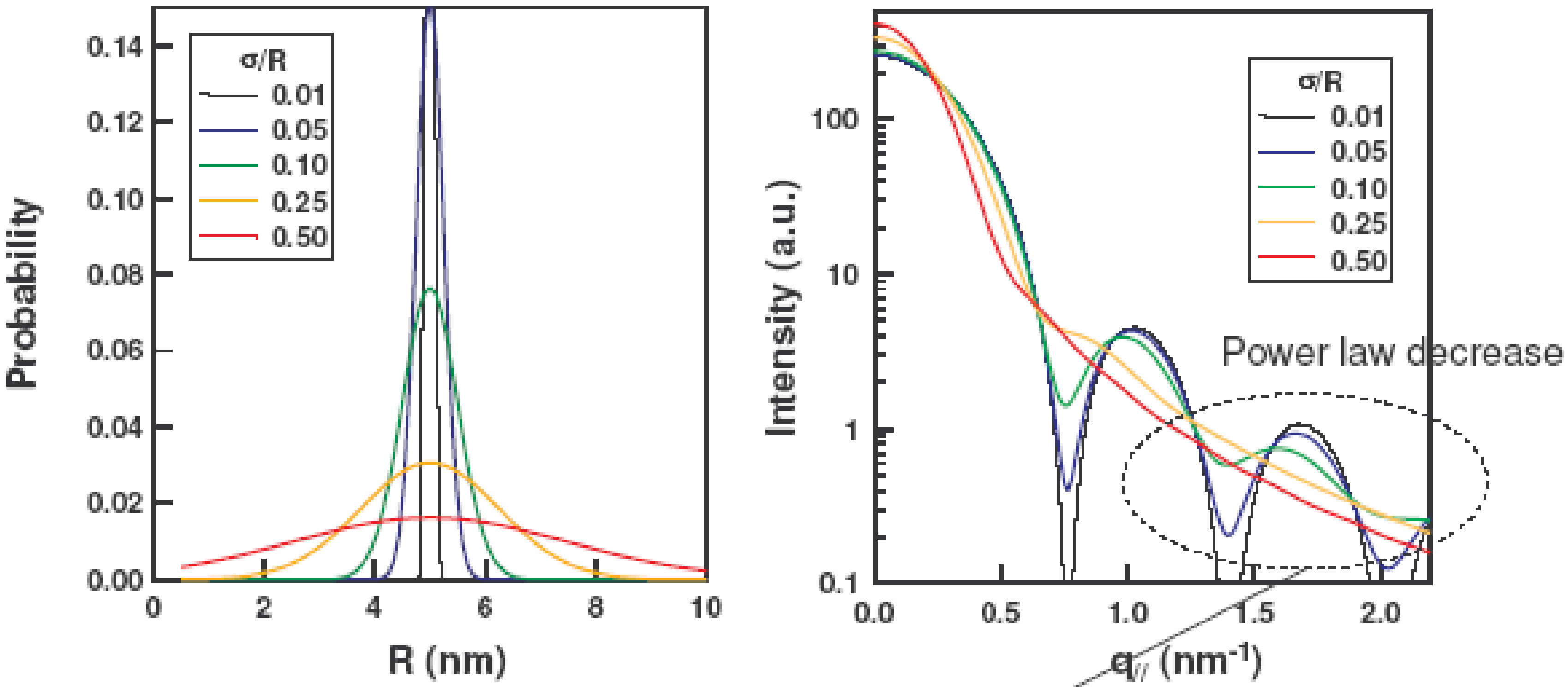

In IsGISAXS : distributions of lateral sizes, of heights, of orientations, of incidence angles, of wavelengths

Porod regime : a signature of the shape !

S from
s with facets

er template for 2D organization : nano-facetted surface

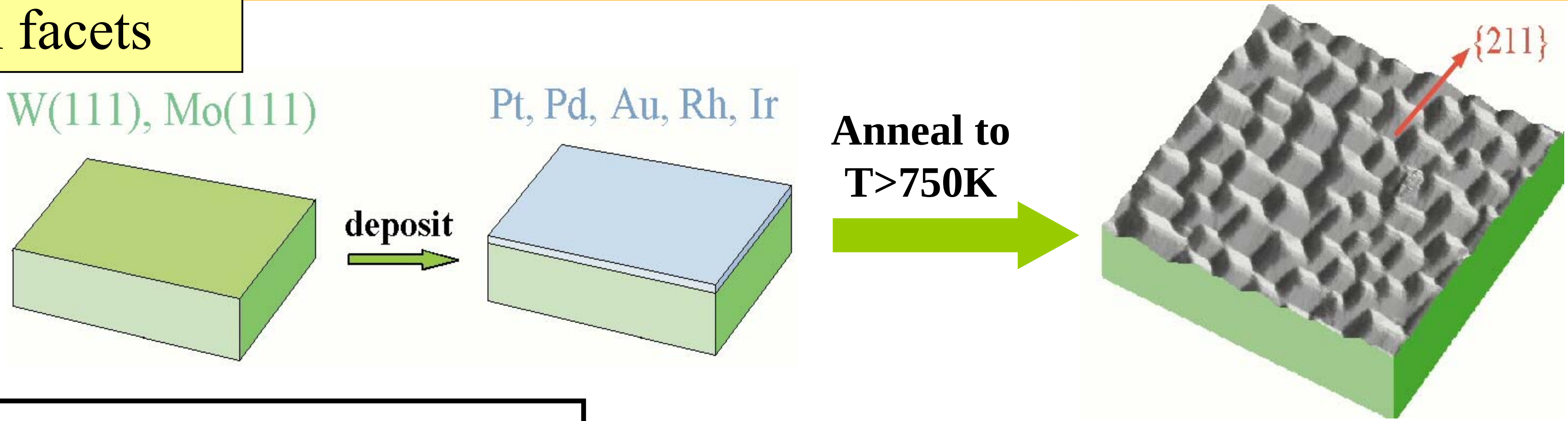

Late stages of facetting:
Large nano-pyramids

$$I(\mathbf{Q}) = |F_{DWBA}(\mathbf{Q}, k_i^z, k_f^z)|^2\, S(\mathbf{Q})$$

Shape: F_{DWBA}

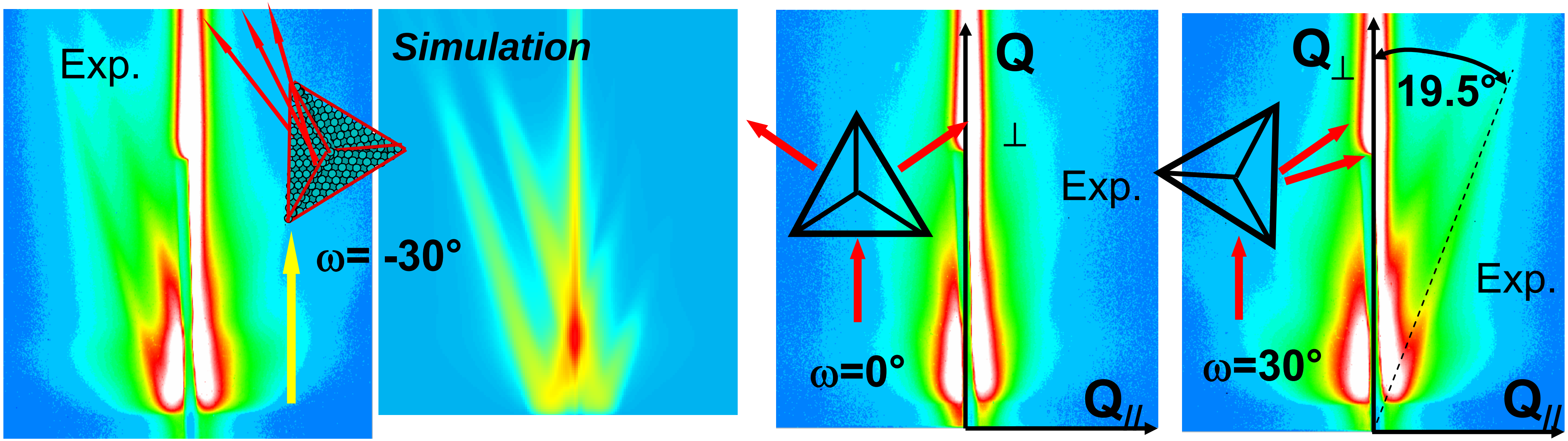

Evolution of facetting as a function of annealing time

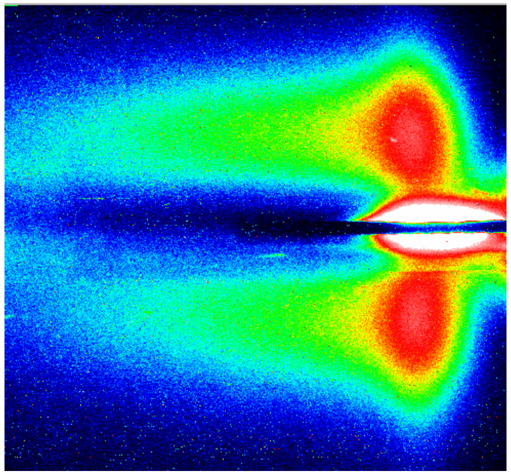

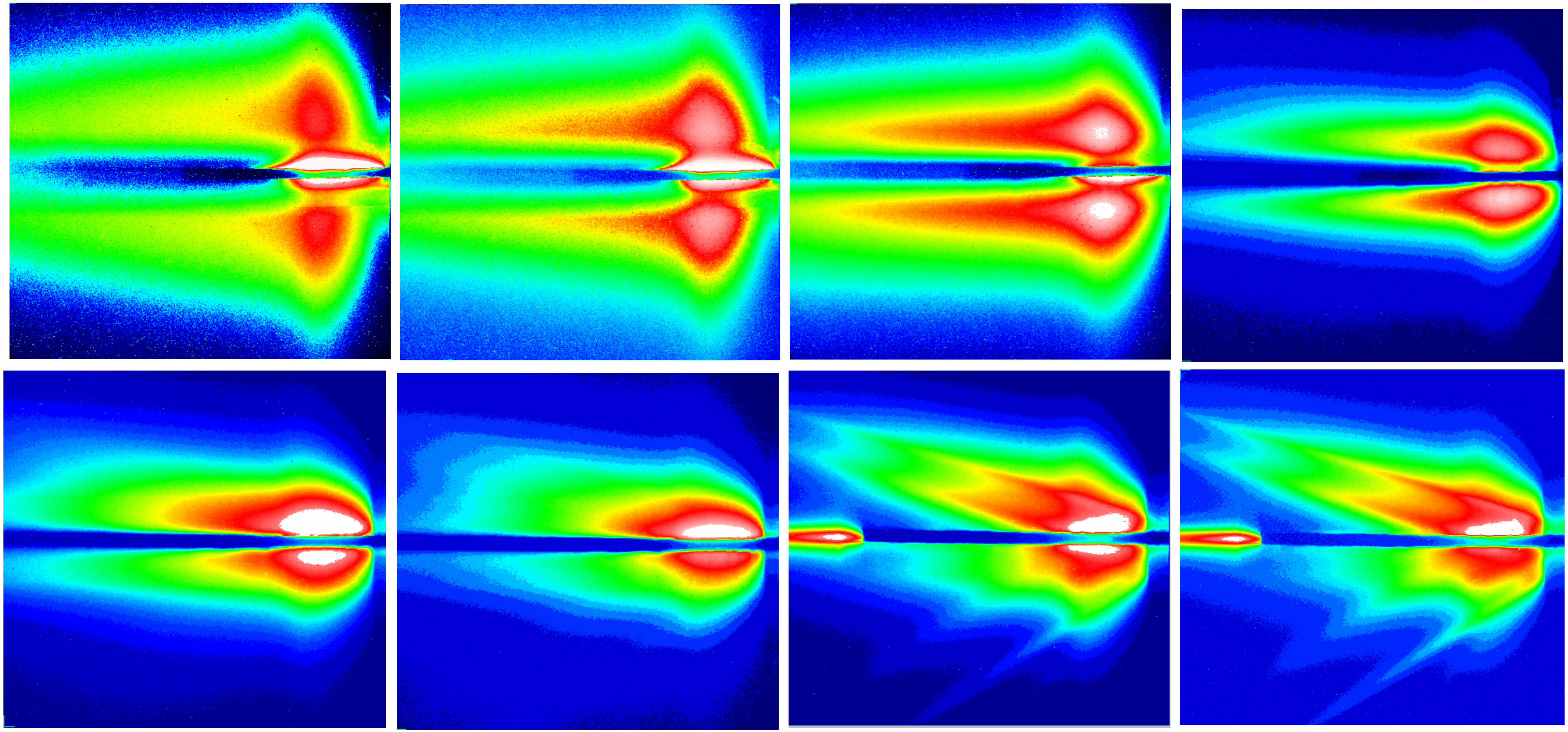

« Super-cristallography » of the Co cluster lattice on Au(111) before coalescence

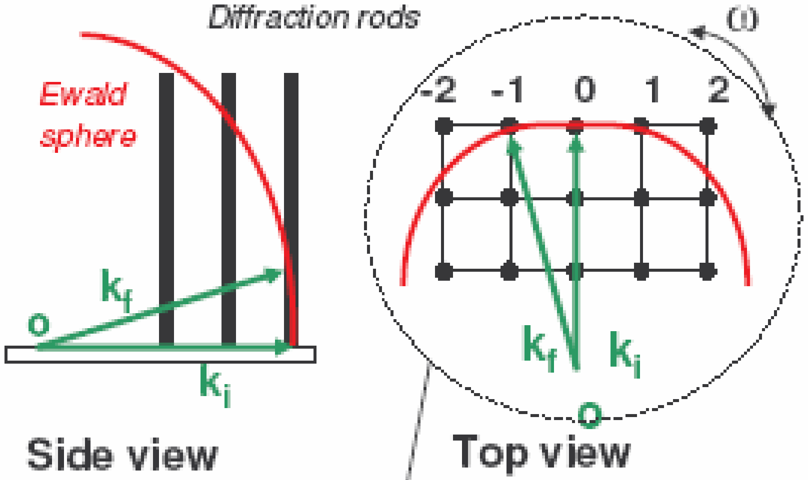

Analysis parameters

- rectangular 2D paracrystal (ΔK) with three variants oriented at 120°
- Triangular islands (R,H and size distribution)
- Centering of the mesh δy

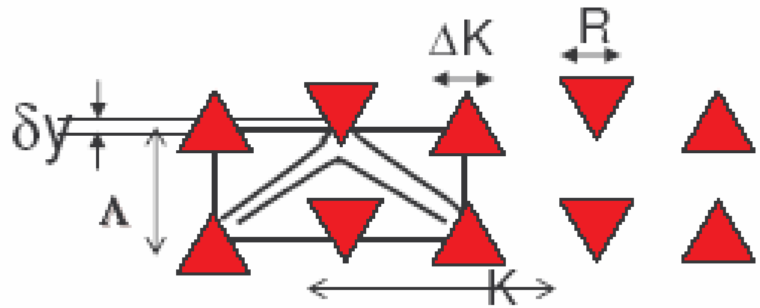

Rebuild cross section of the reciprocal space around $q_z = 0$

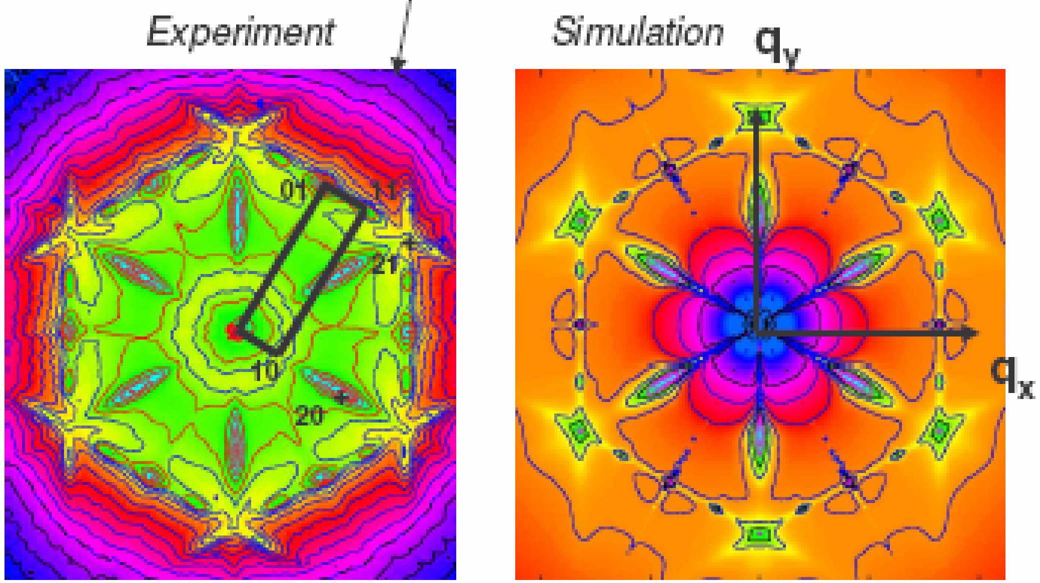

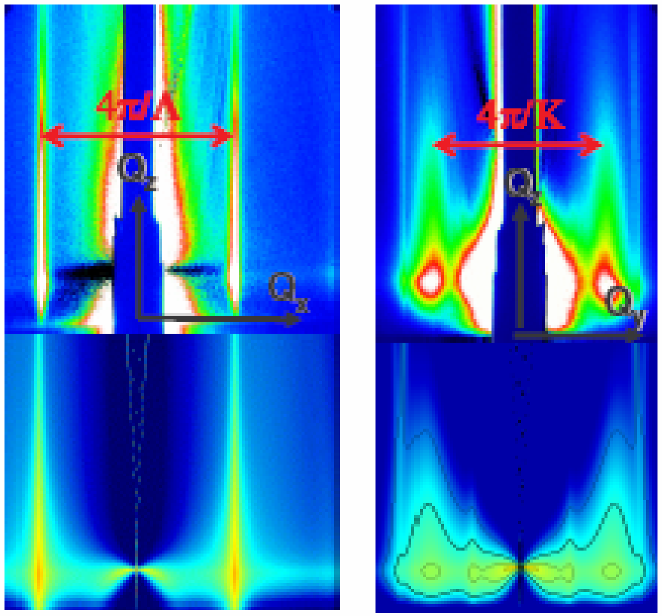

GISAXS on Bimolecules B. Krause, ID01

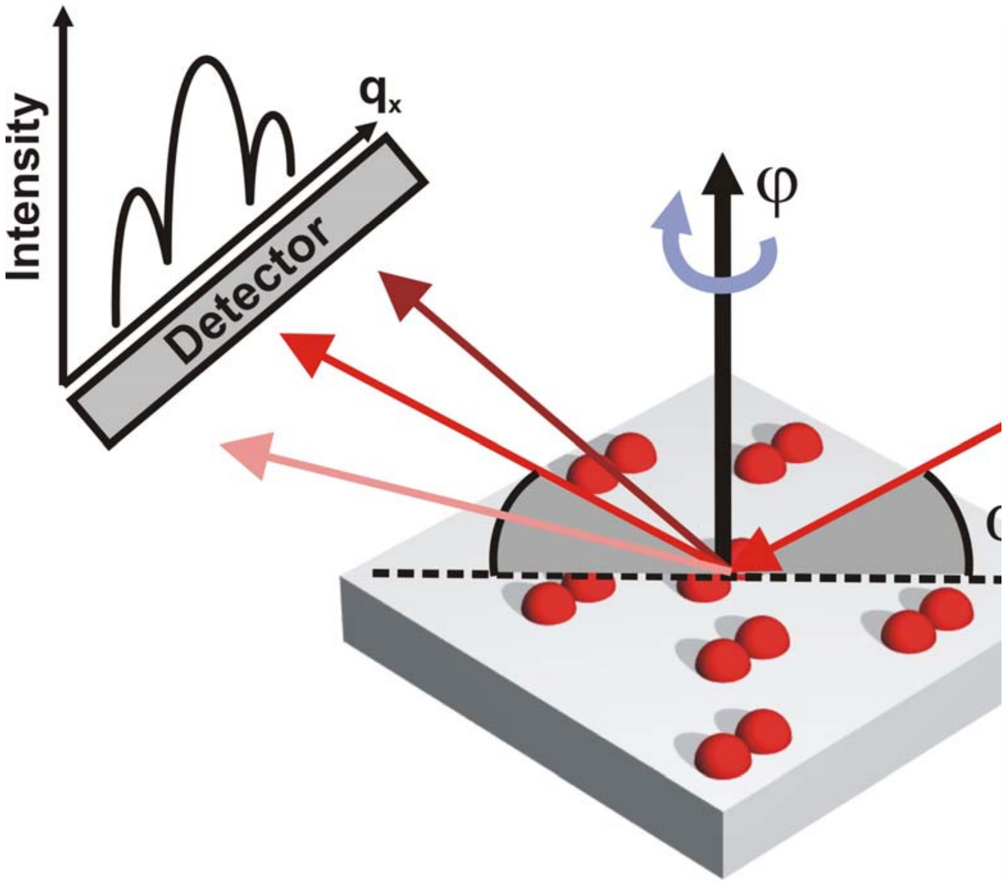

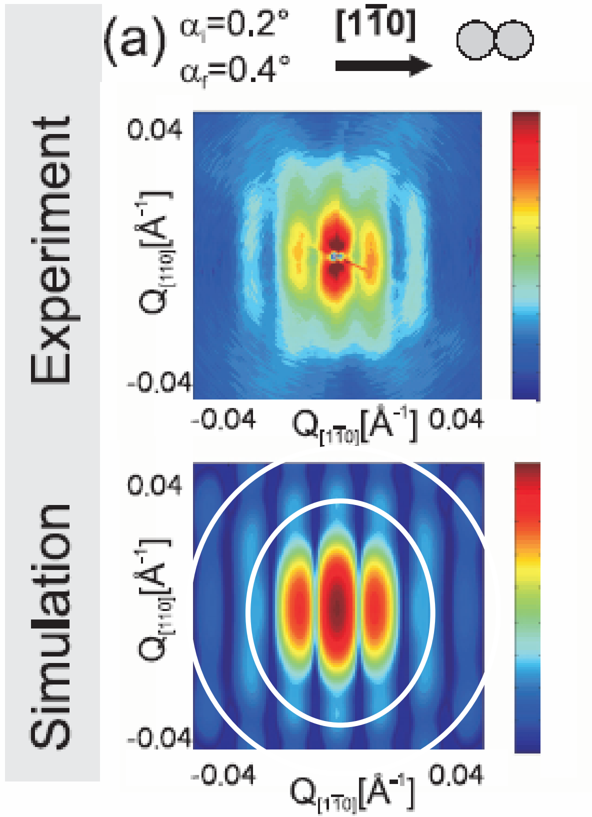

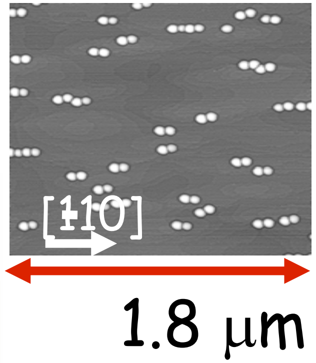

Model: Formfactor of double-disk

R_0=270 Å H=170 Å

R_1=130 Å 10 % size distribution

Scans in 3D reciprocal space

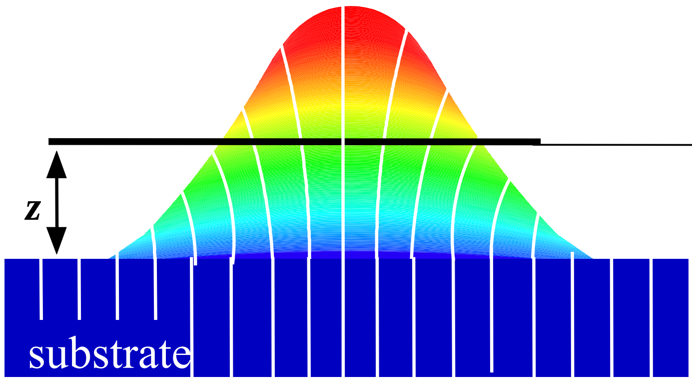

:

information on
- shape ⟺ $q_{angular}$
- strain ⟺ q_{radial}
- depth ⟺ q_z

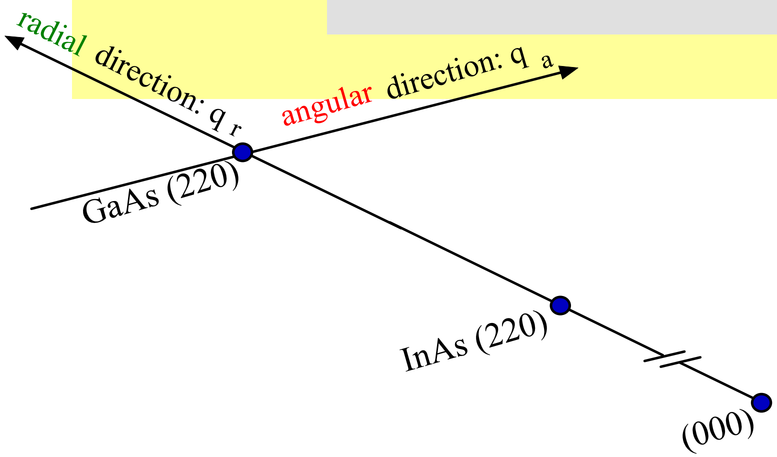

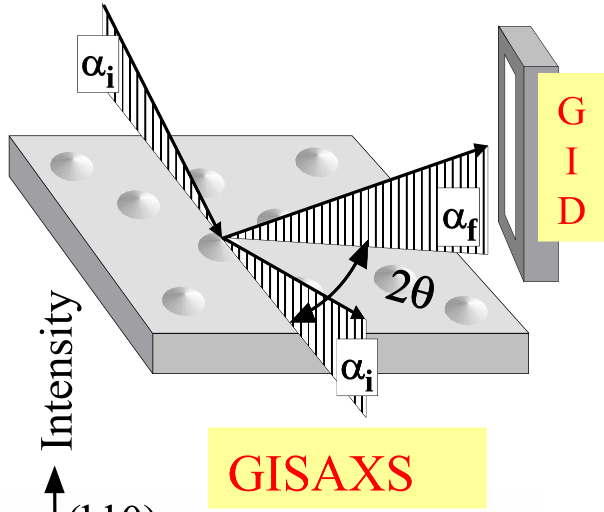

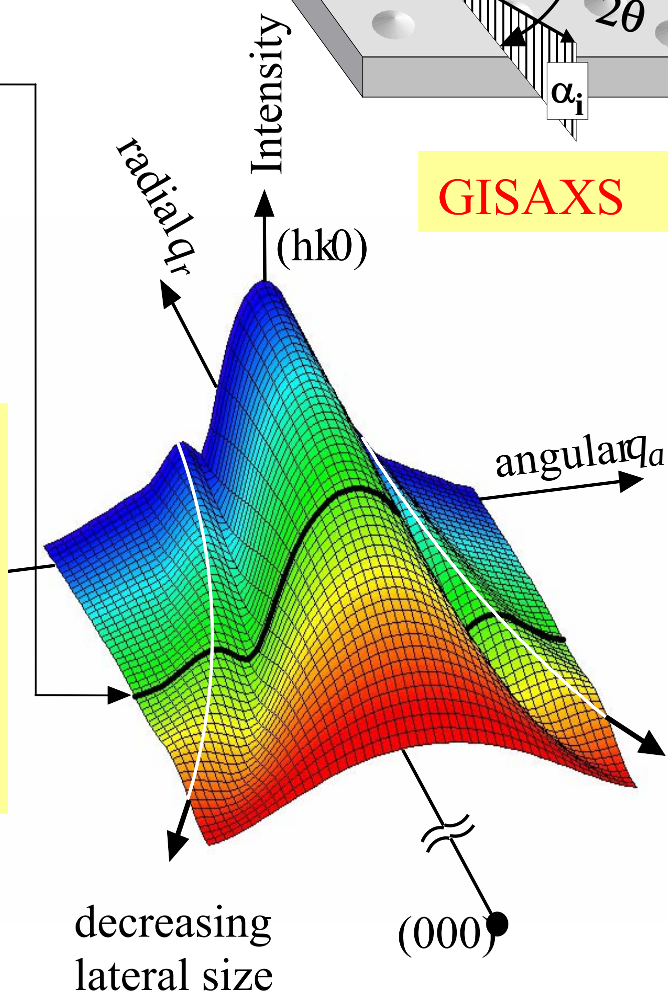

Results: data analysis ISS

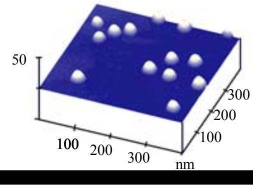

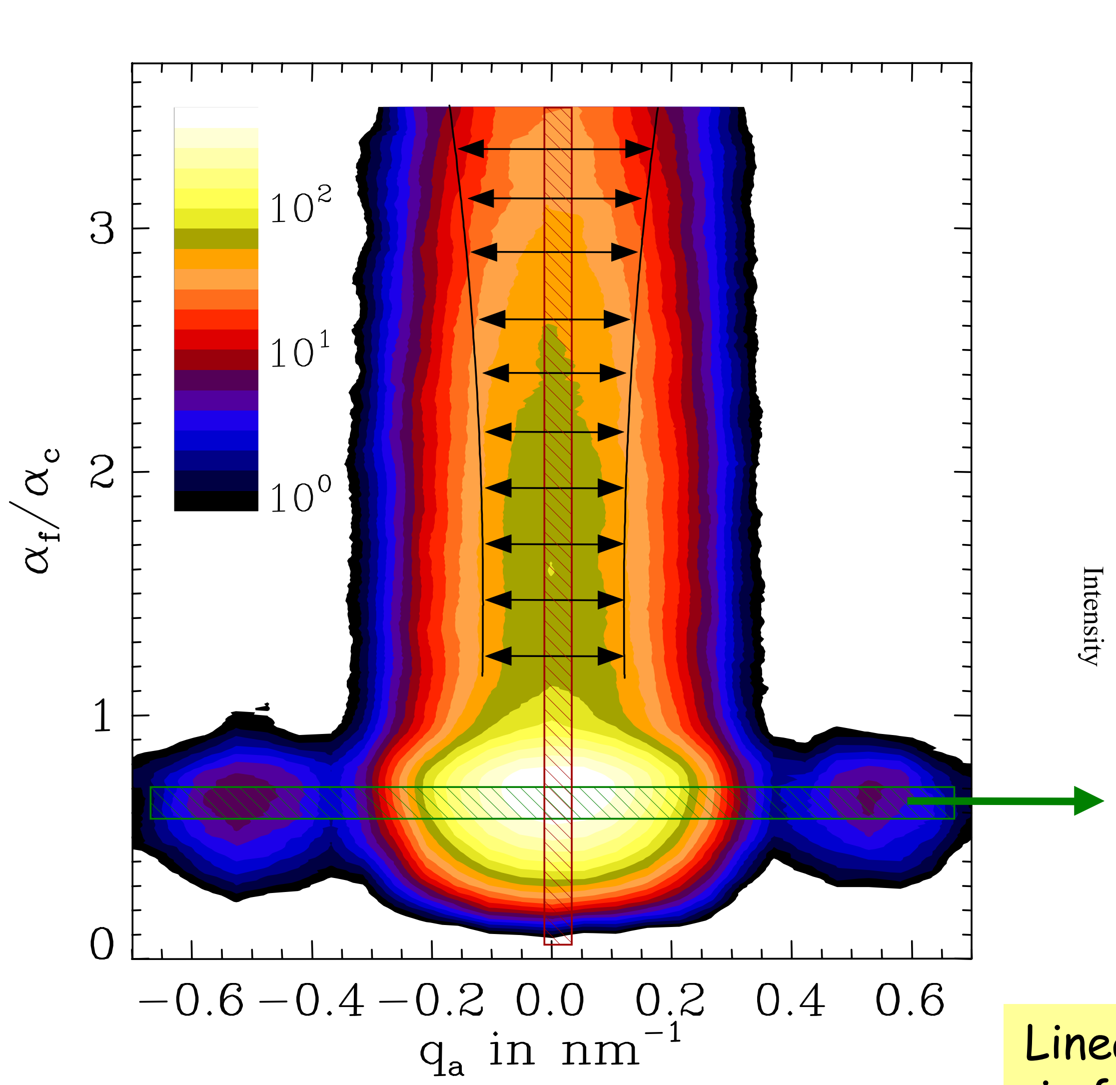

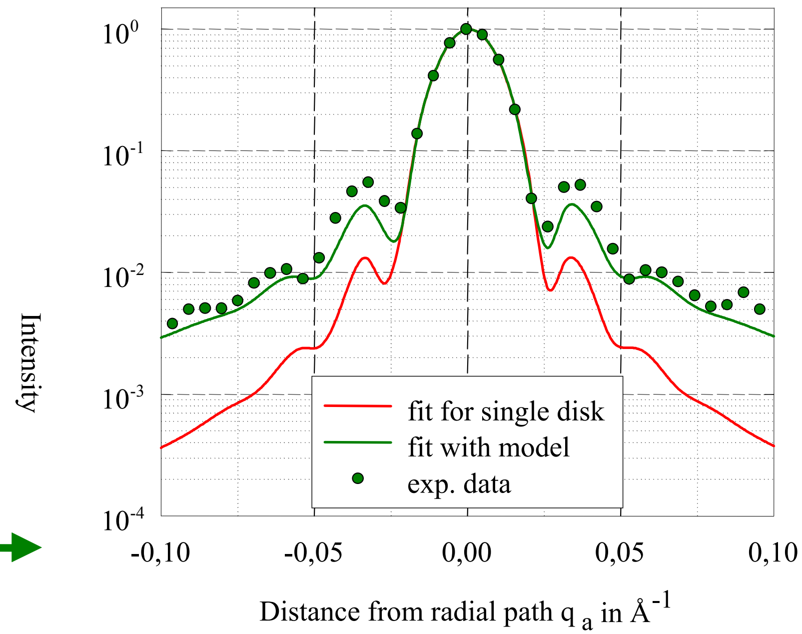

Linear relation between strain and size is found from fits at all radial positions

Example III: composition of Ge domes on Si

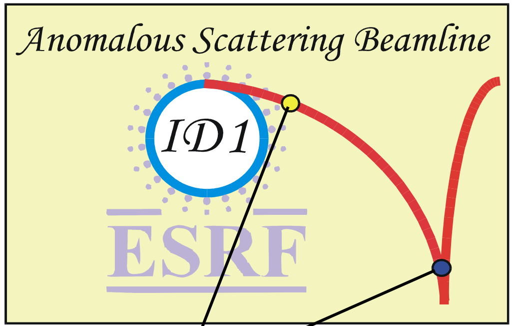

GID with contrast variation

using anomalous ISS

$$f(Q,E) = f_o(Q) + f'(E) + i\, f''(E)$$

Energy dependence

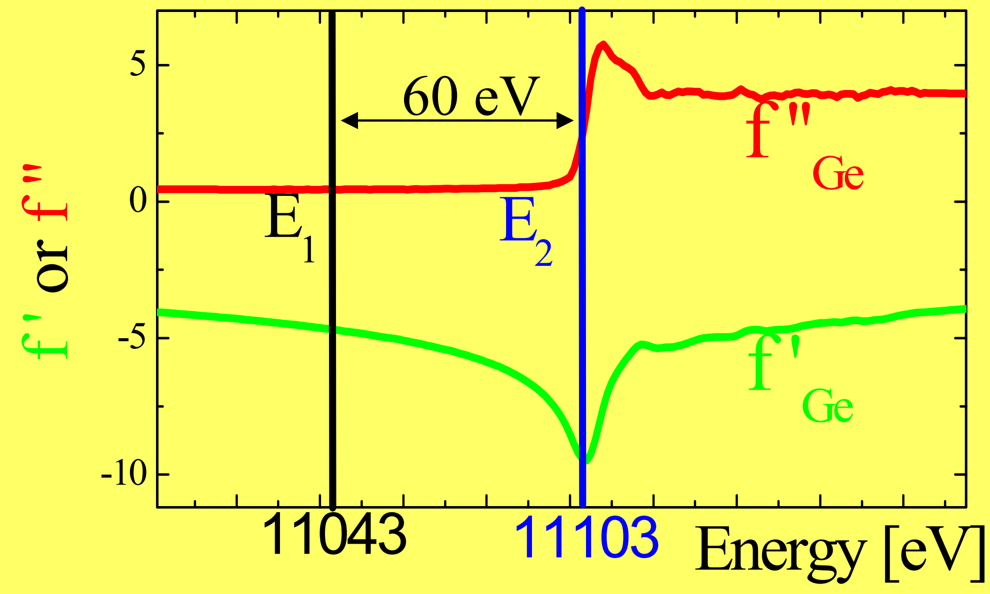

For Si negligible

Use energy and Q dependence

to amplify contrast:

measure at high Q !

T. Schülli et al PRL, 90, 66105 (2003)

Contrast variation: Q dependence

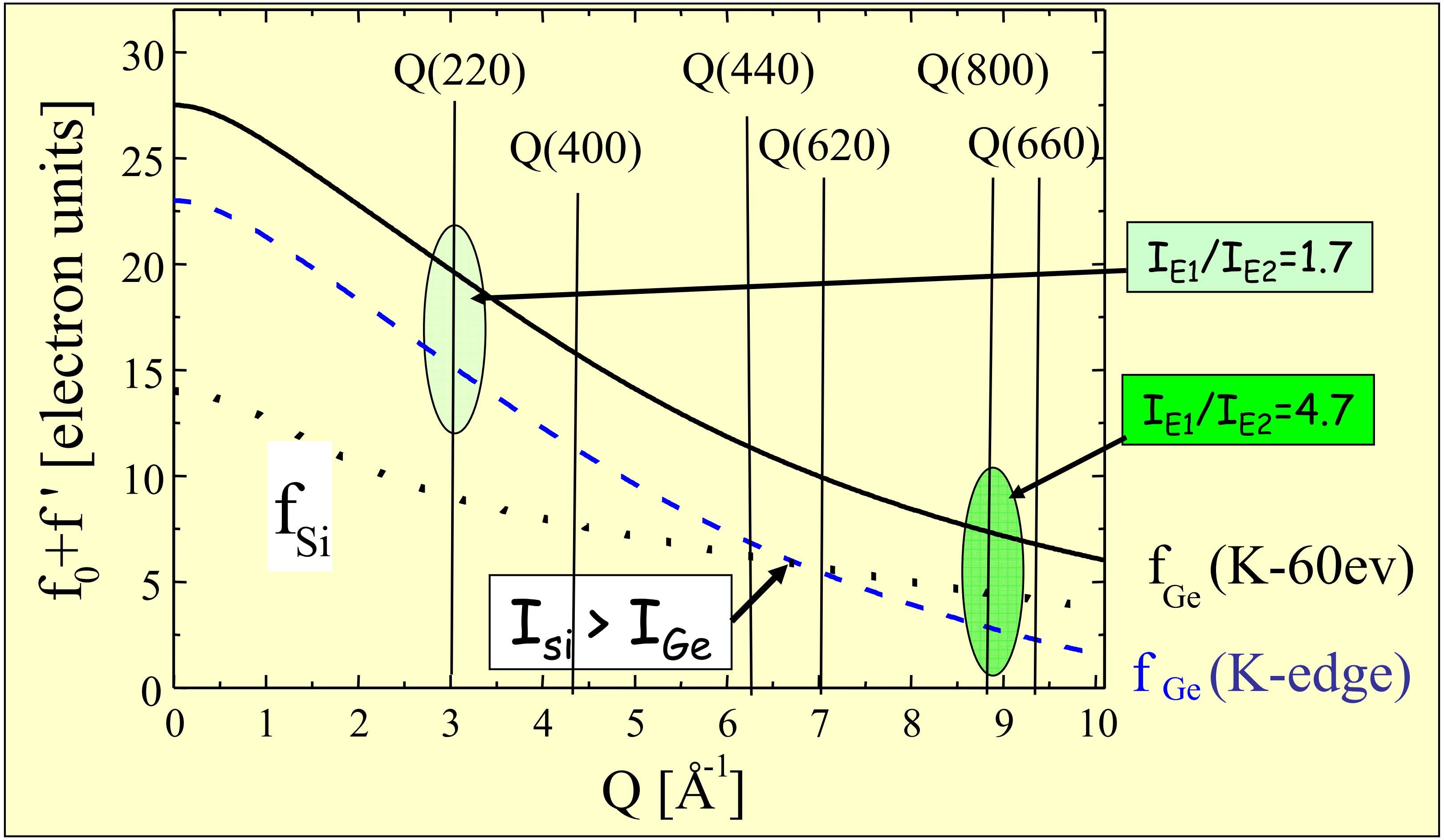

- anomalous correction enhanced at high Q
- higher resolution for $\Delta a/a = -q_r/Q$
- Si content from deviation of I_{E1}/I_{E2} for pure Ge
- All possible GID reflections should be measured

Si interdiffusion : vertical composition profile from (A)-GID at (800)

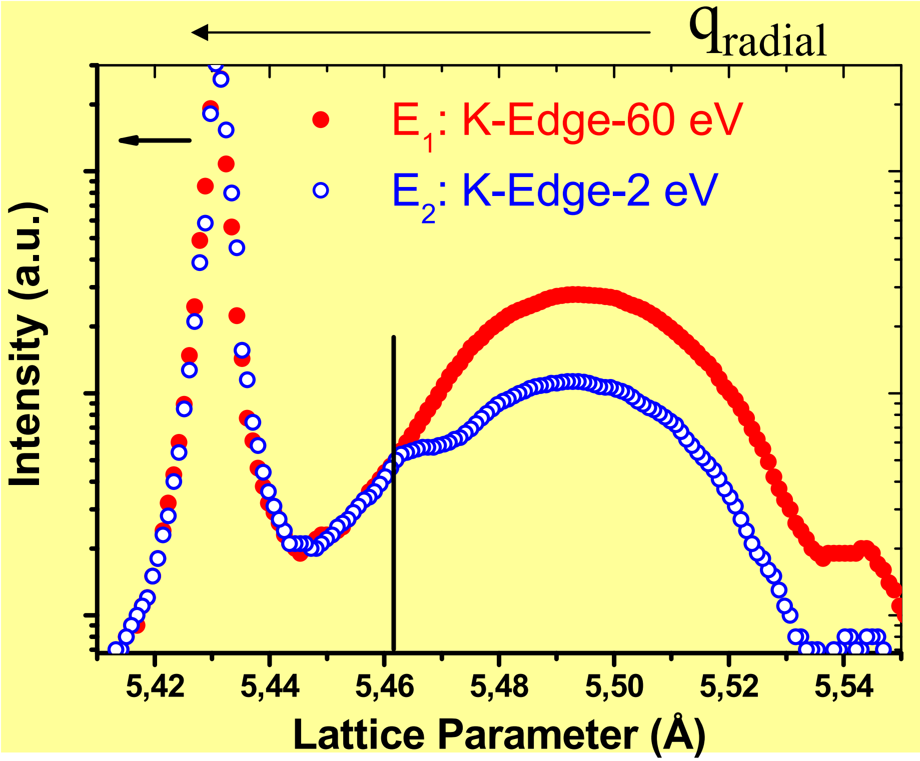

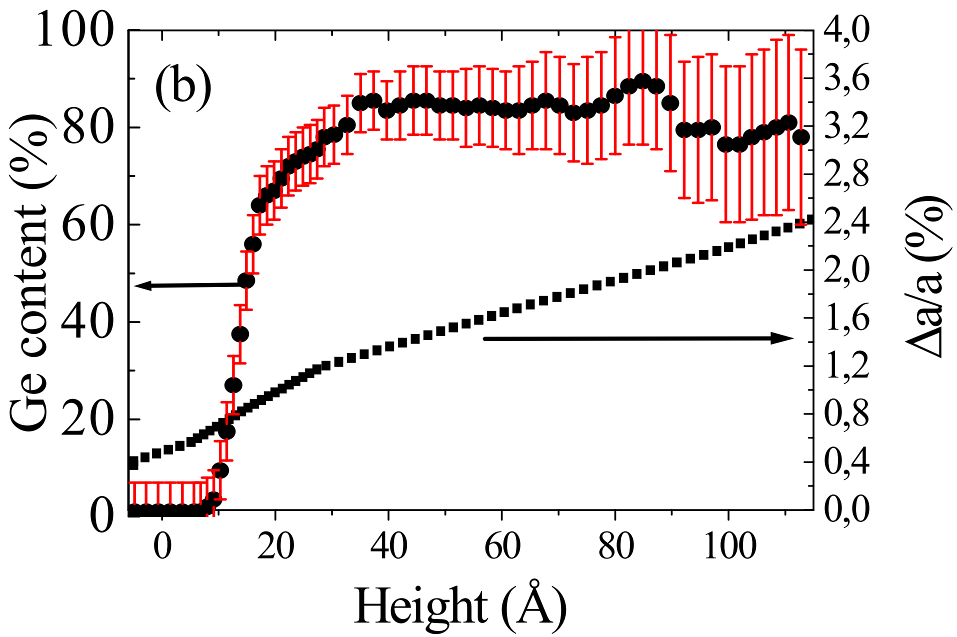

7 ML MBE growth at 600°C

Ge domes

Small size dispersion

Direct method!

RESULTS

- Sharp Si/Ge interface
- Ge plateau at 85%
- Δa/a monotonic
- dot is highly strained

T. Schülli et al PRL, 90, 66105 (2003)

"Nano –Tomography": 3D real space image
shape, size, strain and composition of Ge/Si alloy islands

11.2 ML Ge domes on Si (001) grown by CVD at 600°C

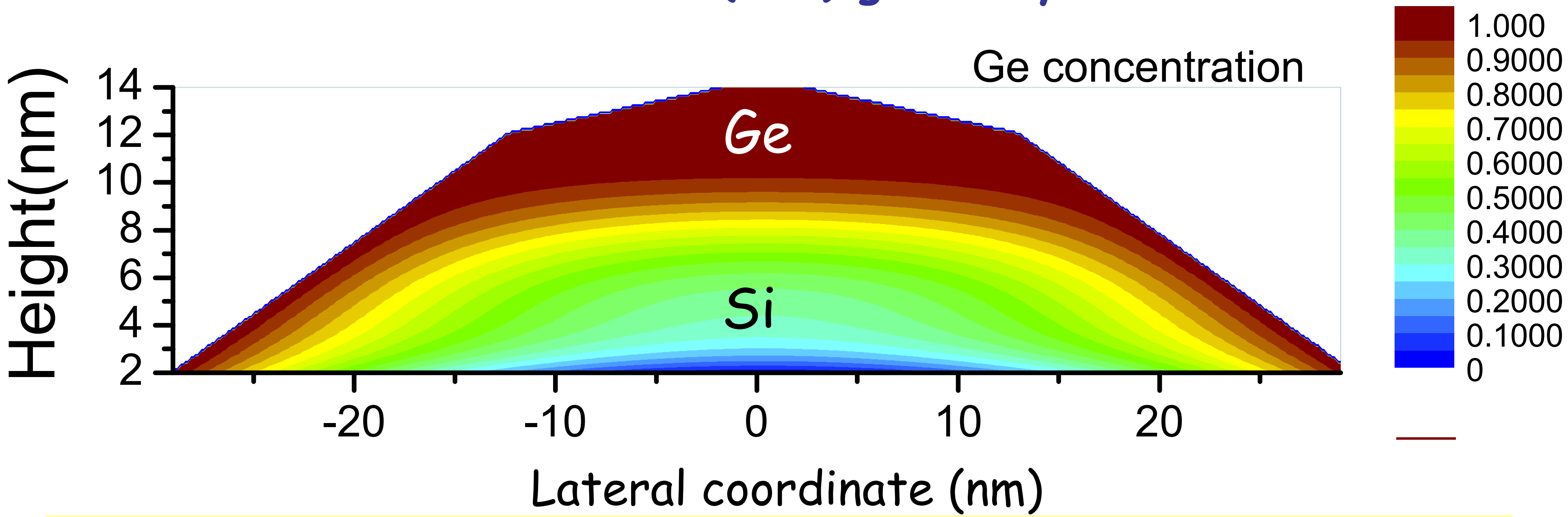

Results:
the lateral variation of the Ge concentration changes with height
Si rich core covered by Ge rich alloy
concentration from pure Si at bottom to pure Ge at top

T.Schülli *et al.* PRL90, 66105 (2003)
A. Malachias *et al.* PRL91, 176101 (2003)

Oxide layer and crystalline core

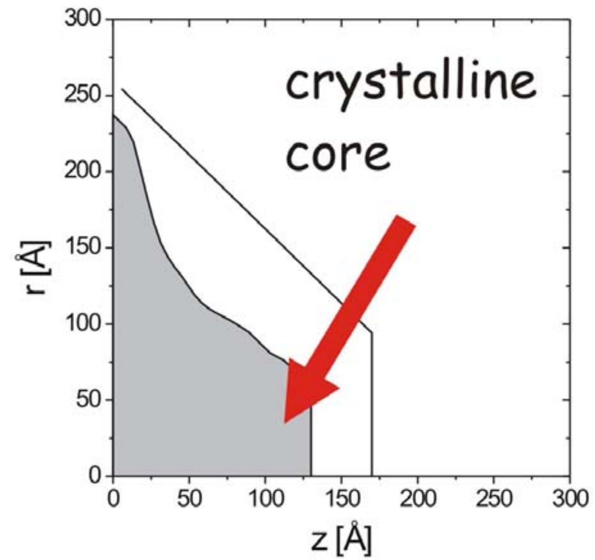

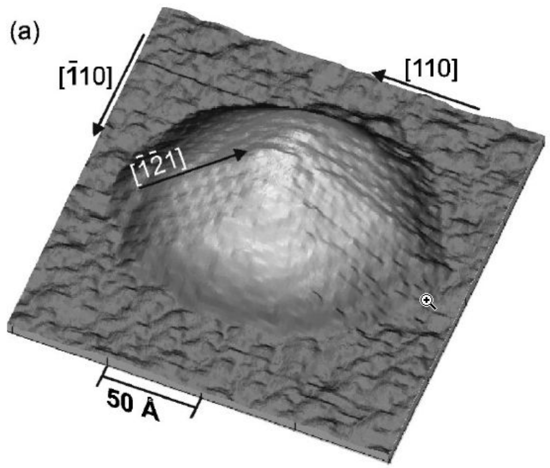

Marquez et al., APL **78** (16), 2310 (2001)

amorphous oxide layer
(2-3 nm)

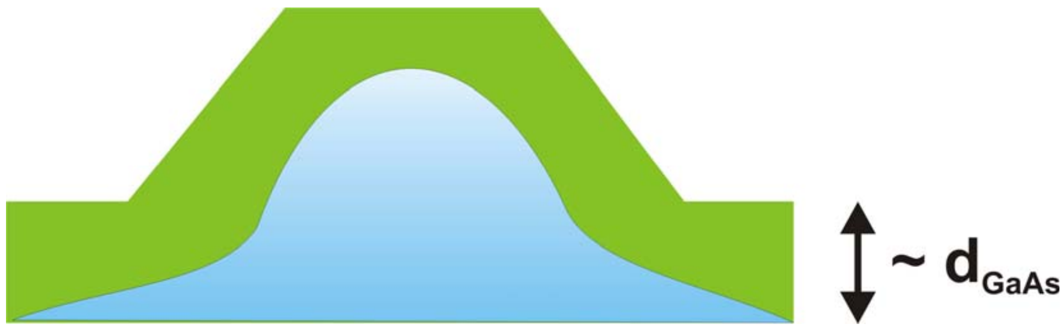

oxidation ⇒ foot of the dot was part of the substrate

Oxide layer and crystalline core

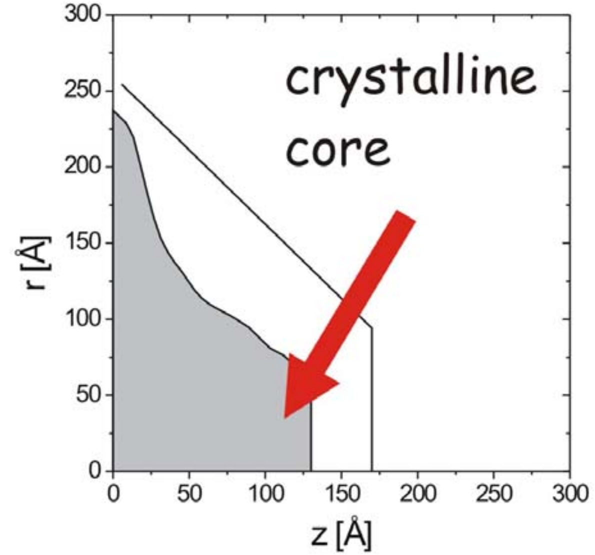

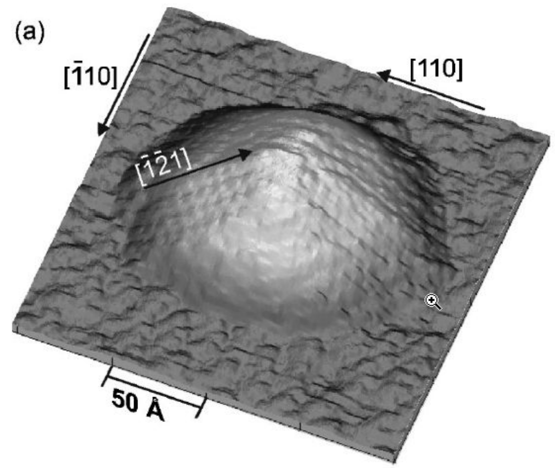

Marquez et al., APL **78** (16), 2310 (2001)

amorphous oxide layer
(2-3 nm)

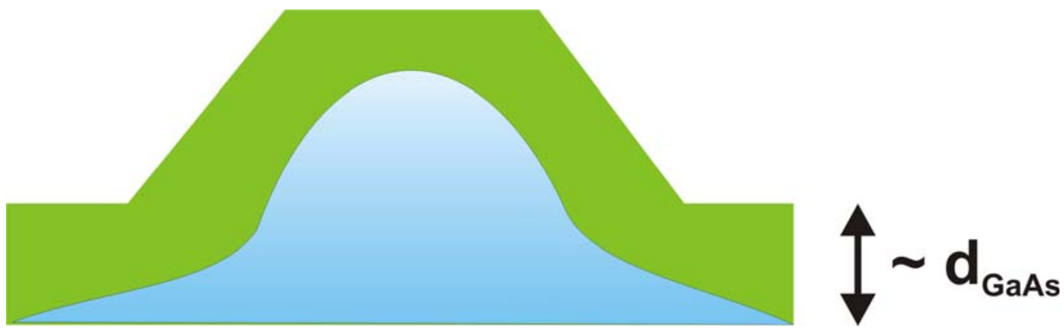

oxidation ⇒ foot of the dot was part of the substrate

Magnetic resonant X-ray scattering from an array of CoPt multilayers

Away from L_3 Co edge 770 eV

Specular peak

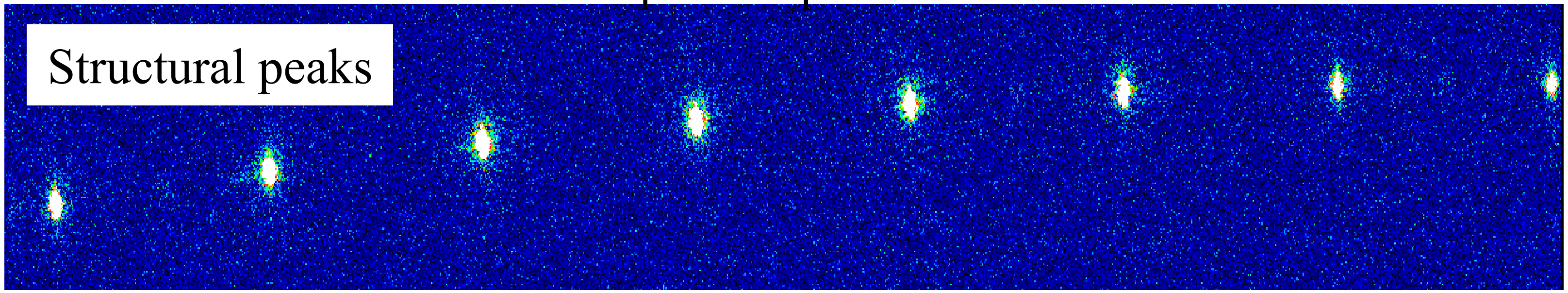

At L_3 Co edge 780 eV

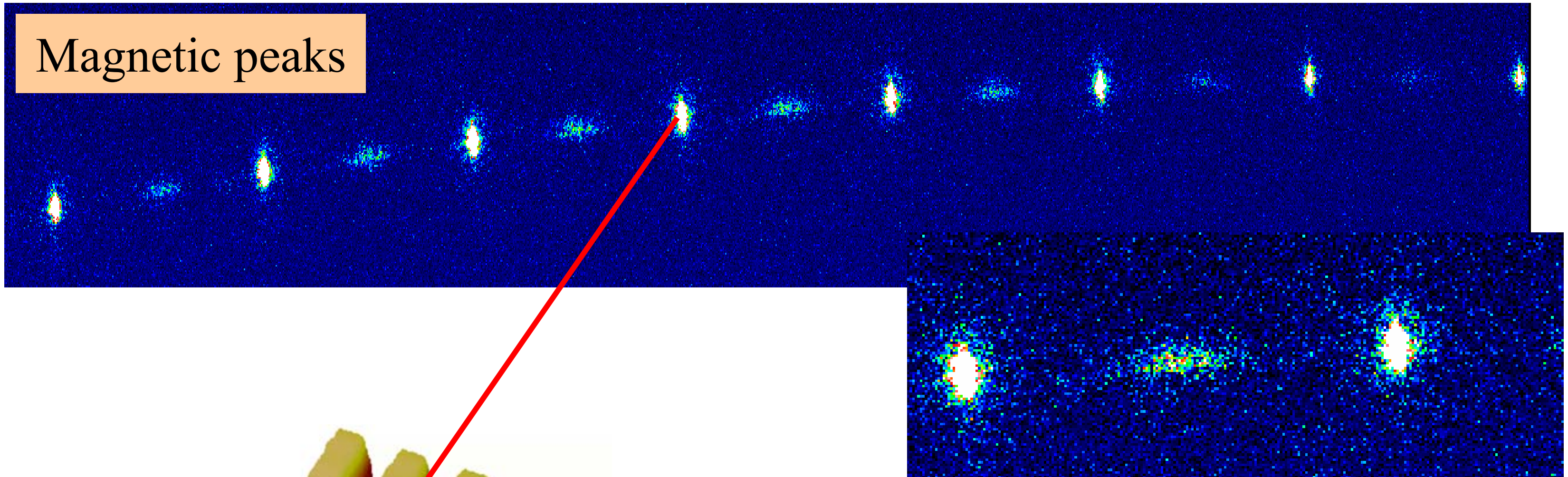

Peak from AF magnetic order

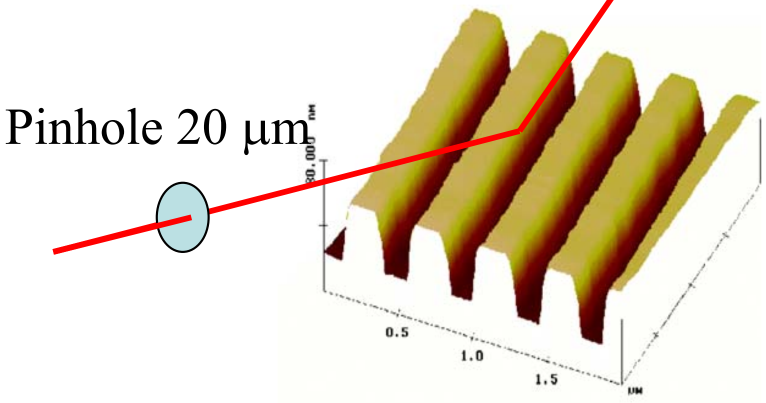

K. Chesnel at al, PRB 2003

Coherent scattering on magnetic microstructures

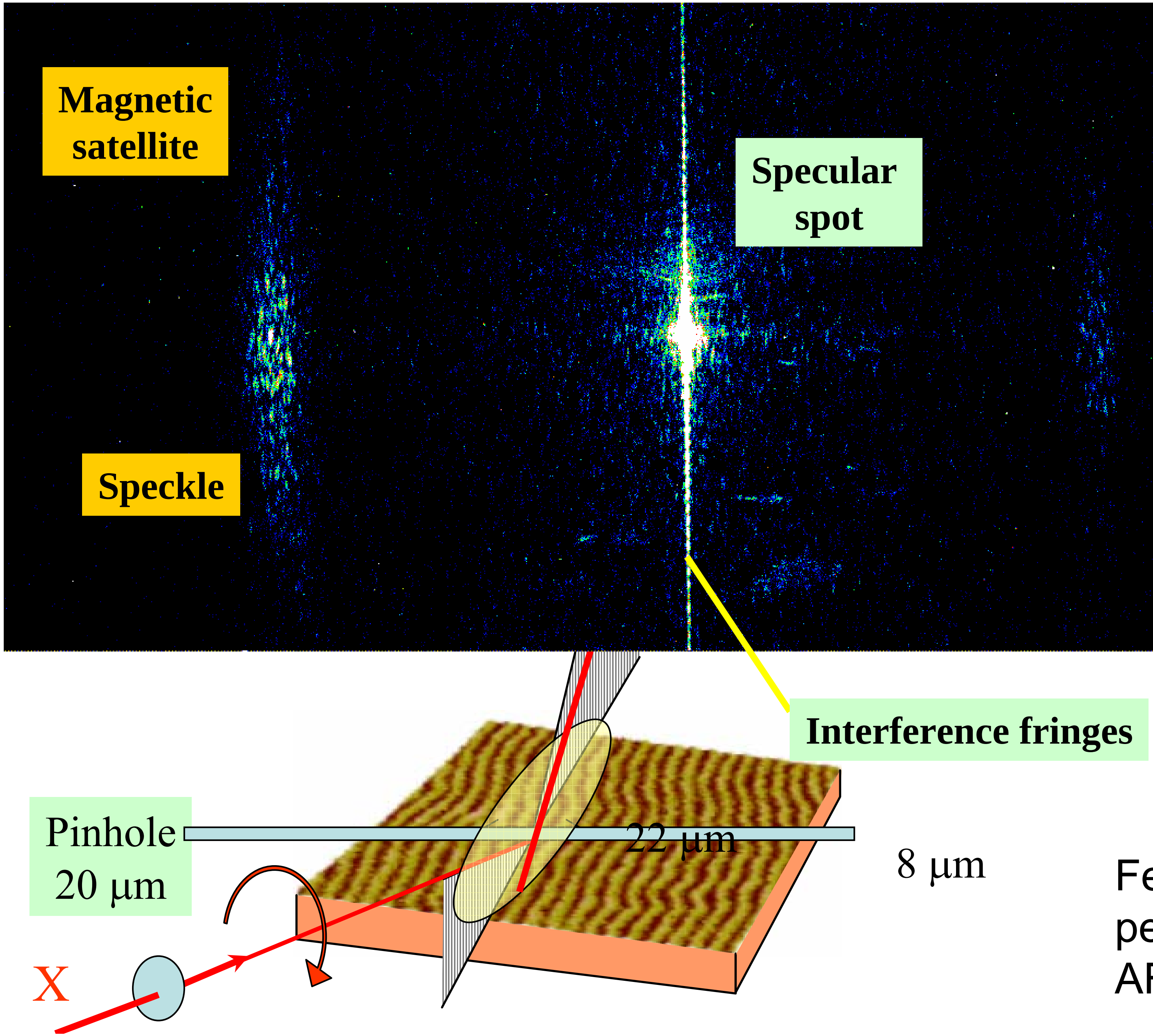

FePd thin film,
perp. magn.
AF order

Beutier – Chesnel

CF les PRBs.

Grazing Incidence X-ray Scattering

In UHV *in situ* during growth

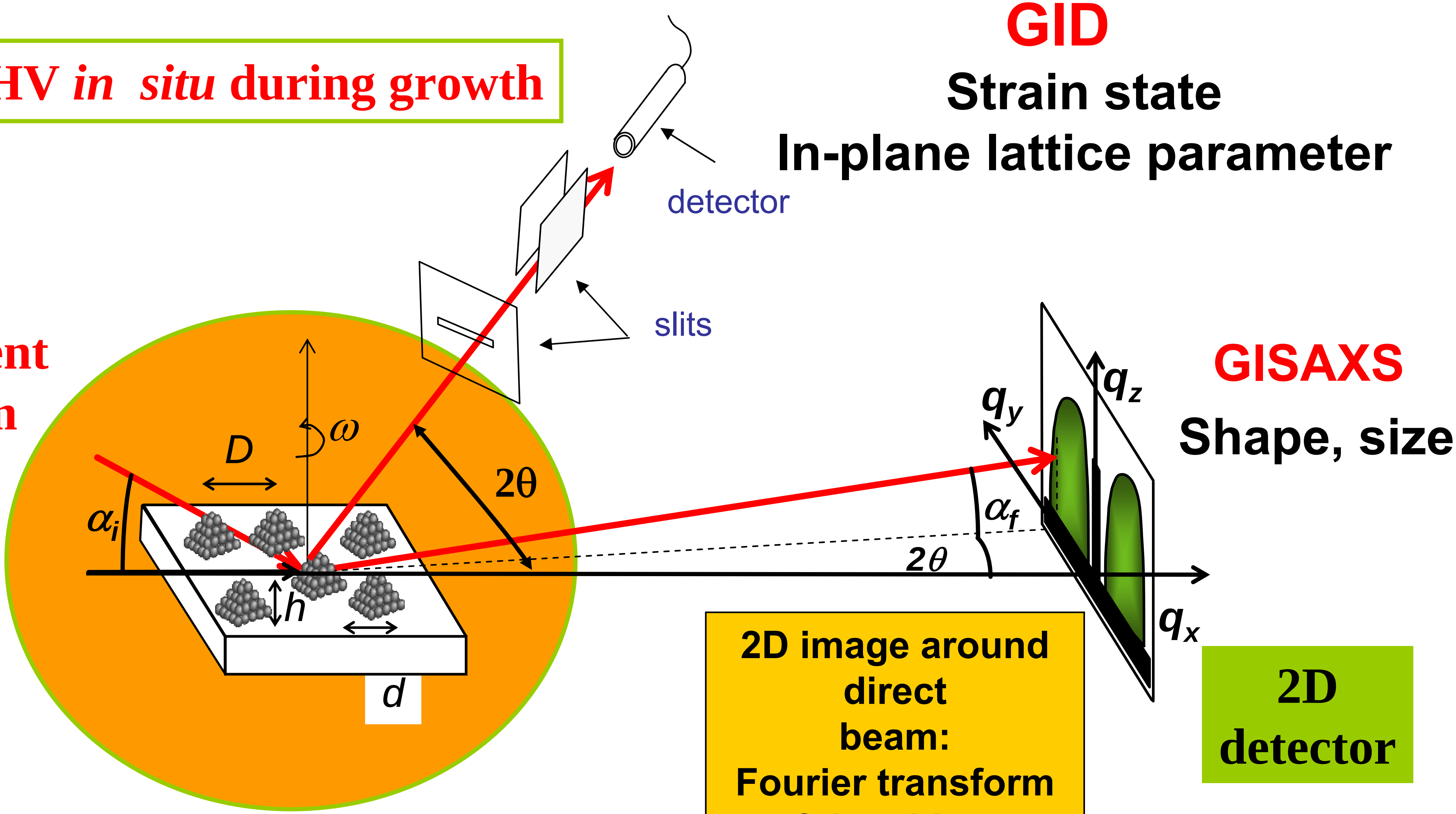

⇨ **to decrease the bulk scattering as much as possible (to be sensitive to surface)**

Coherent Diffraction from a 5 μ  made of Au

Christian Schroer, Edgar Weckert, Andreas Schropp, I. Vartanyants, Hasylab and ID01

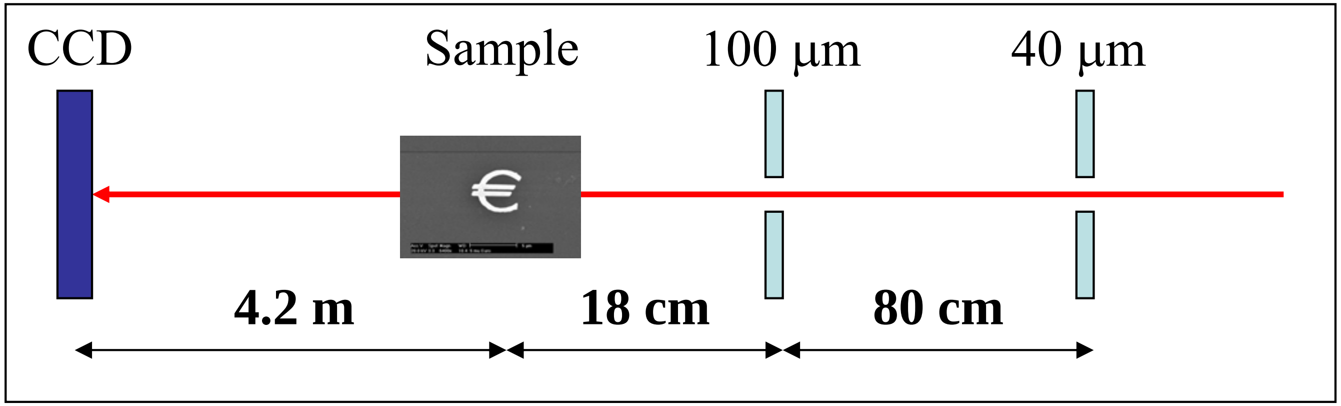

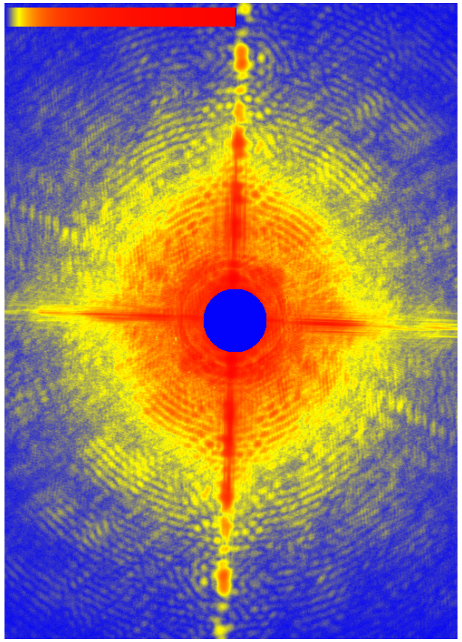

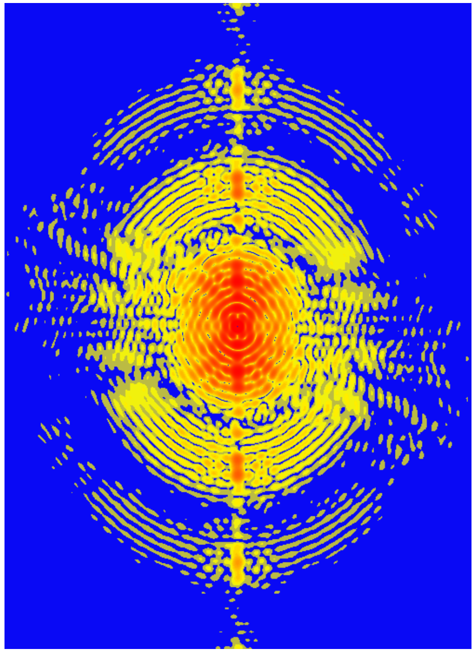

Next steps
Phase retrieval
and reconstruction

Measurement **Simulation**

General references

- Elements of modern X-ray physics, J. Als-Nielsen et D. McMorrow, John Wiley&Son (2001)
- X-ray scattering from soft-matter thin films, M. Tolan, Springer Tracts in Modern Physics, Vol148 (1998)
- High-resolution X-ray scattering from thin films and multilayers, V. Holy, U. Pietsch et T. Baumbach, Springer Tracts in Modern Physics, Vol149 (1998)
- Scattering of X-rays and neutrons at interfaces, D. Dietrich et A. Haase, Phys. Rep. 260 (1995) 1-138
- Critical phenomena at surfaces and interfaces, H. Dosch, Springer Tracts in Modern Physics, Vol126 (1992)
- Surface X-ray diffraction, K. Robinson et D.J. Tweed,Rep. Prog. Phys. 55 (1992) 599-651
- Surface structure determination by X-ray diffraction, R. Feidenhans 'l, Surf. Sci. Rep. 10 (1989) 105-188

Aknowledgments

F. Leroy, C. Revenant, A. Létoublon, T. Schülli, M. Ducruet, O. Ulrich,
CEA-Grenoble (France)

C.R. Henry, C. Mottet
CRMCN, Marseille (France)

O. Fruchart,
LLN, Grenoble, France

R. Lazzari, S. Rohart, Y. Girard, S. Rousset
GPS, Paris (France)

A. Coati, Y. Garreau
LURE, Orsay (France)

Thank you for your attention